UNIVERSIDAD AUTÓNOMA DE MADRID

Programa de Doctorado en Biociencias Moleculares

The Role Of The β3-Adrenergic Receptor In Animal Models Of Cardiac Injury

Andrés Pun García

Tesis Doctoral

PhD Thesis

Madrid, 2019

Departamento de Bioquímica

Facultad de Medicina

UNIVERSIDAD AUTÓNOMA DE MADRID

The Role Of The β3-Adrenergic Receptor In Animal Models Of Cardiac Injury

Memoria que presenta para optar al título de Doctor

por la Universidad Autónoma de Madrid:

Andrés Pun García

Licenciado en Veterinaria y Máster en Investigación en Ciencias Veterinarias

Director de Tesis:

Dr. Borja Ibáñez Cabeza

Centro Nacional de Investigaciones Cardiovasculares Carlos III (CNIC)

Madrid, 2019

Department of Biochemistry

School of Medicine

AUTONOMOUS UNIVERSITY OF MADRID

The Role Of The β3-Adrenergic Receptor In Animal Models Of Cardiac Injury

Doctoral Thesis presented to earn the Doctor of Philosophy degree

of the Autonomous University of Madrid by:

Andrés Pun García

Doctor of Veterinary Medicine and Master of Veterinary Science

Thesis Director:

Dr. Borja Ibáñez Cabeza

Spanish National Center for Cardiovascular Research (CNIC)

Madrid, 2019

Don Borja Ibáñez Cabeza, Doctor en Medicina y Cirugía y director del Departamento de Investigación Clínica del Centro Nacional de Investigaciones Cardiovasculares Carlos III (CNIC),

CERTIFICA que:

Andrés Pun García, Licenciado en Veterinaria por la Universidad Complutense de Madrid, ha realizado bajo su dirección en el Centro Nacional de Investigaciones Cardiovasculares Carlos III (CNIC) el trabajo titulado "**The role of the β3-adrenergic receptor in animal models of cardiac injury**" para la obtención del grado de Doctor, con Mención Internacional, por la Universidad Autónoma de Madrid. El presente trabajo cumple con todos los requisitos de originalidad y contenido exigidos y contribuye de manera significativa al ámbito de la investigación cardiovascular, por lo que autoriza su presentación para que pueda ser juzgada por el tribunal correspondiente.

Para que así conste y surjan los efectos oportunos, firmo el presente certificado en

Madrid, 10 de julio de 2019.

Fdo. Dr. Borja Ibáñez Cabeza

Esta tesis doctoral ha recibido financiación de una Beca de Formación de Personal Investigador (FPI) del Ministerio de Economía y Competitividad con referencia BES-2012-061091 asociada al proyecto SEV-2011-0052-02.

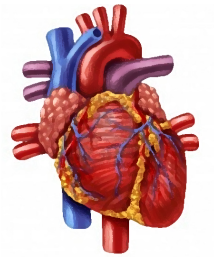

Agradecimientos/Akcnowledgements

Gracias a Borja por esta increíble oportunidad de participar y desarrollar esta etapa tan importante de mi carrera profesional en un centro tan impresionante como el CNIC. Gracias por creer en mí desde el primer día cuando llegué a tu despacho en primavera de 2012. Gracias por el apoyo en los momentos más duros y gracias por haber hecho de mi doctorado algo de lo que puedo estar y siempre estaré orgulloso. Por haberme hecho viajar por medio mundo conociendo otras formas de ver la ciencia. Gracias por ser un referente para mí y por hacerme sentir una admiración constante, esto ha sido sin duda un gran motor para mantener la motivación durante estos 6 años. Gracias por tu generosidad y por seguir siendo el viento que me impulsa y me ayuda a volar. Gracias en definitiva por haberme hecho crecer de una manera que nunca habría imaginado antes de empezar esta aventura.

Gracias a Andrés Hidalgo y Antonio Fernández-Ortiz por formar mi comisión de seguimiento a lo largo de mi doctorado. Gracias a Jaime por haber compartido tu experiencia conmigo y haberme ayudado a dar los primeros pasos en el laboratorio de los que siempre me quedará un buen recuerdo. A David por haber sido un gran guía en mis primeros años como doctorando siempre con una sonrisa en la cara. A Moni por todo tu apoyo y ayuda, tu rigor, tu precisión, tu destreza y por ser la mejor técnico que he conocido en cualquiera de los laboratorios en los que he trabajado en el mundo. A Roci por tu frescura, por tu energía y por tu pasión por la Ciencia, por estar siempre dispuesta a ayudar con una profesionalidad que en poca gente de tu edad he visto. A Agus por todos los buenos momentos que nos has hecho pasar y por aportar tanta brillantez al laboratorio. A Lorena, a Ana y a Eva por vuestro trabajo en las 3 millones de ecocardiografías realizadas a lo largo de estos años siempre de buen humor. A Alba que aunque con un paso fugaz por el laboratorio has sabido hacerte querer como post-doc y como compañera. A Edu por las innumerables conversaciones a las 10 de la noche cerrando el laboratorio, por aportarme su visión de la Ciencia, por haber sido y ser un post-doc ejemplar y estar siempre dispuesto a ayudar a que el grupo crezca todos los días. A Jaume por todos los consejos, por aportar tu visión crítica a mis experimentos y por ser un ejemplo de pasión por la medicina y la ciencia. A toda la parte del equipo confinada horas y horas con los cerdos, a Carlos, a Rodri, a Manu, a Mario, a Jean Paul, a Xavi… A Javi y a Paula por haberme enseñado algo (o eso creo) de resonancia magnética. A toda la gente que ha venido con la ilusión de aprender al laboratorio especialmente a Juan Pablo y a Sergi.

Por supuesto mil gracias a Anabel y a Eeva por toda la ayuda cada vez que tenía que pedir una beca, una ayuda, una convocatoria de estancias o cualquier otra tortura burocrática. La vida de doctorando hubiera sido mucho más difícil sin vosotras. Y lo mismo puedo decir de Edu B. y de Sonia aunque un poco más tarde en mi vida en el CNIC. Cris por todas las risas y por toda tu ayuda con la Universidad y las becas. A Irene por la ayuda con la parte de la gestión bibliográfica. A todos los miembros del CNIC que alguna vez habéis pasado por la primera sur y habéis formado parte de mi día a día en el laboratorio, con los que he compartido risas, angustias, conversaciones trascendentales de la vida, reactivos y cafés. Por mencionar a algunos y sin querer ser exhaustivo gracias por todos esos buenos momentos compartidos Álvaro, Bea, Cris, Javi M., Raquel, Amanda, María C., Alberto, Lara, Jose, Marina, María V., Javi L., Marta C., Irene… Gracias a Juan y a todo su equipo, Fran, Andrés, Marta, Crisss… por todo el apoyo con la parte viral de esta tesis y por haber sido como mi segunda casa en el CNIC. Gracias a todos los miembros de todas las unidades técnicas, servicios y toda la administración y dirección del CNIC por hacer del trabajo en este centro un placer a pesar de la adversidad del trabajo en la Ciencia.

Gracias al Dr. Valentín Fuster por haber dirigido con tanta pasión el CNIC durante estos años y hacer del centro un referente mundial y un hogar para toda la gente que trabajamos en él.

Thanks to everyone that I have met and has helped me during my externships in Philly and NYC. Thanks to Dr. Koch's lab, specially to Nora, Alessandro, CJ and Jessica and the rest of the people who have made my life in Philly a wonderful experience inside and outside the lab especially Talpa. Thanks to Dr. Hajjar's lab too, especially to Ludo, Lahouaria, Eric, Francesca and Julie for your help. And of course to Dr. Roger J. Hajjar and Dr. Walter J. Koch for giving me the opportunity to be part of their amazing laboratory.

Gracias a mis amigos que sin vuestro apoyo esta experiencia hubiera sido menos llevadera. A Carlos, Guille, Jesús y Borja por vuestro cariño, por vuestra amistad y por vuestro apoyo incondicional en todos los momentos buenos y sobre todo en los malos vividos juntos y los que nos quedan por vivir. Gracias a mi familia habichuela, esa gran familia de la que me siento tan afortunado de pertenecer y con la que sé que compartiré muchos momentos importantes de nuestras vidas como éste. Un especial gracias a mi familia del mal, Arancha, Merche, Dani, Ana, Marta y Charli que sois una constante fuente de amor estemos lejos o cerca, en un solo país o en 7 diferentes.

Por supuesto gracias a mi familia, a mi padre, a mi madre, a Álvaro, a Ernesto, a David, a Noel y a Elvira porque un pedacito de este éxito también os pertenece a vosotros. Espero haceros sentir orgullosos de vuestro hijo/hermano tanto por esta tesis doctoral como por todo lo que me ha llevado a este momento de la vida. A mis abuelos, especialmente a la abueli, a mis tíos y tías, cuñados y cuñadas y sobrinos.

Por último gracias a todos los animales que dan su vida por hacer avanzar la ciencia. Como veterinario, como amante de los animales y como ser humano creo que es importante resaltar la gran responsabilidad que se tiene al trabajar con seres vivos en investigación. Todos los animales que han participado en estos experimentos han sido tratados con el mayor de los respetos.

Gracias

“Dans la vie, rien n'est à craindre, tout est à comprendre.”

“Nothing in life is to be feared. It is only to be understood.”

“Nada en la vida es para ser temido, es sólo para ser comprendido.”

Marie Curie

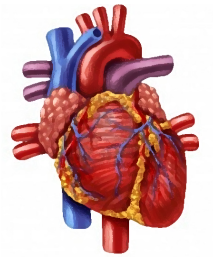

Resumen/Abstract

RESUMEN

El sistema β-adrenérgico es clave en la regulación de la función cardiaca. El papel de los receptores β1 y β2 adrenérgicos está bien establecido y son dianas frecuentes en los tratamientos médicos utilizados en la práctica clínica. Sin embargo el conocimiento que existe sobre el papel del receptor β3 adrenérgico (β3AR) tanto en condiciones fisiológicas como patológicas en el sistema cardiovascular es mucho menor. A pesar de que la expresión del β3AR en el corazón es relativamente baja comparada con los subtipos β1 y β2, estudios previos han demostrado que agonistas del β3AR tienen un efecto cardioprotector en la hipertrofia por sobrecarga de presión, el remodelado hipertrófico neurohormonal y el daño por isquemia/reperfusión. En el corazón el β3AR está presente en los miocitos cardiacos y en las células endoteliales pero la contribución de ambos tipos celulares en la protección proporcionada por la activación del β3AR está aún sin explorar. Con respecto a la insuficiencia cardiaca poco se sabe sobre el papel de este receptor en la progresión de la misma y la literatura presenta resultados contradictorios. Los recientes resultados del primer ensayo clínico con un agonista del β3AR en pacientes con insuficiencia cardiaca exigen ahondar en el conocimiento del papel de este receptor. El objetivo principal de esta tesis doctoral es profundizar en el conocimiento del β3AR en la patología cardiaca. En primer lugar, siguiendo una línea de investigación existente en el grupo, se ha explorado el origen celular de la cardioproteción que ofrece la administración de un agonista del β3AR antes de la reperfusión. En este estudio demostramos por primera vez usando modelos de ratón transgénico nunca antes publicados que la activación del β3AR en el daño por isquemia/reperfusión (IR) protege el corazón debido a su acción en el miocito cardiaco principalmente y no en la célula endotelial. Además un incremento en el número de β3AR en los miocitos cardiacos amplifica la respuesta protectora de su estimulación, señalando la sobreexpresión del β3AR como una potencial terapia para reducir el daño por IR en pacientes con alto riesgo de sufrir un infarto agudo de miocardio. En segundo lugar se ha investigado el papel del β3AR en la progresión de la insuficiencia cardiaca. Ratones transgénicos que sobreexpresan el receptor en los miocitos cardiacos resultaron no desarrollar signos de insuficiencia y la sobreexpresión del receptor mediante terapia génica durante el desarrollo de la insuficiencia detuvo su progresión. Se especula que esta cardioproteción está relacionada con el incremento de la utilización de ácidos grasos por parte del miocito cardiaco, la inhibición el cambio metabólico durante la insuficiencia cardiaca y la protección de las mitocondrias. Este trabajo confirma por lo tanto que la activación del β3AR es una terapia que debe ser considerada para el tratamiento de la insuficiencia cardiaca. En conclusión esta tesis incrementa el conocimiento sobre el β3AR en el sistema cardiovascular aportando fuertes evidencias sobre su potencial terapéutico en la práctica clínica como diana para reducir el daño por IR en pacientes con infarto agudo de miocardio y apoyando el papel beneficioso de su estimulación en el tratamiento de la insuficiencia cardiaca.

ABSTRACT

The β-adrenergic system is a key player in the regulation of the heart function. The role of the β1- and the β2- adrenergic receptors is well established and they are common targets of the medical treatment used in clinical practice. However the role of the β3-adrenergic receptor (β3AR) in the cardiovascular system is still poorly understood in both physiological and pathological conditions. It is known that β3AR expression in the heart is relatively low compared to β1 and β2 subtypes, nevertheless previous studies have shown that β3AR agonists have a cardioprotective effect in pressure overload hypertrophy, neurohormonal hypertrophic remodeling and ischemia/reperfusion injury. In the heart, β3ARs are present in cardiac myocytes and in endothelial cells but it is still unknown what is the relative contribution of these cell types in the cardioprotection afforded by the activation of the β3AR. Regarding heart failure little is known about the role of this receptor in the progression of cardiac dysfunction and contradictory results can be found in the literature. Recent results from the first-in-man clinical trial using a β3AR agonist in heart failure patients demand deeper knowledge about the role of the β3AR. The main aim of this doctoral thesis is to improve the knowledge concerning the β3AR in cardiac diseases. First, following an already existing research line in the laboratory we have investigated the cellular origin of the cardioprotection afforded by β3AR agonists administration before reperfusion. In this study we demonstrate for the first time using transgenic animal models never published before that β3AR activation in ischemia/reperfusion (IR) injury protects the heart by activating mainly the cardiomyocyte β3AR and not the endothelial β3AR. Moreover the overexpression of the receptor in cardiac myocytes amplifies the protection afforded by its activation, pointing out the β3AR overexpression as a potential therapy to reduce IR injury in patients at risk of acute myocardial infarction. Secondly, we have investigated the role of the β3AR in the progression of heart failure. Transgenic mice overexpressing the receptor in cardiac myocytes did not develop heart failure and gene therapy based overexpression of the receptor during the development of heart failure stopped its progression. We speculate that this protection involves increase in free fatty acids utilization by cardiac myocytes, inhibition of myocardial metabolism switch during heart failure and mitochondrial protection. This work confirms that β3AR stimulation is a therapy that should be considered to treat the failing heart. To conclude, this thesis increases the knowledge of the role of the β3AR in the cardiovascular system offering strong evidences of its therapeutic potential in the clinical arena as a target to decrease IR injury in patients with acute myocardial infarction and supporting the beneficial effect of its stimulation in the treatment of heart failure.

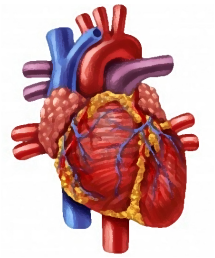

Index

INDEX OF TABLES

INDEX OF FIGURES

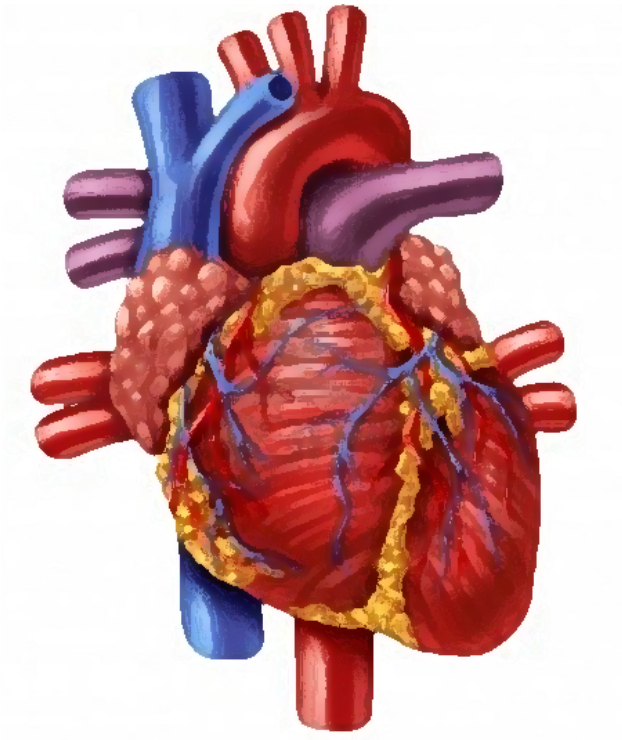

Abbreviations

AAR: area at risk

AAV : adeno-associated virus

ADRB3: Homo sapiens (Human) Beta-3 adrenergic receptor gene

Adrb3: Mus musculus (Mouse) Beta-3 adrenergic receptor gene

AMI: acute myocardial infarction

AMVM: adult mouse ventricular myocytes

cTnT : truncated chicken cardiac troponin-T ()

CVD: cardiovascular disease

EGFP : enhanced green fluorescent protein

eNOS: endothelial nitric oxide synthase

FAO : free fatty acids oxidation

FFA : free fatty acids

GPCR: G-protein-coupled receptors

GRK2: G-protein-coupled receptor kinase 2

GRKs: G-protein-coupled receptor kinases

HF: heart failure

hβ3AR: human Beta-3-adrenergic receptor protein

IR: ischemia reperfusion

IS: infarct size

IVIS : In Vivo Imaging System

LAD: left anterior descending coronary artery

LV: left ventricle

mβ3AR: mouse Beta-3-adrenergic receptor protein

nNOS: neuronal nitric oxide synthase

NO / NOS: nitric oxide / nitric oxide synthase

NRVM: neonatal rat ventricular myocytes

PET-CT : positron emission tomography–computed tomography

PKA: protein kinase A

rAAV : recombinant adeno-associated virus

ROS: reactive oxygen species

sGC : soluble guanylate cyclase

TAC: transaortic constriction

TTC : 2,3,5-triphenyltetrazolium chloride

WT : wild type

β-ARK1: Beta-adrenergic receptor kinase 1

β1AR: Beta-1-adrenergic receptor protein

β2AR: Beta-2-adrenergic receptor protein

β3AR: Beta-3-adrenergic receptor protein

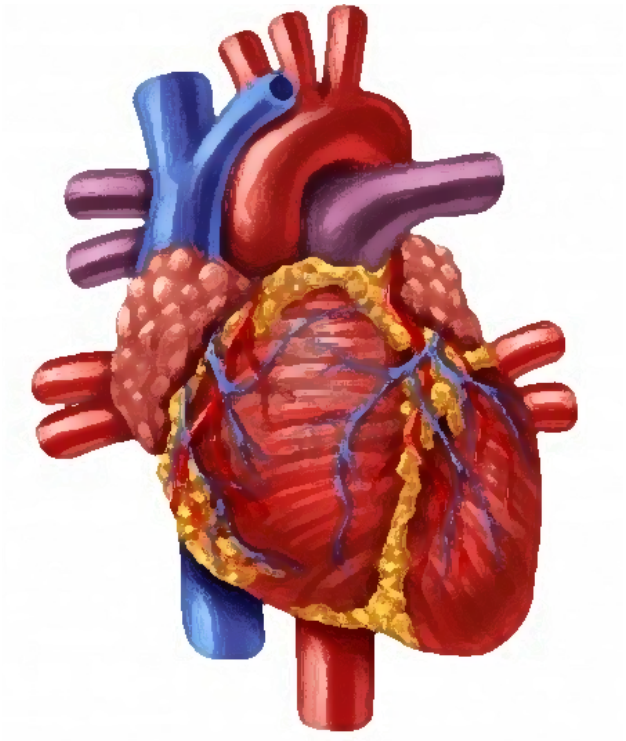

Introduction

1 INTRODUCTION

The topic of study covered in this doctoral thesis is the role of the third subtype of the beta-adrenergic receptors, the β3-adrenergic receptor (β3AR), in cardiac injury. First, this work explores the origin of the cardioprotection afforded by the systemic stimulation of the β3AR in ischemia/reperfusion (IR) injury. Second, this study focuses on the role of the β3AR in the development of HF and its therapeutic use.

1.1 Heart failure

1.1.1 The relevance of heart failure

Heart failure (HF) is a serious pathological condition in which the heart is unable to pump enough blood to meet the needs of the body. Far from being rare, it is one of the most common medical problems affecting 26 million people worldwide and it is the most common cause of hospitalization after normal delivery *(1–3)*. Up to one in five people is expected to develop HF at some point in their life *(4)*. HF is the final consequence of most heart diseases and it is therefore considered a heart "condition" and not a heart "disease" itself.

The advances in the prevention, diagnosis, and management of cardiovascular disease (CVD) in the last 50 years have been spectacular. As a result, there has been a dramatic fall in the mortality rates associated with the acute coronary syndromes, uncontrolled hypertension, valvular and congenital heart disease and many arrhythmias *(5)*. HF however, is a exception to these trends *(1, 6)*. The reason is that many patients who have suffered these kind of disorders develop some myocardial damage, and even if their lives are prolonged, their heart has not been completely cured *(7, 8)*. By instance, a better awareness and management of high blood pressure in the last 40 years has probably delayed the onset of HF to later ages in life *(9)*. In the same way, more effective treatments for acute myocardial infarction could have increased the number of surviving patients, who are then at risk of developing HF years later *(10)*. Therefore, an increasing number of these treated patients become at risk of subsequently developing HF, which might be seen as the price of success in treating CVD. In high-income countries HF has become the most common diagnosis for hospitalization in patients older than

65 years of age *(11)*. Every year, about one million hospital admissions occur for HF in Europe and the picture is similar in the USA *(12–14)*. With the unstoppable aging of the population, the number of HF patients will inevitably increase in the future *(15)*. In fact, a 50% increase in the prevalence of HF is estimated by 2030, unless there is real progress in prevention or treatment, or both *(16)*.

In addition, HF is unfortunately a life-threatening condition. In recent years, survival after a diagnosis of HF has improved in many parts of the world; the age-adjusted death rate has declined *(12, 13, 17)*, and the mean age at death from HF has risen *(18, 19)* as a consequence of the success of modern evidence-based therapies and patient management systems *(20–23)*. However, despite these modest improvements over the past 20 years, the 5-year mortality is still approximately 50% worse than that of many cancers like bowel, breast or prostate cancer *(24, 25)* highlighting the poor prognosis for patients with HF. Across the world, 17–45% of patients admitted to a hospital with HF die within one year of admission and the majority die within five years of admission *(17, 19, 26)*.

1.1.2 The heterogeneity of heart failure

The etiology of HF is complex and varies within and among world regions. There is no agreed single classification system for the causes of HF. The European clinical guidelines *(27)* classifies it in three main groups: diseased myocardium, abnormal loading condition and arrhythmias (Table 1) although there is an overlap between categories. The true is that many patients have several different pathologies (cardiovascular and extra-cardiovascular) that add up and contribute to cause HF.

Regarding the treatment, there is heterogeneity in these patients. The reason is that HF can arise from different pathologies concerning the structure or function of the heart, some of which are more difficult to treat than others. In patients with chronic HF with reduced ejection fraction, β-adrenoceptor blockers, angiotensin-converting enzyme inhibitors, angiotensin receptor blocker, I_f channel inhibitor, aldosterone antagonists, isosorbide dinitrate and hydralazine and an angiotensin receptor-neprilysin inhibitor improve both the survival and quality of life *(27–29)*. Devices, including pacemakers, which improve cardiac synchronization and implanted cardiac defibrillators *(30, 31)* have also shown important benefits. However, in many patients the progression of HF cannot be slow down and modern therapies are not capable of prolonging life. Therefore, new therapies are needed for patients

suffering HF and huge efforts are done worldwide to encourage international research to improve the understanding of how heart failure develops and how it can be prevented and treated.

Table 1: Etiologies of heart failure defined by the European Society of Cardiology Clinical Guidelines *(27)*

DISEASED MYOCARDIUM	Ischemic heart disease
	Toxic damage
	Immune-mediated damage and inflammatory infiltration
	Metabolic derangements
	Genetic abnormalities
ABNORMAL LOADING CONDITIONS	Hypertension
	Valve and myocardium structural defects
	Pericardial and endomyocardial pathologies
	High output states
	Volume overload
ARRHYTHMIAS	Tachyarrhythmias
	Bradyarrhythmias

Nowadays, ischemic heart failure is the most common type of heart failure *(32)* and therefore among all the causes of HF ischemic heart disease is thought to be the most important risk factor for HF *(33–35)*.

1.1.3 Acute myocardial infarction

The Global Burden of Disease 2010 study *(32, 36)* reported that from 1990 to 2010, ischemic heart disease was the most common cause of death worldwide. Acute myocardial infarction (AMI) is the main cause of ischemic heart disease. AMI is the result of the sudden occlusion of an epicardial coronary artery. Subsequently, the blood flow is interrupted, the blood carrying oxygen and nutrients is not able to reach the myocardium distal to the occlusion site and this area becomes ischemic. This blood flow deprivation causes permanent damage to the myocardium that was previously supplied by the occluded artery. The heart is an organ with high metabolic needs because of its unstoppable activity. For this reason, a short

time under ischemic conditions is enough lead to a fatal damage of the myocardium *(37)*. The damaged myocardium becomes necrotic and is replaced by fibrous scar tissue that lacks contractile function. The volume of necrotic tissue is called infarct size (IS). If the IS is large, the global left ventricular (LV) contractile function is impaired, resulting in progressive chronic HF *(38)*. Therefore, IS is the main determinant of long-term mortality and HF and for this reason limiting its extent is of great individual and socioeconomic interest *(39)*.

Forty years ago, studies in animal models demonstrated that an early reperfusion of the ischemic myocardium was able to limit the final amount of dead tissue and therefore improve the survival rate of the patients suffering these events *(40–42)*. In light of this evidence, therapies to reduce time under ischemia based on reperfusion strategies have been incorporated into clinical practice during the last three decades. The fibrinolytic drugs therapy was the first to reach the clinical arena and show a reduction in mortality in patients with AMI *(43)*. Years later, the mechanical reperfusion by percutaneous coronary intervention improved the outcomes of the previous strategy *(39, 44)*. Since then reestablishment of the coronary blood flow in order to reduce ischemic injury has been established as the main indication in the clinical guidelines for the treatment of patients with AMI *(45)*. These therapies have remarkably reduced the mortality of patients with AMI *(46)* but as a downstream consequence of survival these patients develop post-infarction HF. The reason is that reperfusion reduces the final IS and this helps to save the patient right after the event but there is still some myocardium that is injured and with time it becomes a non-contractile scar leading to HF.

Unfortunately, few additional therapies have shown to be able to reduce short and long term mortality in patients with AMI besides early reperfusion *(39)*. Although the age-standardized incidence of AMI has decreased worldwide, the prevalence of ischemic HF has increased *(32)*. For this reason, there is an urgent need to develop new therapies to reduce IS and to prevent myocardial dysfunction after AMI. The only way to do so is by targeting the pathophysiological mechanism involved in ischemia and reperfusion leading to myocardial damage.

1.1.4 Basis of myocardial ischemia/reperfusion injury

When the coronary artery is occluded during AMI, normally by a thromboembolism, the myocardium supplied by this artery becomes at risk of ischemia and consequent death. This portion of the myocardium is known as area at risk (AAR) (Figure 1). In reperfusion

strategies, the coronary artery is reopened and blood flow is reestablished supplying again blood full of nutrients and oxygen and saving the myocardium from ischemic death. Even with short times of hypoxia, some cells have already become necrotic by the time of reperfusion and cannot be saved. The extension of the final amount of dead myocardium is called infarct size (IS) as already mentioned (Figure 1). Without reperfusion all the AAR dies in a time-dependent manner until the IS is equal to the AAR. With reperfusion, the cells that are still not so damaged benefit from the nutrients and oxygen provided by the reestablished blood flow and are saved from necrosis. This is known as salvaged myocardium. Paradoxically, reperfusion itself can contribute to further damage the ischemic and fragile cells increasing the final IS. This phenomenon is known as reperfusion injury *(39)*. Hence, reperfusion injury can be defined as "the injury caused by the restoration of blood flow after an ischemic episode, leading to the death of cardiac cells that were reversibly injured at the time of blood flow restoration" *(37)*.

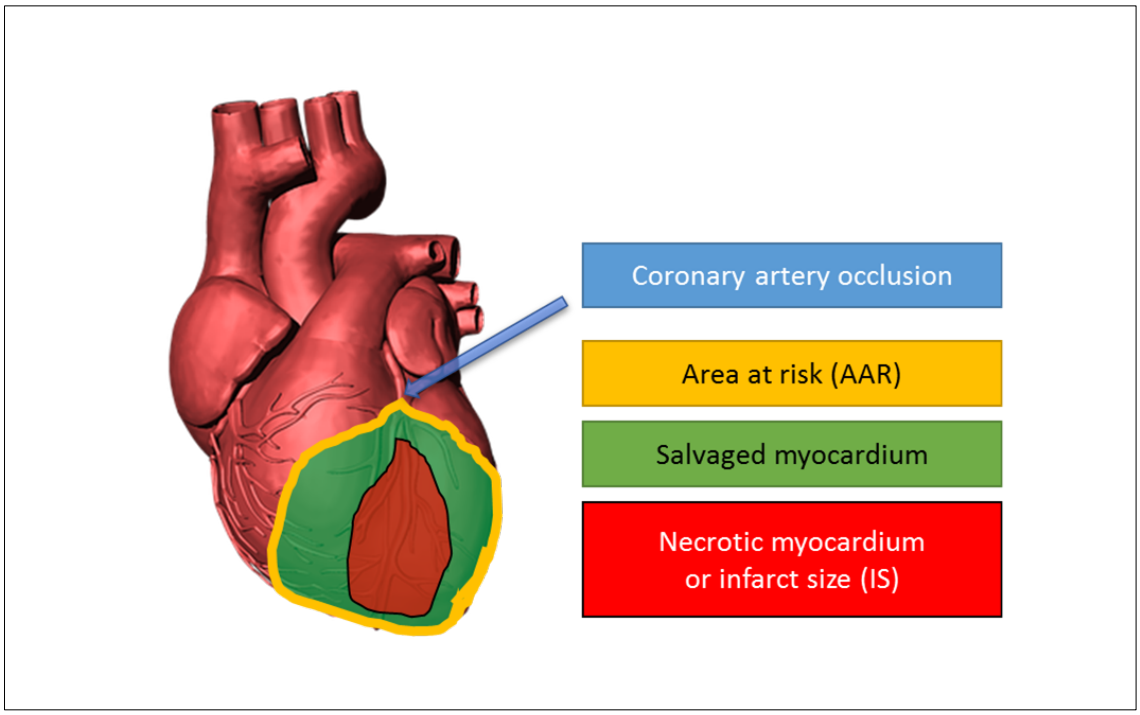

Figure 1: Acute myocardial infarction

After coronary artery occlusion the myocardium supplied by this artery becomes at risk of ischemia and consequent death. This portion of the myocardium is known as area at risk (AAR). The reestablishment of the coronary blood flow by reperfusion strategies saves this myocardium from necrosis (salvaged myocardium) however some tissue cannot be rescued and becomes necrotic (infarcted area).

Different contributors of reperfusion injury have been described *(47)*. Some factors contributing to IR injury alter the capacity of the microcirculation to correctly reperfuse the myocardium. During the reperfusion process, thrombus material and other plaque debris can be distally embolized and generate microvascular obstruction. Activated platelet and leukocytes attracted by the inflammatory milieu can also form plugins that can embolize distally contributing to microvascular obstruction. This process of microembolization prevents a full recovery of the blood flow in some areas of the myocardium that will finally die because of the maintained ischemia. The generation of tissue edema following reperfusion can also result in external compression of the microcirculation, reducing the perfusion capacity of the capillary network. Capillaries that are injured during ischemia allow the leakiness of circulating cells into the interstitial space when blood flow is reestablished. Extravasated red blood cells are especially harmful due to the release of iron, which can contribute to the subsequent inflammatory reaction inducing an additional damage to the myocardium. Therefore maintaining capillary integrity can be a way to decrease IR injury.

Some others factors directly affect the viability of the cardiac myocytes that are intact but fragile at the end of ischemia. Four major pathways have been described. The first pathway involves pH. During ischemic conditions, anaerobic glycolysis, poor washout of metabolic end products, and the loss of ionic pump activity secondary to high-energy phosphate depletion (ATP) take place. As a result ischemic myocytes become overloaded with Na^+, H^+, and Ca^{2+} before reperfusion. Reperfusion with oxygenated blood and normal pH (7.4 pH) generates a rapid shift in ionic equilibrium. The large amount of H^+ inside cardiomyocytes is rapidly corrected through activity of the Na^+/ H^+ exchanger and the Na^+ / $HCO3^-$ symporter, pumping out of the cell the H^+ but at the same time increasing the concentration of Na^+. In order to compensate the Na^+ overload, the Na^+ /Ca^{2+} exchanger through reverse function pumps inside the cells large amounts of Ca^{2+} that have fatal consequences for the cell. Therefore, slowing down the rapid recovery of extracellular pH from acidotic conditions to normal pH values may have an important effect in limiting lethal reperfusion injury *(48)*.

The second pathway involves calcium. The rapid increase of Ca^{2+} inside the cell targets three mechanisms that can affect cell viability. The first one is the activation of calpains and other degradative enzymes. Once activated, these enzymes can weaken the cytoskeleton of the myocytes rendering the cell more fragile and its membrane more likely to physical disruption *(49–51)*. The second is the activation of the contractile function of the myocytes that can result in a hypercontracture. This phenomenon occurs as a consequence of the

resumption of ATP generation by mitochondria in the presence of normal or elevated calcium levels *(52)*. Hypercontracture generates a physical stress leading to cell death *(53)* and its inhibition has been demonstrated to be cardioprotective in reperfusion injury *(54)*. The third important consequence of increased calcium influx is the effect in mitochondrial function and membrane permeability. Under this condition, mitochondria increases calcium uptake, its membrane becomes more permeable and this results in severe mitochondrial swelling. The main responsible of mitochondrial membrane permeability is a protein channel known as mPTP (mitochondrial Permeability Transition Pore). Increased calcium fluxes, increased reactive oxygen species (ROS), and increases in inorganic phosphate concentration are factors that render this channel more susceptible to remain open *(55, 56)*. An uncontrolled opening of this channel results in a collapse of the inner mitochondrial membrane potential and uncoupling of the respiratory chain leading to mitochondrial failure. Mitochondrial swelling can also trigger cytochrome c enzyme release to the cytoplasm, acting as a potent activator of apoptotic pathways. Inhibition of mPTP opening has been shown to decrease infarct size and has already been explored as a therapy in humans with the use of cyclosporine A *(57)*. The ongoing multicenter, randomized, placebo-controlled CIRCUS (Cyclosporine and Prognosis in Acute Myocardial Infarction Patients) trial is now exploring the effects of this therapy in a bigger cohort of patients.

The third pathway involves cell swelling. During the ischemic period, the metabolism goes from free fatty acid-dependent Krebs cycle–based metabolism to anaerobic glycogen-dependent glycolysis. This generates large amounts of lactate as the end product of glycolysis. This metabolite accumulation makes the intracellular and extracellular spaces hyper-osmotic. At reperfusion, an osmotic gradient between the blood and the hyper-osmotic spaces is created and this results in cell swelling. Cell swelling as an isolated phenomenon has been shown to induce a substantial physical stress resulting in cell death *(51)*.

The fourth pathway is oxidative stress. Large amounts of reactive oxygen species (ROS) including superoxide anion, hydrogen peroxide, and hydroxyl radical and other radical species, including nitric oxide (NO) are generated during early reperfusion. ROS are generated in small amounts during the normal cellular activity as an essential part of the aerobic survival of the cell and are involved in multiple pathways. To avoid harmful effects of ROS the cell has several defense mechanisms such as catalase, glutathione peroxidase, and superoxide dismutase that are able to protect organelles and proteins from oxidation. However, on reperfusion and the associated reintroduction of oxygen, the amount of ROS produced exceeds the defensive

capacity of the cell causing widespread damage. ROS can affect a large variety of targets such as the sarcoplasmic reticulum and ionic pumps impairing the calcium-handling machinery. This results in calcium overload, protein oxidation leading to cross-linking and eventual breakdown of critical proteins. When lipids are affected, there is a subsequent disruption of cholesterol-containing membranes, opening of the mPTP, and activation of apoptotic pathways *(58, 59)*. It has also been describe that oxidative stress may also influence recruitment of neutrophils and neutrophil activation, interaction with platelets and generation of microvascular obstruction and no-reflow effect as well as generation of peroxynitrite during lipid peroxidation, and ROS-mediated disruption of cellular signaling pathways *(60)*.

All these pathways lead to necrosis and subsequent myocardial dysfunction and HF. However, many animal models have been described to explore the complexity of the HF in human medicine.

1.1.5 Exploring heart failure: the role of the animal models

There are multiple models of HF. The pathophysiological basis of all of these models have always something in common, they are either pressure overload or volume overload. Pressure- or volume-overload lead to remodeling to normalize systolic wall stress, this in turn leads to cardiomyopathy and HF *(61, 62)*. Volume overload causes eccentric hypertrophy through an increase in myocyte length. Eccentric hypertrophy allows the ventricle to receive the increased volume; normalizing systolic wall stress but increases end-diastolic wall stress *(63)*. Clinically, the example for pure volume overload is atrioventricular valve regurgitation or intracardiac shunts such as an atrial septal defect. Experimentally, volume overload is typically achieved by an aorto-venous (AV) shunt. Pressure overload leads to concentric hypertrophy through an increase in myocyte volume but not length *(64)*. Concentric hypertrophy normalizes wall stress at the beginning according to the law of Laplace; this is typically called “compensatory hypertrophy”. The rapid increase in wall thickness is known to affect mechanical function in the heart and as an early consequence diastolic dysfunction may develop *(65)*. Later, the capillary network may be inadequate and insufficient for supplying these thickened walls with increased pressure and higher oxygen demands *(64)*. In the clinical setting, the classic example is aortic stenosis and for research purposes, the classic pressure overload animal model is thoracic aortic constriction (TAC). In this model, the aorta is surgically constricted, resulting in chronic elevation of LV end-systolic pressure. Animals subjected to TAC classically display an initial remodeling with concentric hypertrophy and progression to

HF. A recent comparison between TAC and AV shunt models has demonstrated that they have different molecular mechanism involved with 160 differentially expressed transcripts *(66)*. The myocardial infarction model is a mixture of both. The infarcted heart is initially subjected to a volume overload. This sudden volume overload results in a pressure overload. The TAC is the most common model when using rodents and it is the one chosen for this thesis. It is important to mention that these animal models are important for research purposes but they are far from the reality in the clinical arena. HF in humans as previously seen is a condition that develops over the years and in the presence of many comorbid conditions that contribute to their underlying heart disease. These facts contribute to the molecular heterogeneity of clinical HF that is not present in animal models. These confounding issues need to be considered when applying the results of animal models to humans.

Nevertheless, these animal models are a key tool to understand underlying pathways and signaling cascades that regulate HF and the causes that can lead to it like the IR injury. HF is defined by the deterioration of the cardiac function and the main regulator of the cardiovascular function is the β-adrenergic system.

1.2 The β-adrenergic system

In 1906, Dale discovered the adrenergic receptors and he predicted the existence of two different types *(67)*. In 1948, Ahlquist *(68)* was the first to differentiate the adrenergic receptors pharmacologically into α- and β-adrenergic receptors using their differential response to the catecholamines adrenaline, noradrenaline and isoprenaline. In 1967, Lands et al. *(69)* described two different subtypes of βARs (β1AR and β2AR) using adrenergic agonists. In 1989, Emorine et al. *(70)* cloned the third subtype of the βARs (β3AR) completing the classification of the βARs family as it is known today *(71)*. Nowadays, the physiological relevance of the β-adrenergic receptors is obvious and it is reflected in the fact that James Black in 1988 and Robert J. Lefkowitz and Brian Kobilka in 2010 were awarded with the Nobel Prize for Medicine (1988) and for Chemistry (2010) regarding discoveries related to these receptors *(72, 73)*.

1.2.1 Structure of the βARs

The β-adrenergic receptors (βARs) belong to the superfamily of the G-protein-coupled receptors (GPCR). GPCRs are involved in the cellular response to different external neuro and autocrine stimuli. A pocket formed by seven transmembrane domains that contains the binding sites for the agonists and competitive antagonists characterizes them. As part of the GPCR family, the βARs also contain three extracellular and three intracellular loops. The first and second extracellular loop are coupled via a disulfide bridge and play an important role in the development of the tertiary structure of the protein *(74–76)*. The molecular structure of these receptors also includes an extracellular N-terminal domain and a cytosolic C-terminal tail. The latter contains the phosphorylation sites of G-protein-coupled receptor kinases (GRKs). A second phosphorylation site for the protein kinase A (PKA) is localized on the third intracellular loop of the receptor *(77)*.

1.2.2 Agonist-induced desensitization of the βARs

The process of receptor desensitization involves several mechanisms that may be divided into acute responses (uncoupling) and chronic responses (internalization and downregulation). Intense activation of the receptor by agonists is known to promote phosphorylation of the receptor by GRK and the PKA. These two kinases phosphorylation sites are extremely important for the regulation of βARs. The β-adrenergic receptor kinase 1 (β-ARK1) also known as G-protein-coupled receptor kinase 2 (GRK2) is a serine/threonine kinase, in charge of the specific phosphorylation of G-protein-coupled receptors and is expressed in the mammalian heart *(78)*. The phosphorylation of the βAR in the C-terminal tail by β-ARK1 or GRK2 allows the binding of the cytosolic protein β-arrestin to the receptor and preventing its coupling to the G-protein therefore blunting the signal transduction. This process is known as uncoupling of the receptor. PKA also phosphorylates the receptor but it is described as heterologous desensitization since this kinase phosphorylates other proteins also and not exclusively GPCRs. Hence, the phosphorylation and subsequent desensitization of the receptor is an effective negative feedback mechanism to modulate the responsiveness of the β-adrenergic receptor-mediated signal transduction cascade. After the phosphorylation, the uncoupled receptors translocate from the sarcolemma to a vesicle fraction in a process known as internalization or sequestration. From this vesicle, fraction the receptor can be dephosphorylated and sent back to the plasma membrane *(79)* or it can be degraded. Prolonged exposure to adrenergic agonists leads to a decline in the total number of receptors by a slow process known as downregulation. This process can take several days and it involves

reduction in mRNA levels and protein levels *(80, 81)*.

1.2.3 βARs in the cardiovascular system

The β-adrenergic stimulation is one of the most important mechanisms for the modulation of cardiovascular function. The cardiac βARs population is predominantly composed by β1-adrenergic receptors (β1AR, about 70-80%) *(82)* which mediate an increase in inotropy and chronotropy upon stimulation induced by endogenous catecholamines such as adrenaline and noradrenaline *(83)*. Positive inotropic and chronotropic effects of β1AR are mediated by stimulation of G-protein G_s followed by activation of adenylate cyclase, increase production of cAMP and activation PKA. β2-adrenoceptors (β2AR) are also present but they are expressed in a smaller proportion in the myocardium (30-20%). For that reason, their physiological role has not been fully understood yet. There is evidence that they may have positive inotropic effects via stimulation of G-protein G_s but they may as well oppose β1-adrenergic stimulation by interacting with inhibitory G-protein G_i and endothelial nitric oxide synthase (eNOS) *(84, 85)*.

Regarding the vasculature, βARs are present in two different kinds of cells responsible for the control of blood pressure and vascular tone, the endothelial cells and the smooth muscle cells. Depending on the location and the type of the vessel (resistance or conductance), different distributions of the βARs have been described *(86)*. Traditionally, it was thought that β2AR was the only βAR mediating the vascular response *(69)*. Nowadays, both β1AR and β2AR have been implicated in the catecholamine-mediated vasodilatation *(87)*. The role of β1AR in vasodilation has been linked to the increase in cAMP through adenylate cyclase activity in smooth muscle cells. β2AR activation in both smooth muscle cells and endothelial cells can lead to vasodilation through NO/cGMP pathway *(88)*. Present in both vasculature and cardiac tissue, a third subtype with different characteristics completes the family of the βARs, the β3AR.

1.2.4 The β3-adrenergic receptor

1.2.4.1 Location

Cloned by Emorine et al. in 1989 *(70)*, the third subtype of the βARs family (β3AR) was initially discovered in adipocytes, where it mediates the adrenergic β-oxidation of fatty acids. For this reason, the scientific community started to study its potential as a target for obesity

(89–94). Later studies demonstrated its presence also in other tissues like gall bladder, gastrointestinal tract, prostate, urinary bladder detrusor, brain as well as in myometrium *(95, 96)*. Regarding cardiac tissue, as early as 1996, Gauthier et al. reported the expression of transcripts of β3AR in biopsies of human hearts *(97)*. Years later, researchers demonstrated the presence of β3AR protein in human atrial and ventricular cardiac myocytes, as well as in endothelial cells of the small coronary resistance vessels *(98–100)*. Although its total contribution in the heart was found to be low in physiological conditions (2-3% of the total number of βARs) *(101)*, the interesting characteristics of this receptor put it under the spotlight.

1.2.4.2 Functional structure

In humans, the gene is localized in chromosome 8. Unlike the gene encoding the other two subtypes, β3AR gene contains introns. The number of exons and introns are controversial and vary depending on the species but it is accepted that the human β3AR is formed by 408 amino acids and only one variant has been found to date *(102)*. In the case of the mouse β3AR, alternative splicing can lead to two variants with differential expression across tissues *(103)*. The homology between human and mouse sequences is around 80%, being the C-terminal tail and the third intracellular loop the sites where more differences can be found. The amino acid sequences for the human β3AR shares 51% and 46% identity with β1- and β2AR, respectively. Despite its similarities with the β1AR and β2AR, the β3AR has its own singularities that make it different (Figure 2).

One of the most interesting features of the β3AR that makes it different from the other two subtypes is that it lacks the consensus sequences for phosphorylation by PKA and GRKs. As seen before, phosphorylation by these two enzymes promotes recruitment of β–arrestin, uncoupling from G-proteins and therefore desensitization of the receptor. Lacking these phosphorylation sites makes the β3AR more resistant to the progressive loss of function by prolonged catecholamines stimulation *(104)*. However, is not the only differential feature granted by its primary structure. Because of its molecular characteristics, this subtype is less sensitive to endogenous catecholamine activation. Therefore, the β3AR is activated at higher catecholamine concentrations than β1AR and β2AR *(70)*.

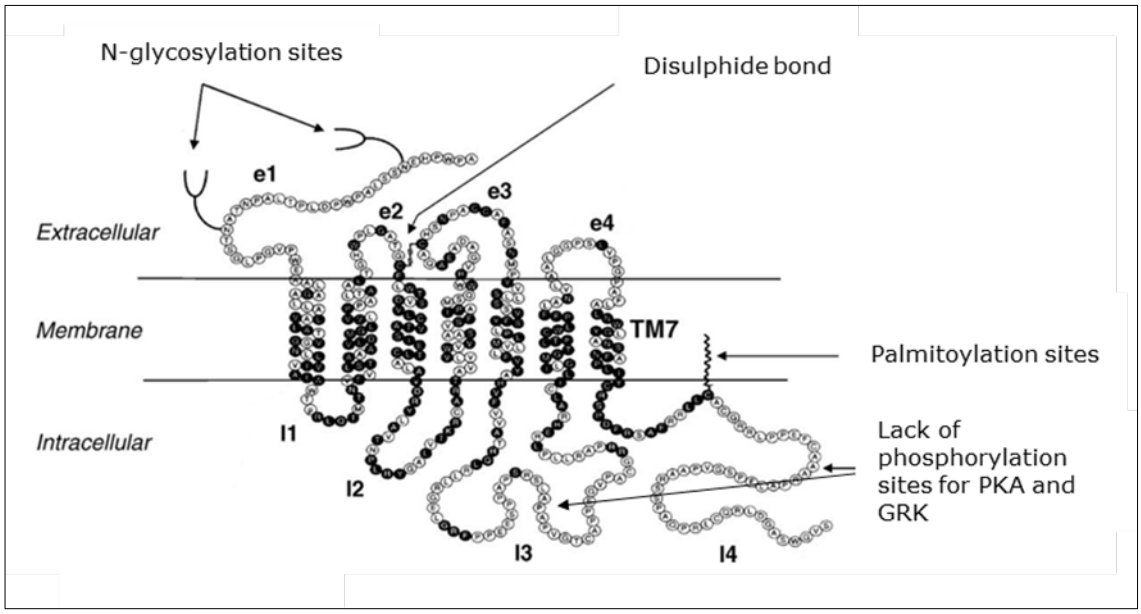

Figure 2: Primary structure of human β3AR

The dark circles represent amino acids identical in the three different βAR subtypes. e: extracellular loop; i: intracellular loop; TM: transmembrane domain. Figure adapted from Rozec et al. *(105)*

1.2.4.3 Signaling and function in the cardiovascular system

Similarly to the β2AR, the β3AR has been reported to couple with both, G_s and G_i protein. In the vasculature, depending on the vessels, β3ARs are expressed in both vascular smooth muscle cells and endothelial cells, or just in the endothelium. In smooth muscle cells, it increases cAMP levels promoting vasorelaxation through the classical cAMP/PKA pathway as observed in β1AR activation *(106)*. Stimulation of β3ARs in endothelial cells produces an endothelium-dependent relaxation through endothelial nitric oxide synthase dependent and independent mechanisms. This has been demonstrated in aortic and resistance vessels from different species *(107)* and particularly in human coronary resistance vessels *(98)*.

Concerning cardiac myocytes, a dual G_s and G_i coupling has also been reported. The β3AR coupling with G_i has been linked with increased nitric oxide production in human cardiac biopsies *(108)*. Two different isoform of the nitric oxide synthase (NOS) inside the cardiomyocyte have been implicated in the β3AR dependent NO production, the endothelial NOS (eNOS) and the neuronal NOS (nNOS). The contribution of both isoforms has been investigated in different settings and both seem to be activated through differential

phosphorylation or enhanced expression *(109–112)*. A recent report has pointed β3AR/NOS/sGC/cGMP pathway as a possible initial part of the downstream pathway of the receptor *(113)*. Some reports have also suggested that the β3AR can couple with G_s in cardiac myocytes *(114)* leading to an increase in cardiac contractility. G_s is known to activate the PKA/Akt/eNOS protective pathway suggesting a cardioprotective role of the β3AR, similarly to β2AR *(115, 116)*. Regarding the effects in contractility, ex-vivo experiments with human cardiac biopsies from transplanted hearts showed that β3AR activation leads to a negative inotropic effect. Experiments in vivo in a sheep model showed that stimulation of the β3AR resulted in a negative inotropic effect but the same experiment conducted in HF animals resulted in a positive inotropic effect suggesting a shift in the β3AR coupling under pathological conditions. Two different groups have generated a transgenic mouse with cardiac restricted expression of the human β3AR. In 2001, Kohout et al. described a positive inotropic effect performing in vivo experiments in response to a β3AR agonist in these transgenic mice *(114)*. Tavernier et al. two years later showed a negative inotropic effect ex vivo in cardiac tissue of their own transgenic mice in response to different agonists *(117)* similar to what was already observed in the human biopsies. The discrepancies in studies performed in vitro and in vivo described the complexity of β3AR pharmacology suggesting a pronounced inter-species variability and the heterogeneous pharmacological profiles of β3AR agonists in a given species and the difference between physiological and pathological conditions.

1.3 Role of the β-adrenergic receptors in heart failure

It is clear that the β-adrenergic receptors govern the cardiovascular system activity in physiological conditions. During heart failure, the ability of the heart to correctly pump the blood through the body is impaired. In the middle 80's scientists started to explore the link between the β-adrenergic system and heart failure.

1.3.1 Implication of the β-adrenergic system in heart failure

In 1985, Lefkowitz et al. demonstrated that βARs were downregulated and desensitized after exposure to agonist *(118)*. The following year, Bristow et al. published that β1AR were downregulated by 60% in failing human hearts explanted at the time of transplantation *(82)*. In light of these findings, a debate started on whether βARs

downregulation was a cardioprotective mechanism to reduce catecholamine induced damage or a pathological feature of HF. If βARs downregulation was a cause leading to cardiac dysfunction, then restoring receptors density should rescue HF. To answer this question, mice overexpressing βARs were generated. Mice with 5 to 15-fold overexpression of the β1AR developed with age in basal conditions dilated cardiomyopathy, increased fibrosis and HF at young age, similarly to a chronic catecholamine overstimulation *(119)*. Mice with 50 to 200-fold increase in β2AR expression displayed an enhanced contractility at baseline *(120)*. However, with age mice with 100-fold increase of β2AR or more developed progressive myocardial fibrosis and eventually a dilated cardiomyopathy, HF and premature death. Interestingly, the authors found that the higher the level of overexpression the faster the progression of the remodeling. Importantly, 60-folds overexpression enhanced basal cardiac contractility without detrimental consequences and the authors did not find a correlation between adenylate cyclase activation and early or delayed decompensation *(121)*. β2AR was then studied as a therapeutic approach in genetic models of HF with negative results *(122)* and high levels of the receptor (200-fold increase) was found to be deleterious in the TAC mouse model *(123)*. Nevertheless, β2AR was proven to rescue βAR signaling in myocytes from a HF rabbit model *(124)* and moderate levels of this receptor improved cardiac function and hypertrophy in the $G_{\alpha q}$ overexpression HF model *(125)*. These findings reinforced the hypothesis that excessive βAR signaling, at least from β1AR and β2AR, is ultimately detrimental to cardiac function.

1.3.2 β3-adrenergic receptor in heart failure and IR injury

Contrary to β1AR and β2AR, the β3AR was found to be upregulated in cardiac tissue from patients with HF *(100)*. As previously mentioned, β3AR is resistant to desensitization and has a lower affinity to endogenous catecholamines. These facts suggest that in HF conditions where there is a prolonged activation by the sympathetic nervous system the β3AR-mediated response is likely to be preserved contrary to β1AR and β2AR. All together, these data support the idea that the β3AR plays a dominant role in regulating beta-adrenergic function in HF.

Whether the increase in β3AR was a contributing factor of HF or a protective mechanism was a matter of intense debate. To answer this question, different animal models have been explored. Some authors suggested that the β3AR pharmacological stimulation contribute to progression of HF in dog *(126)* and that chronic blocking of the receptor improve cardiac function in a rat model of HF *(127)*. However, many others have positioned the β3AR

as a therapeutic target. Zhou et al. *(128)* showed antiarrhythmic properties in a dog model. In the mouse, animals lacking this receptor developed cardiac hypertrophy with age and more severe LV dilation, myocyte hypertrophy and enhanced fibrosis when subjected to TAC *(129)*. Following this line, the same group showed that wild-type mice were protected against TAC induced remodeling when they were treated with the β3AR agonist BRL 37344 *(130)*. The cardioprotection afforded by exercise in the pressure overload model has also been link to the β3AR *(131)*. In a rat model of pressure overload, autoantibodies against β3AR with agonist-like effects obtained from HF patients were able to protect against cardiac dysfunction *(132)*. These opposed findings could be explain by an interspecies variability in the distribution and characteristics of the β3AR and the different pharmacological profile of the β3AR agonists used.

A transgenic mouse model overexpressing the human β3AR was proposed as a tool to overcome these difficulties. This model gave the opportunity to investigate the properties of the human receptor without the pharmacological heterogeneity of the different the β3AR agonists. To this day, only the group of Prof. Balligand has explored the effects of the overexpression of the human β3AR in a mouse model under pathological conditions. Transgenic mice with cardiac restricted overexpression of the human β3AR seem to be protected against cardiac hypertrophy and fibrosis in a neurohormonal induced remodeling model using isoproterenol and angiotensin II pumps *(113)*. In a second publication, this group explored the anti-fibrotic effects of the β3AR finding a paracrine signaling from cardiac myocytes to fibroblast *(133)*. However, whether these findings result in a final improvement of cardiac function in HF models is still unknown.

Different groups have explored the role of the β3AR in IR. In a early study, a single dose of nebivolol (a β3AR agonist, β1- β2AR antagonist) before reperfusion was able to reduce IS in a IR murine model *(134)*. The authors corroborated the result using two other β3AR agonists and they pointed nNOS and eNOS as mediators of this cardioprotection. This same mechanism seems also to be responsible for the beneficial effects of exercise in IR *(135)*. Our group demonstrated that a single dose of a β3AR agonist before reperfusion was beneficial in the pig model too resulting in a decrease in IS, a better cardiac function after IR and we have implicated the delay of mPTP opening in this cardioprotective effect *(136)*. Sustained β3AR stimulation was also found to be beneficial in a mouse model of chronic ischemia by an eNOS and nNOS activation and a decrease in apoptosis *(137, 138)*. However, the contribution in this cardioprotection of the β3AR activation in the different cellular types is still not clear. Besides

the effect in the cardiomyocytes, the stimulation of β3AR in endothelial cells has shown a clear benefit in the myocardium in chronic ischemia models *(139)*. Therefore, further studies need to dissect the cellular origin of the cardioprotective effect of the β3AR in IR.

1.3.3 Clinical Trials in Cardiology with β3-adrenergic receptor agonist

All these pre-clinical data and specially the experiments performed in the sheep model of HF *(140)* led to the first pilot trial, the phase II trial BEAT-HF (NCT01876433) *(141)*, to examine the potential beneficial effect of β3AR activation in cardiac diseases. This trial was designed to examine the effect of mirabegron, a β3AR agonist, on patients with HF with reduced ejection fraction (HFrEF). Mirabegron was already approved in Europe, USA, and Japan for the treatment of the overactive bladder disease given its myorelaxant properties mediated by the activation of β3AR in the detrusor muscle *(142)*. BEAT-HF primary end point was the increase in LV ejection fraction (LVEF) monitored over 6 months. This trial ended in 2016 and surprisingly the primary end point was only reached in a non pre-specified subgroup of patients with severe LV dysfunction (LVEF < 40 %).

Currently, the phase IIb BETA3_LVH clinical trial (NCT02599480) *(143)* monitors additional parameters over a longer period of 12 months. This trial examines LV mass and diastolic function as well as fibrosis, exercise capacity, endothelial function, and various metabolic parameters of patients with cardiac structural remodeling with, or at risk of developing, HF with preserved ejection fraction (HFpEF). This multicenter, randomized, placebo-controlled study is based on the evidences of the antihypertrophic and antifibrotic effect of β3AR activation *(113, 133)* and therefore its primary endpoints are the reduction in LV mass and the improvement in diastolic function. The trial will be completed in 2020 so there are still no available results.

Finally, our lab has demonstrated that β3AR agonists can reduce pulmonary vascular resistance associated with an improved right ventricular function in a porcine model of pulmonary hypertension *(144)*. This has led to the phase II SPHERE-HF clinical trial (NCT02775539). This trial aims to evaluate the effect of mirabegron on pulmonary vascular resistance in patients with chronic pulmonary hypertension secondary to HF. This study will follow the patients for 4 months and is expected to be completed in 2019.

Preclinical studies have shown the benefits of β3AR activation in the treatment of cardiovascular diseases. The relevance of these findings has positioned the β3AR as a potential target for HF and the first results in human patients are encouraging. However, in light of the results of the BEAT-HF clinical trial it is evident that more studies are needed to elucidate the beneficial effects of treatments targeting this receptor and that we should rethink new therapeutic avenues in this regard.

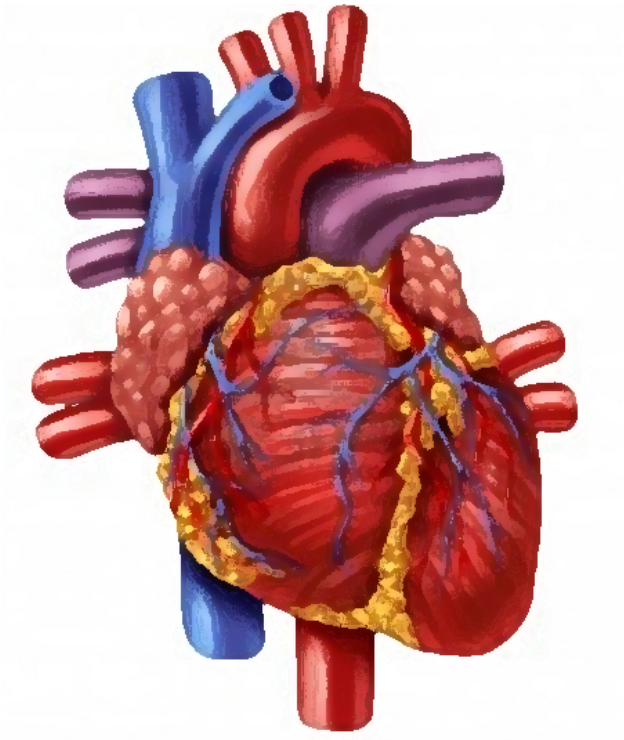

Objectives

2 OBJECTIVES

Heart failure is a devastating medical condition and nowadays acute myocardial infarction and the injury caused after the reperfusion is the main leading cause. Previous studies have reported interesting characteristics of the β3AR that could be beneficial in the treatment of cardiovascular diseases. However, the β3AR is present in different kinds of cells in the cardiac tissue and little is known about the contribution of each type of cell in the cardioprotection provided by β3AR agonists. Moreover, there are controversial results regarding the role of the β3AR in the progression of heart failure and results from recent clinical trials raise questions about the therapeutic potential of β3AR agonists in human patients. Due to the interest of our group in translational medicine, the following objectives were set for the present thesis:

1. To generate animal models with cell specific expression of the human β3AR:
    a. Transgenic mouse lines with constitutive expression of the human β3AR.
    b. Human β3AR expression by adeno-associated virus based gene therapy.

2. To define the contribution of the endothelial cells and the cardiac myocytes in the protection afforded by the stimulation of the β3AR during ischemia reperfusion injury in the myocardium.

3. To determine the role of the β3AR in the progression of heart failure in a mouse model of pressure overload.

4. To explore the therapeutic potential of the β3AR as a target for the treatment of heart failure.

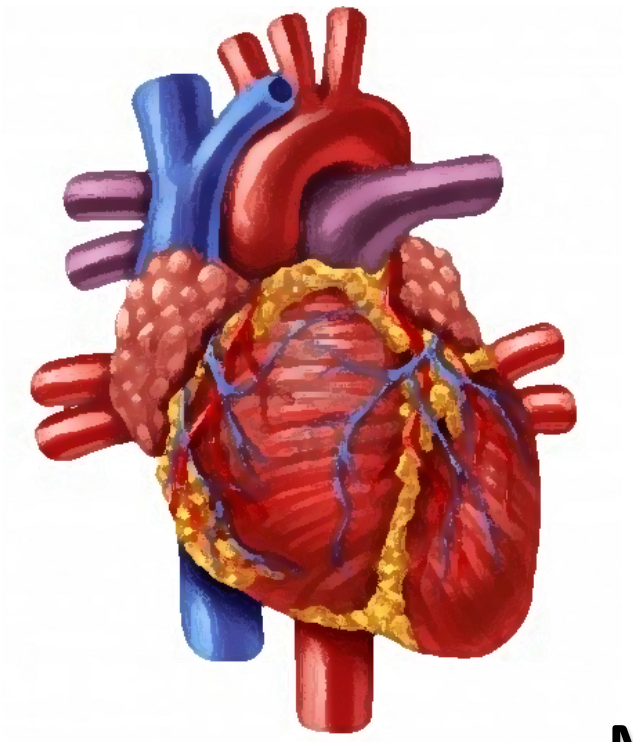

Materials And Methods

3 MATERIALS AND METHODS

3.1 Mice

All experimental and other scientific procedures with animals conformed to EU Directive 2010/63EU and Recommendation 2007/526/EC, enforced in Spanish law under Real Decreto 53/2013. Animal protocols were approved by the local ethics committees and the Animal Protection Area of the Comunidad Autónoma de Madrid. C57BL/6J wild-type (WT) mice and the following transgenic lines on a C57BL/6J genetic background were used in this thesis. All mice in this study were males.

Generation of *R26-ADRB3* transgenic mouse line

To target the human β3AR transgene (*ADRB3*) into the *R26* locus by homologous recombination into embryonic stem (ES) cells, we have generated a construct with a *PGK-Neo* cassette plus a transcriptional stop flanked by loxP elements followed by *ADRB3* cDNA and an *IRES-EGFP*. Upon Cre recombination, *R26* promoter will control the transgene expression. Complete cDNA from human *ADRB3* was obtained from clone IMAGE. The sequence was PCR amplified with Phusion High-Fidelity DNA Polymerase (NEB) and primers containing *EcoR*I sites and was cloned into the *EcoR*I site of a *pCDNA3.1-IRES-EGFP* plasmid previously generated by cloning a *Sal*I *IRES-EGFP* fragment into the *Xho*I site of *pCDNA3.1*. The resulted plasmid was digested with *Xba*I, treated with DNA Polymerase I, Large Klenow Fragment (NEB) to form blunt ends and digested with *Nhe*I to obtain a *Nhe*I-blunted *Xba*I *ADRB3-IRES-EGFP* fragment. The fragment was cloned into *Nhe*I-blunted *Not*I sites of the pBigT. We got the *Pac*I-*Asc*I-cassette containing loxP-*PGK-Neo-STOP*-loxP-*ADRB3-IRES-EGFP* by digestion and cloned it into the *Pac*I-*Asc*I sites of modified *pROSA26*-1 plasmid. The final construct was linearized with *Xho*I and electroporated into G4 ES cells derived from 129S6/SvEvTac x C57BL/6Ncr cross *(145)*. After G418 (200 μg/ml) selection for 7 days, 192 clones were picked. Homologous recombination was identified by Southern Blot of DNA digested with *EcoR*V and hybridized with 5' and 3' probes. Four clones resulted positive and we selected two to confirm karyotype. One clone was injected into B6CRL blastocyst to generate chimaeras that were analyzed for germ line transmission. This human β3AR transgenic mouse line (*ADRB3*$^{tg/tg}$) was crossbred with C57BL/6J mice to achieve a pure genetic background.

Generation of transgenic mouse lines expressing the human β3AR

Upon Cre recombination, the stop codon between the *R26* promoter and the *ADRB3*-IRES-*EGFP* sequence is removed, and the *R26* promoter drives *ADRB3* expression. Lines with Cre recombinase enzyme endothelial-specific expression (*Tie2* $^{Cre/+}$) *(146)* and cardiomyocyte-specific expression (*cTnT*$^{Cre/+}$) *(147)* kindly provided by Dr. de la Pompa laboratory at CNIC were used to drive hβ3AR expression. Thus, **e-hβ3tg** mice with endothelial-specific overexpression (*Tie2*$^{Cre/+}$*;ADRB3*$^{tg/tg}$) and **c-hβ3tg** mice with cardiomyocyte-specific overexpression (*cTnT*$^{Cre/+}$*;ADRB3*$^{tg/tg}$) of the β3AR (human β3AR expression on top of mouse endogenous β3AR expression) were generated. Their corresponding wild type (**WT**) littermates with normal levels of the murine β3AR (*Tie2*$^{+/+}$*;ADRB3*$^{tg/tg}$ and *cTnT*$^{+/+}$*;ADRB3*$^{tg/tg}$) were used as controls.

The hβ3tg lines were also crossbred with a knockout line with a targeted disruption of the murine β3AR gene (*adrb3*) *(148)*, in order to generate **e-hβ3tg mβ3KO** mice with sole expression of the β3AR in endothelial cells (*Tie2*$^{Cre/+}$*;ADRB3*$^{tg/tg}$*;adrb3*$^{-/-}$) and **c-hβ3tg mβ3KO** mice with sole expression of the β3AR in cardiomyocytes (*cTnT*$^{Cre/+}$*;ADRB3*$^{tg/tg}$*;adrb3*$^{-/-}$). Their corresponding **mβ3KO** littermates with no expression of the β3AR (*Tie2*$^{+/+}$*;ADRB3*$^{tg/tg}$*;adrb3*$^{-/-}$ and *cTnT*$^{+/+}$*;ADRB3*$^{tg/tg}$*;adrb3*$^{-/-}$) were used as controls.

3.2 Binding assay

Snap frozen hearts were crushed and200-400 mg of tissue was mixed with 50 mM Tris–HCl (pH 7.5). The samples were homogenized using an ultrasonic cell disruptor (MicrosonTM ultrasonic cell disruptor) keeping the sample on ice and they were filtered using nylon mesh. Next, the samples were centrifuged at 4ºC for 15 min at 1000 g. Protein in the resulting supernatant was quantified using the Bradford method and 2 mg of protein was incubated in duplicate for 60 min at 37 °C with different concentrations of [3H]-CGP 12177 (from 0.25 to 120 nM) (Perkin Elmer, Waltham, MA, USA) in 50 mM Tris–HCl (pH 7.5). Experiments were terminated by rapid filtration through fiberglass filters (Schleicher and Schuell, GF 52), presoaked in 0.3% polyethyleneimine, using a Brandel cell harvester (M24R). The filters were then washed three times with 4 ml of ice-cold 50 mM Tris–HCl buffer (pH 7.5), and the filter-bound radioactivity was determined by liquid scintillation counting (2480 WIZARD, PerkinElmer, Waltham, Massachusetts, USA). Nonspecific binding was measured in the presence of 1 mM propranolol (Sigma). Specific binding is defined as total binding minus nonspecific binding. The saturation data were analyzed by non-linear regression using Prism

version 4.0 (GraphPad Software; San Diego, California, U.S.A) to determine the maximum number of binding sites (Bmax) expressed as fmol/mg of protein.

3.3 Western Blot

Cells and tissue samples (0.1 mg) were lysed in RIPA buffer containing protease inhibitors (complete-Roche, Indianapolis, IN, USA) and phosphatase inhibitors (PhosSTOP-Roche, Indianapolis, IN, USA). The supernatant was separated by centrifugation at 12000g for 15 min at 4ºC, and total protein concentration was detected with the BCA protein assay kit (Thermo Fisher, USA) using bovine serum albumin (BSA) as the standard. Equal amounts of protein (15ug) were separated by SDS-PAGE and transferred to a nitrocellulose membrane using a transfer apparatus according to the manufacturer's protocol (BioRad). After incubation with 5% of nonfat milk or BSA in TBST for 60 min, membranes were incubated overnight at 4ºC with primary antibodies against GFP (1:1000; Living Colors® Full-Length GFP Polyclonal Antibody, 632592, Clontech) and GAPDH (1:10000; Abcam, ab8245). Membranes were washed 3 times for 5 min each with TBST and incubated for 1 h with HRP-conjugated anti-mouse or anti-rabbit antibodies (1:5000). Bound antibody signals were developed with the ECL (Luminata) system. Quantitative densitometry analysis was performed using Fiji (ImageJ) software.

3.4 Histology and immunofluorescence

For histology, heart specimens were fixed in 4% formaldehyde, dehydrated to xylene, and embedded in paraffin. After deparaffinization and rehydration, 5-µm sections were cut at 3 levels, mounted on glass slides, and stained with hematoxylin and eosin and with 1% Sirius red in picric acid (Sigma-Aldrich) to detect interstitial fibrosis. All sections were examined with a Nikon Eclipse Ni microscope and scanned with a NanoZoomer-RS scanner (Hammamatsu), and images were exported with NDP.view2. The percentage of fibrosis was quantified using Fiji (ImageJ) software in at least three sections per heart, and the mean was used for statistical analysis.

For immunofluorescence, hearts were fixed in 4% formaldehyde, dehydrated through 15% sucrose in PBS and then 30% sucrose overnight at 4ºC, and embedded in Tissue-Tek® OCT compound (SAKURA, Netherlands). Cryostat sections were blocked and permeabilized for 1

hour at RT in PBS containing 0.3% Triton X-100 (90002-93-1, Sigma), 5% BSA (A7906, Sigma), and 5% normal goat serum (055-000-001, Jackson InmunoResearch). Sections were then incubated overnight at 4ºC with anti-GFP (Living Colors® Full-Length GFP Polyclonal Antibody, 632592, Clontech) diluted (1:500) in PBS containing 0.3% Triton X-100 and 2.5% normal goat serum. After washes, samples were incubated for 2 hours at RT with a secondary antibody (Alexa Fluor, Invitrogen) and the nucleic acid stain Hoechst 33342 (B2261, Sigma) and were mounted in Fluoromount G imaging medium (4958-02, Affymetrix eBioscience).

For cell immunofluorescence, adult mouse ventricular myocytes (AMVM) and neonatal rat ventricular myocytes (NRVM) were fixed with 4% paraformaldehyde in PBS for 10 min. Cells were then washed 1-3 times with PBS and blocked with 2% BSA (in PBS) for 1 hour at RT. Samples were incubated overnight at 4°C with primary antibodies (anti hβ3AR; A4854 Sigma and anti α-actinin; A7811 Sigma). After 1-3 washes with PBS, cells were incubated with Alexa Fluor secondary antibodies for 1 hour at RT. Cells were then washed 1-3 times with PBS and incubated for 5 min with DAPI (1:10000 in PBS) and washed again 1-3 times with PBS. AMVMs were additionally incubated with FITC-conjugated lectin for 1 hour (L4895, Sigma) before a final wash in PBS. Stained cells were mounted in Fluoromount G imaging medium (4958-02, Affymetrix eBioscience).

3.5 Mouse left ventricular catheterization and PV loops

Ventricular catetherization was performed as previously *(149)*. Mice were anesthetized (sevoflurane 1.5%) and intubated. A skin incision was made to visualize the diaphragm, which was heat cauterized to expose the heart apex. The pericardium was removed gently with forceps. Using a 25–30 gauge needle, a stab wound was made near the heart apex into the left ventricle (LV). The catheter tip (Transonic, NY, USA) was inserted retrogradely into the LV until the proximal electrode was just inside the ventricular wall. The catheter position was adjusted to obtain rectangular shaped pressure-volume (PV) loops. After allowing the signal to stabilize for 5 min, recordings were made of baseline PV loops, heart rate, maximal derivative of LV pressure (dP/dtmax), minimal derivative of LV pressure (dP/dtmin), left ventricular end-systolic pressure (LVESP), minimal derivative of LV pressure (dP/dtmin), and time constant of isovolumic relaxation (Tau). The same parameters were recorded after the injection a single dose of mirabegron (1µg/kg) through the femoral vein. At the conclusion of the experiment, the catheter was removed by gently pulling it back through the stab wound, and the animal was euthanized.

3.6 Blood pressure measurement

Blood pressure and heart rate measurements were performed in conscious mice using the BP2000 noninvasive automated tail-cuff system (Visitech Systems). All experiments were performed in the morning to avoid variability related to circadian oscillations in the arterial pressure *(150, 151)*. Animals were trained during five consecutive days (first week) and then experimental data was collected during five consecutive days (second week). For each mouse, at least 10 measurements of arterial pressure and pulse rate were registered each day. Final measurement was preceded by 10 preliminary measurements to allow the animal to settle. Values that were equal to 0 (which arose from equipment error or animal movements) were excluded from analysis. For each day, the median was calculated for the pulse rate and systolic pressure. The mean from 5 days was used for further analysis.

3.7 Myography for ex-vivo arterial contractility

Wire myography was performed as previously described *(152)*. Briefly, thoracic aortas were obtained from 11-13-week-old mice and cleaned of fat and connective tissue. Aortas were cut into 2 mm long rings, mounted on two tungsten wires in a wire myograph system (620M, DMT) and immersed in 37ºC Krebs Henseleit Solution (KHS: 115 mM NaCl, 2.5 mM $CaCl_2$, 4.6 mM KCl, 1.2 mM KH_2PO_4, 1.2 mM $MgSO_4$, 25 mM $NaHCO_3$, 11.1 mM glucose, and 0.01 mM EDTA) with constant gassing (95% O_2 and 5% CO_2). In order to set the vessels up to their optimal distension, diameter-tension relations were determined by stepwise stretching the tissue, increasing its passive diameter by augmenting the distance between the wires. Force and distance between the wires were recorded in each step. The diameter of vessel segments was calculated from these data when the force is equivalent to 100 mmHg (L100) using the Laplace Equation (Tension=[pressure*radius]/thickness). Arterial segments were then set up at their optimal distension (0.9 of L100), which was maintained for the rest of the experiment. After stabilization for 30 minutes, arteries were exposed to 120 mM KCl to check their functional integrity. Endothelial integrity was checked by examining acetylcholine dependent vasodilation after precontraction with phenylephrine 1µM. The response to β3AR activation was analyzed by recording dose-dependent vasodilation induced by mirabegron (from 0.1nM to 1µM) in aortic rings precontracted with U46619 0.1µM. Data are presented as

the percentage of the previous precontraction (mean ± SEM). To determine the role of the nitric oxide synthase (NOS) in mirabegron-induced vasodilation, experiments were also performed in the presence of the specific NOS inhibitor L-NAME 0.1 mM.

3.8 Adeno-associated virus production and in vivo delivery

HEK293T cells were transfected using linear polyethylenimine hydrochloride with two plasmids, pDG-9 or pDG-6 and an AAV transfer plasmid where the transgene (*ADRB3* or *EGFP*) is placed between two ITRs. pDG-9 is a plasmid encoding for Rep78, Rep68, Rep52, Rep40 (required for the AAV life cycle), serotype 9 VP1, VP2, VP3 (capsid proteins) and genes from adenovirus E4, E2a and VA (mediating AAV replication) and it was used to generate AVV-9. Similarly pDG-6 encodes for the same genes except for VP1 ,VP2 and VP3 from serotype 6 and it was used to generate AVV-6. An AAV transfer plasmid encoding for *ADRB3* under the control of the troponin T promoter was used to generate recombinant AAV (rAAV) for hβ3AR cardiac-specific expression (Figure 3A). An AAV transfer plasmid encoding for *EGFP* instead of *ADRB3* was used to generate control rAAV (Figure 3B). In addition, AAV transfer plasmid contained an IRES sequences followed by the luciferase gene after the transgene sequence (*ADRB3* or *EGFP*). Luciferase activity was used as a reporter to check viral transduction in vivo.

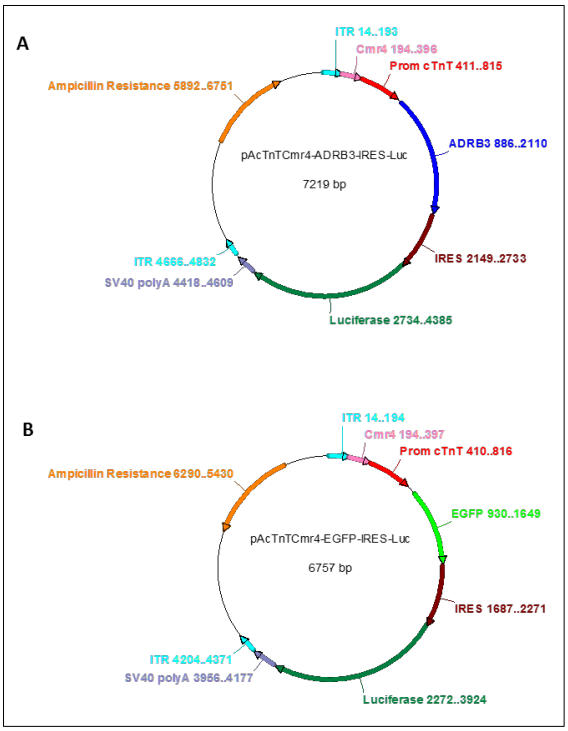

Figure 3: Scheme of the plasmids used to generate the recombinant adeno-associated virus (rAAV) (**A**) Plasmid used for hβ3AR-rAAV production (**B**) Plasmid used for control EGFP-rAAV production. ITR, recognition site for AVV packaging. Cmr4, enhancer sequence. Prom cTnT, Troponin T promoter sequence for cardiomyocyte specific expression. ADRB3, c-DNA sequence of the human β3AR receptor. EGFP, enhanced Green Fluorescent Protein sequence. IRES, Internal Ribosome Entry Site. Luciferase, firefly luciferase sequence. SV40 polyA, simian virus 40 polyadenylation signal. bp, base pairs.

Cells were harvested 3 days after transfection, lysed, frozen and thawed three times, and digested with benzonase (150 units/mL). The final supernatant containing the virus was then purified on an iodixanol gradient in an optiseal polypropylene tube (361625, Beckman Coulter). The concentrated and purified viral fraction was collected between the 40% and 60% iodixanol layers after ultracentrifugation (350,333 g, 18ºC for 1 hour).

Adult mice were anesthetized and maintained on 1–2% isoflurane. A skin incision was made on the medial face of the hindlimb, and the femoral vein was exposed. A dose of $3x10^{11}$ viral genomes (vg)/mouse in 50µl saline was injected using a 31G insulin syringe, and the skin was closed with a 6/0 silk thread. AAV-9 was used for in vivo delivery.

3.9 In vivo and ex vivo imaging system for luminescence detection

To verify correct viral transfection, 875 µg of D-luciferin (Xenogen, Alameda, CA) was administered to mice in a volume of 50 µl by intraperitoneal injection. Three minutes later, animals were anesthetized and maintained on 1–1.2% isoflurane in oxygen. Six minutes after D-luciferin administration, all mice were imaged using a Xenogen IVIS100 imaging system. Emitted photons were collected and integrated over 2 min periods. Images were processed using Xenogen Living Image software. For *ex vivo* bioluminescence imaging, animals were killed, organs were removed and quickly dipped in D-luciferin (17.5g/mL), and images were captured with a supercooled charge-coupled camera. Emitted photons were collected and integrated over 2 min periods. Results are expressed as mean luminescence intensities (photons/s/cm2/sr).

3.10 RNA extraction and cDNA preparation

Tissues were homogenized using TissueLyser (Qiagen), and total RNA was extracted with QIAzol reagent (Qiagen). The RNA pellet was dissolved in RNase-free water, and concentration was measured in a NanoDrop spectrophotometer (Wilmington). RNA (2µg) was transcribed to cDNA using the High Capacity cDNA Reverse Transcription Kit (Applied Biosystems).

3.11 PCR detection of ADRB3

cDNA (100ng) was amplified by PCR using DNA polymerase (Biotools, Spain). PCR products were separated on a 2% agarose gel containing ethidium bromide. Images were taken with a Molecular Imager® Gel Doc™ XR+ System (BioRad). Primers were designed specifically to match only the human β3AR cDNA sequence and not the mouse sequence: (Forward primer: TGCCAATTCTTGCCTTCAACC; Reverse primer: CAGGCCTAAGAAACTCCCCA).

3.12 Adult mouse ventricular myocytes isolation

The protocol for mouse adult ventricular myocyte (AMVM) isolation was performed as previously described *(136)*. Briefly, 10- to 12-week-old mice were heparinized (50 USP units) and anesthetized with a mixture of ketamine (140 mg/kg), xylazine (33 mg/kg), and atropine (9 mg/kg). Once pedal pinch reflexes were completely inhibited, animals were placed in a supine position, ventral thoracic regions were wiped with 70 % alcohol, and animals were euthanized. The heart was quickly removed, cannulated through the ascending aorta, and mounted on a modified Langendorff perfusion apparatus. The heart was then retrogradely perfused (3 mL/min) for 5 min at room temperature (RT) with pre-filtered Ca^{2+}-free Perfusion-Buffer [NaCl (113 mmol/L); KCl (4.7 mmol/L); KH_2PO_4 (0.6 mmol/L); Na_2HPO_4 (0.6 mmol/L); $MgSO_4$-$7H_2O$ (1.2 mmol/L); $NaHCO_3$ (12 mmol/L); $KHCO_3$ (10 mmol/L); Phenol Red (0.032 mmol/L); HEPES-Na salt (0.922 mmol/L); taurine (30 mmol/L); glucose (5.5 mmol/L); 2,3-butanedione-monoxime (10 mmol/L), pH 7.4]. Enzymatic digestion was performed with digestion-buffer [perfusion-buffer with Liberase™ (0.2 mg/mL), Trypsin 2.5% (5.5 mmol/L); DNase ($5x10^{-3}$ U/mL) and $CaCl_2$ (12.5 µmol/L)] for 20 min at 37ºC. At the end of enzymatic digestion, both ventricles were isolated and gently disaggregated in 5 mL of Digestion Buffer. The resulting cell suspension was filtered through a 100µm sterile mesh (SEFAR-Nitex) and transferred for enzymatic inactivation to a tube with 10 mL of stopping-buffer-1 [perfusion-buffer supplemented with fetal bovine serum (FBS, 10 % v/v) and CaCl2 (12.5 µmol/L)]. After gravity sedimentation for 20 min, cardiomyocytes were resuspended in stopping buffer-2 containing lower FBS (5 % v/v) for another 20 min. Cardiomyocyte Ca^{2+}-reintroduction was performed in stopping-buffer-2 with five progressively increased CaCl2 concentrations (62 µmol/L, 112 µmol/L, 212 µmol/L, 500 µmol/L and 1 mmol/L). Cells were resuspended and allowed to decant for 10 min in each step, contributing to the purification of the cardiomyocyte

suspension. The homogeneous suspension of rod-shaped cardiomyocytes was then resuspended in M199 supplemented with Earle's salts and L-glutamine, penicillin–streptomycin (1 %), 0.1x insulin–transferin–selenium-A, bovine serum albumin (BSA, 2 g/L), blebbistatin (25 µmol/L) and FBS (5 %). Cells were plated in single drops onto 22-mm2 glass coverslips precoated with 200 µL of mouse laminin (10 mg/mL) in phosphate-buffered saline (PBS) for 1 h.

3.13 cGMP quantification

cGMP levels of ether-extracted samples were measured by EIA according to kit manufacturer protocol using Cayman Chemical kit.

3.14 Mouse model of myocardial IR injury

The protocol for the mouse model of myocardial IR injury was performed as previously described *(136)*. Male 8- to 12-week-old mice were subjected to 45 min of left anterior descending (LAD) coronary artery occlusion followed by reperfusion. For IS evaluation, reperfusion was maintained for 24 h. For the LAD procedure, mice were intra-peritoneal anesthetized with ketamine (60 mg/ kg), xylacine (20 mg/kg), and atropine (9 mg/kg). Once deeply asleep, and under direct visualization of the trachea, animals were orally intubated using a blunted 22G cannula and mechanically ventilated throughout the entire procedure (SAR-830. CWE Inc.). Temperature was controlled (BAT-12, Physitemp Instruments) and kept constant at 37ºC with a heated operating table (V500VStat, Peco Services) to prevent hypothermic cardioprotection. A nylon 8/0 monofilament suture was passed beneath the LAD approximately 2 mm below the tip of the left atrium appendage. After stabilization for 5 min, regional ischemia was induced by tightening a simple snare to stop coronary blood flow. A short segment of PE-10 tubing was placed between the tissue and the suture to minimize damage and allow for complete reperfusion after the ischemic period. Successful LAD occlusion was confirmed by ST-segment elevation on ECG (MP36R, Biopac Systems Inc.) and the appearance of myocardial pallor. During ischemia, the thorax was covered with parafilm to prevent dehydration. Anesthetic mixture was injected intra-peritoneally when needed. Five minutes before the onset of reperfusion, mice were randomized to receive a single bolus injection (50 µl, with an insulin syringe) of the B3AR agonist Mirabegron (1 µg/kg) or saline into

the femoral vein. The thorax was closed with a 6/0 silk thread, and animals were recovered with 100 % O2 and analgesized with buprenorphine (S.C., 0.1 mg/kg) until the end of the procedure.

3.15 Mouse infarct size quantification

The protocol for mouse infarct size quantification was performed as previously described *(136)*. Mice reperfused for 24 h were briefly re-anesthetized at the end of the reperfusion period, and were then intubated and the LAD re-occluded by ligating the suture in the same position as the original infarction. Animals were then killed and 1 mL of 1 % (w/v) Evans Blue dye infused i.v. to delineate the Area at Risk. The heart was then excised, the LV was isolated and cut into seven 1-mm-thick transverse slices, and pictures were taken from both sides. In order to differentiate infarcted from viable tissue, slices were incubated in triphenyltetrazolium chloride (TTC, 1 % (w/v) diluted in PBS) at 37ºC for 15 min. The slices were then re-photographed and weighed. Regions negative for Evans Blue staining (AAR) and negative for TTC (infarcted myocardium) were calculated by a blinded observer using the computer-assisted planimetry function in ImageJ 6.0 (NIH, Bethesda, MD). IS for each slice was calculated as the average percentage of infarcted myocardium from both sides of each section. Total weight in mg of AAR and IS for each slice was calculated using the individual weight of each slice. Finally, absolute IS was determined as the ratio Σmg of IS/Σmg of AAR. This methodology takes into account individual AAR variability.

3.16 Hypoxia/reoxygenation in adult mouse ventricular myocytes

The protocol for hypoxia/reoxygenation in AMCM was performed as previously described *(136)*. Prior to being subjected to induced hypoxia/reoxygenation, plated isolated adult mouse cardiomyocytes were washed and stabilized for 30 min at 37ºC with normoxic-buffer (NB) [NaCl (113 mmol/L); KCl (4.7 mmol/L); KH_2PO_4 (0.6 mmol/L); Na_2HPO_4 (0.6 mmol/L); $MgSO_4 \cdot 7H_2O$ (1.2 mmol/L); $NaHCO_3$ (12 mmol/L); $KHCO_3$ (10 mmol/L); HEPES-Na Salt (0.922 mmol/L); Glucose (10 mmol/L); $CaCl_2$ (1 mmol/L) and pH 7.4]. Hoechst 33342 (H42, 1 µg/mL) was added for cell recognition, and propidium iodide (PI, 1 µg/mL) was added to evaluate cell viability. Simulated ischemia was induced at 1 % O2 by placing cells in a H35 Hypoxystation chamber (Don Whitley Scientific Limited, UK) in ischemic-buffer (IB), in which

glucose and HEPES were replaced with lactate-Na (10 mmol/L) and PIPES (10 mmol/L), at pH 6.8 for 30 min (IB was preequilibrated at 1 % O2 for 1 h prior to use). After the hypoxia incubation, NB with Mirabegron (1µM) was added on top of IB at a proportion of 1IB:4NB for 1 h to simulate reperfusion. Fluorescent images were acquired with a Nikon Time-lapse microscope after 15, 30, 45 and 60 min of reoxygenation. An average of 350 rod-shaped cells/well observed from 4 wells per condition in 4 independent experiments were analyzed by a blinded using ImageJ 6.0 (NIH, Bethesda, MD, USA). Cell death, indicated by internalization of red fluorescence (Red, PI positive) was expressed as relative cell death compared to the percentage PI positive cell of the total number of cardiomyocytes (Blue, H42 positive) in the wells with cardiomyocytes from mβ3KO mice at 15min.

3.17 Neonatal rat ventricular myocytes isolation

The protocol for hypoxia/reoxygenation in neonatal rat ventricular myocytes (NRVMs) was performed as previously described *(153)*. Ventricular cardiomyocytes were isolated from 1- to 2-day-old neonatal rat hearts. Hearts were prewashed in ADS buffer (116 mM NaCl, 20 mM HEPES, 0.8 mM Na_2HPO_4, 5.6 mM glucose, 7 mM KCl, and 0.8 mM $MgSO_4 \cdot 7H_2O$; pH 7.35) to remove blood and then placed in dishes containing 7 mL ADS. Hearts were then minced into small pieces with sterile razor blades, and the tissue suspensions were then transferred to flasks containing 7 mL of enzyme solution (ADS containing 0.6 mg /mL pancreatin, 8820 U /L collagenase II, and 50 mM $CaCl_2$) and incubated for 10 min at 37 °C. The supernatant from this predigestion step was discarded, and the tissue pieces were incubated in 15 mL of digestion solution for 15-min periods at 37 °C. At the end of each incubation period, the supernatant was collected in 50 mL conical tubes containing 19 mL F-10 medium and 20% FBS preheated to 37 °C. Three-six fractions were collected and centrifuged at 1400*g* for 10 min, the supernatant was discarded, and cells in each tube were washed with 5 mL FBS. The cells were then centrifuged at 1400*g* for 10 min, and the supernatant was discarded. The resulting pellet containing NRVMs was resuspendend in HAM's F10 complete medium supplemented with 10% horse serum (HS), 5% FBS, and 1% P/S, pH 7.4. The cell suspension was filtered through a 70 µm filter and preplated for 2 h on a Nunc Nunclon 100 mm cell culture dish (Thermo Fisher Scientific, Waltham, MA, USA) to separate fibroblasts from the myocyte fraction. The supernatant, containing mostly myocytes, was collected and plated on culture dishes in Hams F-10 complete medium. The fibroblasts attached to the Nunclon dishes were cultured in DMEM containing 1% P/S. Cells were maintained in medium without HS and

supplemented only with 10% FBS and 1% P/S. Experimental treatments and controls were conducted in serum-free medium.

3.18 Neonatal rat ventricular myocytes transfection

Recombinant AAV6 were generated encoding the hβ3AR gene under the control of a truncated chicken cardiac troponin-T (cTnT) promoter and strengthened by the Cmr4 enhancer. The luciferase reporter gene placed after the hβ3AR gene was used to confirm expression and track transduced cells. The β3AR and luciferase genes were separated by an IRES sequence to prevent formation of a fusion protein that could alter β3AR function. A polyA sequence was added at the end to confer mRNA stability. The gene construct was flanked by ITR sequences for AAV machinery recognition. NRVMs were isolated and cultured for 24h before being transfected with recombinant AAV-6 at the MOI indicated in each figure. A 10 K MOI was used in NRVM hypertrophy and chronotropy experiments. Transfections were performed in free-serum medium for 12 h, Ham's F-10 complete medium was added, and transgene expression was allowed for 72h before experiments.

The efficiency of AAV6 transduction of NRVMs was checked at 48 h and 72 h by monitoring luciferase activity in cells transduced with the AAV6-EGFP control virus. Luciferase reporter luminescence identified a 10K MOI as the appropriate dose for subsequent experiments.

3.19 Neonatal rat ventricular myocytes luciferase assay

NRVMs ($2x10^5$ cells per well in a 24-well multi-well dish) were transduced with AAV-6 containing the luciferase gene. NRVMs were washed three times with ice cold PBS and collected in passive lysis buffer (Promega, Madison, WI, USA). Luciferase activity was measured with a luciferase assay system kit (Promega) and a plate reader (Infinite M1000 PRO-TECAN).

3.20 Neonatal rat ventricular myocytes hypertrophy

The protocol for NRVMs hypertrophy was performed as previously described *(153)*. After isolation, NRVMs (~3 × 10^5 cells per well) were plated in a six-well multi-well dish,

transfected for 72 h with AAV6, and stimulated as indicated in each figure. NRVMs were then fixed in 3% PFA for 10 min, washed three times with ice cold PBS, and permeabilized with 0.2% Triton X-100. The cells were then incubated with 1% BSA for 30 min and incubated overnight at 4 °C with anti-α-sarcomeric actinin (α-SMA, A7811, Sigma-Aldrich) diluted 1:200 in 1% BSA. After washes, cells were incubated with FITC-conjugated secondary antibody anti-mouse (Sigma-Aldrich; 1:200). Cells were examined with a Nikon Eclipse Ni microscope, and images were acquired with a Nikon digital camera. For each sample, five to six fields (~50 cells per field) were acquired.

3.21 Neonatal rat ventricular myocytes beating rate

Neonatal rat ventricular myocytes (NRVM) plated in 6 well plates and transduced with AAV6 were recorded for 15 seconds/well using a Nikon Time-lapse microscope. Videos were recorded in 10 different positions of 6 independent wells per condition immediately after isoproterenol (10µM) addition and 3, 4 and 5 days later in the presence or absence of L-NAME (100µmol/L).

3.22 Mouse model of Transaortic Constriction

Male 8- to 12-week-old mice were intraperitoneally anesthetized with ketamine (60 mg/ kg), xylacine (20 mg/kg), and atropine (9 mg/kg). Once deeply asleep, animals were orally intubated under direct tracheal visualization using a blunted 22G cannula, and mechanical ventilation was maintained throughout the procedure (SAR-830. CWE Inc).

Partial thoracotomy to the second rib was performed under a surgical microscope, and the sternum was retracted with a chest retractor. Fine tip 45° angled forceps were used to gently separate the thymus and fat tissue from the aortic arch. After identification of the transverse aorta, a small piece of a 7.0 prolene suture was placed between the brachiocephalic and left carotid arteries. Two loose knots were tied around the transverse aorta, and a small piece of a blunt 27 gauge needle was placed parallel to the transverse aorta. The knots were quickly tied against the needle, and the needle was removed, leaving 0.36mm diameter constriction. In sham-operated control mice, the entire procedure was identical except that the aortic ligation of the aorta was omitted. The chest retractor was removed, and the ventilator outflow was pinched off for 2 seconds to re-inflate the lungs. The rib cage was

closed with a 6.0 silk suture using an interrupted suture pattern. The skin was closed with a 6.0 silk suture using a continuous suture pattern. Animals were allowed to recover in a warmed cage with a 98% oxygen supply.

3.23 Echocardiographic analysis

Echocardiographic evaluations of mice were performed by an experienced observer blinded to the study at baseline and at 1, 3, 4, 5, 8, 10, and 12 weeks post-TAC, depending on the experiment. Mice were lightly anesthetized with 0.5-2% isoflurane in oxygen, administered via a nose cone and isoflurane delivery adjusted to maintain a heart rate of 450±50 bpm. Anesthetized mice were placed in a supine position on a heated platform, and warmed ultrasound gel was used to maintain normothermia. Mice were examined with a 30-MHz transthoracic echocardiography probe and a Vevo 2100 ultrasound system (VisualSonics, Toronto, Canada). A base-apex electrocardiogram (ECG) was continuously monitored through 4 leads placed on the platform and connected to the ultrasound machine. Images were transferred to a computer and were analyzed off-line using the Vevo 2100 Workstation software. For the assessment of LV systolic function, standard 2D parasternal long axis views were acquired at a frame rate > 230 frames/sec. End-systolic and end-diastolic LV volumes (LVESV and LVEDV) and LV ejection fraction (LVEF) were calculated using the area-length method. LV mass was calculated from short-axis M-mode views using end-diastolic left ventricular wall thickness.

3.24 Lung water content

Lungs were first weighed and then dried for 7 days in a 60ºC oven. The mass of the dry lung was then measured, and water content was calculated as the difference in mass between the dry and wet lung, expressed as a percentage.

3.25 Positron Emission Tomography – Computed Tomography

All PET-CT studies were performed with a small-animal PET-CT device as previously described *(154)*. Briefly, animals were fasted overnight, and anatomic thorax CT scans were performed 1 hour after [^{18}F]FDG injections, followed by metabolic PET static acquisition for 15

min. Prefused and prereconstructed images were analyzed with Osirix (Aycam Medical Systems, LLC); we selected myocardium of the whole heart and calculated the mean myocardial standardized uptake value (SUV med) for each animal.

3.26 Transmission Electron Microscopy

The protocol for transmission electron microscopy (TEM) was performed as previously described *(155)*. Immediately after excision, LV samples were fixed in 4% formahaldehyde: 1% glutaraldehyde in cacodylate buffer, and postfixed in 1% osmium tetroxide. Tissues were then washed in PBS, dehydrated through graded alcohols followed by acetone, and then infiltrated with Durcupan ACM Fluka resin and polymerized at 60 ºC for 48h. Blocks were cut with a Leica ultracut UCT ultramicrotome (Leica, Heerbrugg, Switzerland), and sections (60–70 nm) were mounted onto 200-mesh grids. Sections were stained with a 2% solution of aqueous uranyl acetate for 10 min, followed by lead citrate staining for 10 min. Stained sections were viewed with a JEOL JEM-1010 transmission electron microscope (Tokyo, Japan) operating at 80 kV through 6000×, 10,000×, and 40,000× objectives. Images were acquired with a GATAN Orius 200SC digital camera. Mitochondrial morphometry was analyzed using ImageJ (National Institutes of Health).

3.27 Seahorse

The bioenergetic response of AMVM was measured with the Seahorse Bioscience XF96 Flux Analyzer, as previously described *(154)*. For glucose and palmitate tolerance experiments, cells were preincubated for 30 minutes in 160uL unbuffered DMEM supplemented with 4 mM glutamine, 1 mM pyruvate, 5 mM glucose, 0.1 mM pyruvate, 0.5 mM L-carnitine, and BSA (0.17mM)-conjugated palmitate (0.4mM) for 30 min. The XF96 automated protocol consisted of a 10 min delay after microplate insertion, baseline OCR/ECAR measurements [3x (3 min mix, 3min measure)], followed by injection of port A (20uL) containing the β3AR agonist BRL37344 (1µM), and OCR/ECAR measurement [3x (3 min mix, 3min measure)]. PortB, PortC, and Port D were injected and measured similarly to Port A. Final concentrations of glucose (10, 20, and 40 mM) were adapted to the final volume increase: 200uL after Port B injection, 220uL after Port C, and 240 after Port D. Final concentrations for palmitate characterization were 0.03mM after Port B, 0.3mM after Port C, and 3mM after Port D. All values were first normalized to protein

content in each well and then normalized to baseline values in order to compare 8 independent experiments.

3.28 Statistics

Experimental data are presented as mean ± standard error of the mean (SEM) and were analyzed with Prism software (Graph pad, Inc.). For normally distributed variables, comparisons between two groups were made by unpaired two-tailed Student t-test; for nonnormally distributed variables, the nonparametric Wilcoxon-Mann–Whitney test was used. Comparisons between more than two groups were made by two-way ANOVA with Tuckey's post hoc test. Comparisons between more than two groups in response to increasing drug dose, substrate concentration, or time exposure were made by two-way ANOVA with Sidak's multiple comparisons test. Power calculations were used to obtain statistical significance at p-values below 0.05; * $p<0.05$, ** $p<0.01$, *** $p<0.001$, **** $p<0.0001$.

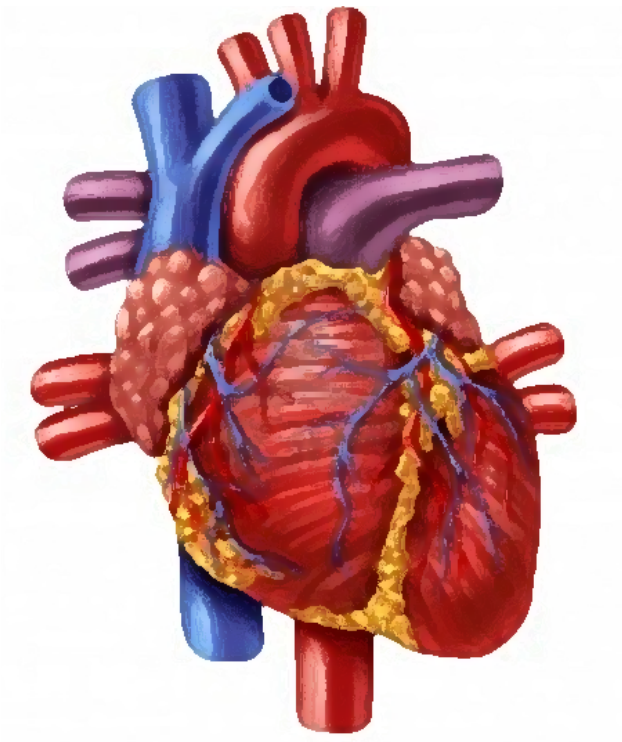

Results

4 Results

4.1 Generation of a transgenic mouse model expressing the human β3-adrenergic receptor

4.1.1 Generation of a mouse model with constitutive expression of the human β3-adrenergic receptor

Two different groups have generated transgenic mice with cardiac constitutive expression of the human β3AR (hβ3AR) with contradictory results regarding the function of this receptor. Kohout et al. proved an enhancement of cardiac contractility in vivo mediated by the hβ3AR *(114)*. Tavernier et al. reported a negative inotropic effect of this receptor in ex vivo experiments using cardiac tissue from these transgenic mice *(117)*. Both groups used the myosin heavy chain (MHC) promoter to control the expression of the transgene and to ensure a cardiac specific expression. Differences in these results may be due to differences in the models used, in vivo vs ex vivo. For this thesis, we have generated our own transgenic animals. The hβ3AR gene followed by an EGFP reporter gene was introduced in the *ROSA26* locus. A stop codon flanked by LoxP sequences was placed between the *ROSA26* promoter and the transgene silencing the transgene. The expression of the transgene is only possible when a Cre enzyme is present and deletes the stop codon by recombination of the LoxP sequences. Therefore, this genetic construction is very versatile since different mouse lines with tissue specific expression of the Cre enzyme are available. This allows the expression the hβ3AR specifically in different tissue by crossbreeding the hβ3AR transgenic line with tissue specific Cre lines.

4.1.1.1 Generation of a mouse model with constitutive expression of the human β3-adrenergic receptor in cardiomyocytes

Mice with cardiomyocyte specific expression of the hβ3AR (c-hβ3tg) were achieved by crossbreeding the hβ3AR transgenic mouse line (*ADRB3*$^{tg/tg}$) with a mouse with Cre expression under the control of the Troponin T promoter (*cTnT*$^{Cre/+}$). The myocardial-specific *cTnT-Cre* line is active from day 8.0 of embryonic development onwards *(147)*. We first evaluate the expression of the transgene in embryos (Fig. 4A) observing a clear expression of the EGFP reporter gene in the heart of fresh embryos using confocal microscopy imaging. Expression of EGFP in myocytes of adult animals was observed by immunoblot analysis of isolated cardiac myocytes (Fig. 4B) and by immunostaining analysis in cardiac tissue (Fig. 4C). The presence of the hβ3AR protein in the heart of adult animals was proved by binding assays using the radioactive ligand [^{3}H]CGP12177 *(156, 157)*. This ligand binds

to βARs with higher affinity for β1AR, then β2AR and finally β3AR. Using high concentrations of the radioligand, we obtained saturation data that were used to we determine the maximum number of binding sites (B_{max}) indicative in this experiment of the amount of β3AR receptor present in the cardiac tissue. Transgenic animals as expected had an increased number of β3ARs in the cardiac tissue.

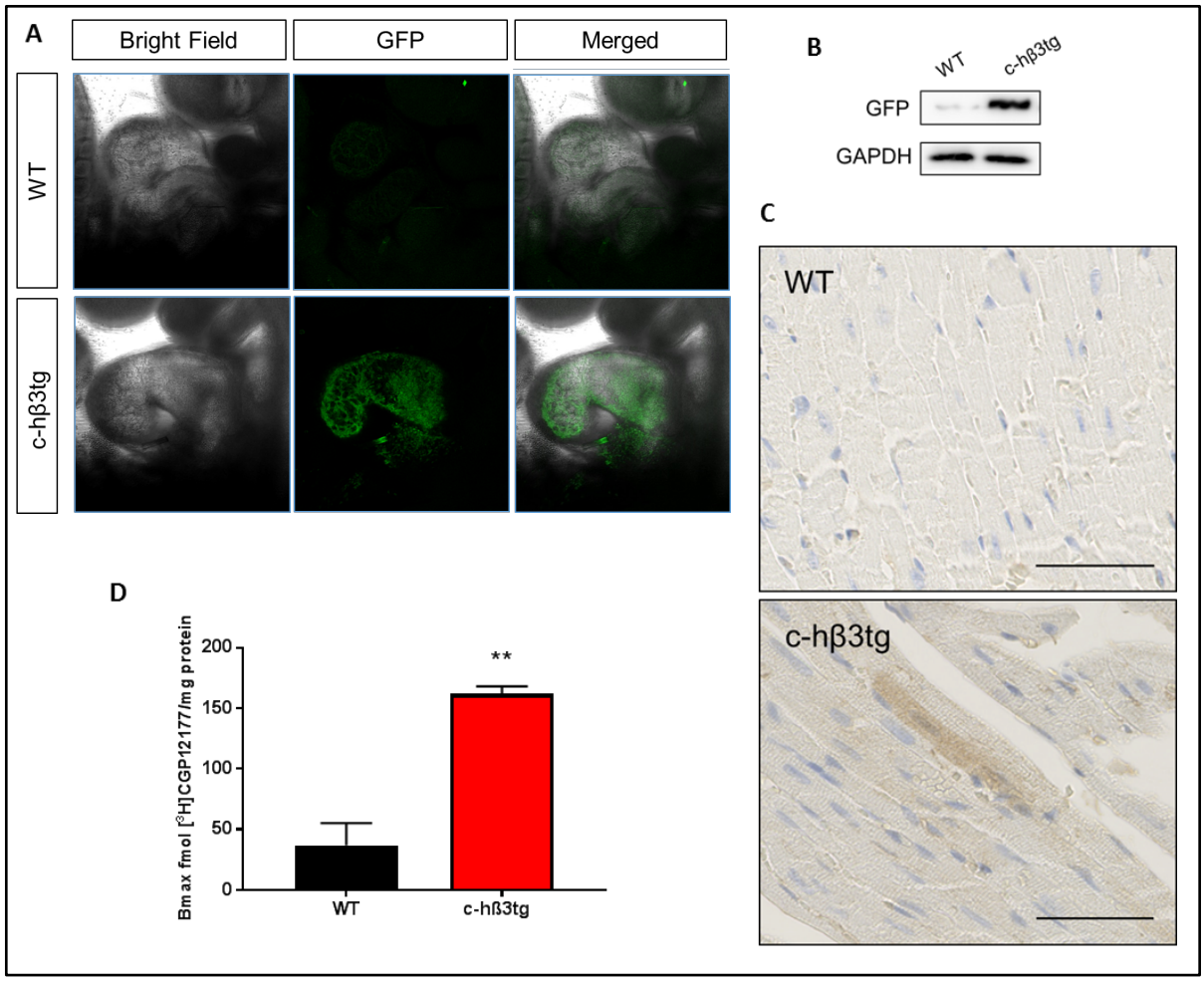

Figure 4: Transgenic mice with cardiac specific expression of the human β3AR efficiently express the *ADRB3-EGFP* transgene in cardiac tissue

(**A**) Confocal microscopy images of embryos at 9.5 days from $cTnT^{+/+};ADRB3^{tg/tg}$ (WT) and $cTnT^{Cre/+};ADRB3^{tg/tg}$ (c-hβ3tg) mice showing the presence of GFP signal restricted to cardiac tissue during embryonic development. (**B**) GFP is also present in cardiomyocytes of adult c-hβ3tg mice. Immunoblot analysis for GFP in isolated cardiac myocytes from adult mice. (**C**) Immunostaining analysis for GFP in cardiac tissue. Scale bar, 50µm. (**D**) The levels β3AR protein are increased in c-hβ3tg mice. Radioligand binding assays were performed on membranes prepared from c-hβ3tg (red, n=3) and WT (black, n=3) hearts and incubated with [^{3}H]CGP12177. The concentration corresponding to the maximum binding (B_{max}) normalized by total protein loaded was determined for a high range of [^{3}H]CGP12177 concentrations characteristic of β3AR binding. Data are means ± SEM. t test, **P=0.003.

In order to determine whether the receptor was functional or not, we performed in vivo studies of the LV function of these animals using an invasive Millar catheter. To elucidate the role of the β3ARs in cardiomyocytes without β3AR vascular response that could influence the results, we crossbreed the c-hβ3tg mice with mice lacking the β3AR (mβ3KO). The resulting mice (c-hβ3tg mβ3KO) had a cardiomyocyte-restricted expression of the β3AR with no β3AR expression in any other cell of the body. We measured the LV function in basal condition and after IV injection (through the femoral vein) of a single dose of mirabegron, a β3AR specific agonist, at 1µg/kg. No differences in basal condition were observed between transgenic and control mice however, after administration of mirabegron c-hβ3tg mβ3KO mice showed a positive chronotropic and inotropic response. Increased in heart rate (Fig. 5A) was accompanied by an increase in contractility. Enhanced systolic function was determined by an increase in left ventricular systolic pressure (Fig. 5C-D) and an increase in dP/dt_{max} (Fig. 5B). Improvement in diastolic function was determined by an increase in $-dP/dt_{min}$ (Fig. 5E-F) and a decrease in the time constant of isovolumic relaxation Tau (Fig. 5G). Pressure-volume relation revealed a shift upwards and to the left after mirabegron injection in c-hβ3tg mβ3KO mice indicating an increase in LV pressure and smaller LV end-systolic volumes characteristic of an increase in contractility. Mirabegron had no effect in mβ3KO control animals.

Altogether, these data demonstrate that the recombination strategy by LoxP-Cre system using a *cTnT-Cre* line successfully generates transgenic mice that express the human β3AR protein in cardiac myocytes in an efficient manner. Despite being a human protein, this receptor is also functional in the mouse cardiac myocytes since it generates a response in cardiac contractility. This means that the protein undergoes the correct posttranslational modifications and processing necessary for membrane insertion and coupling with other molecules to generate an intracellular response. In addition, these functional experiments shed light on the role of the cardiac β3AR. Given that β3AR is only express in the cardiomyocytes of these animals and that mirabegron has no effect in mβ3KO mice, we can conclude that the response that we have observed is exclusively due to the activation of the β3AR in cardiomyocytes. This excludes the possibility that the observed hemodynamic effects were secondary to an unspecific effect of mirabegron on another βAR subtype or on other β3ARs in a different location. The obtained results unequivocally demonstrate an increase in contractility in the cardiac myocytes mediated by the β3AR leading to a positive chronotropic an inotropic effect in these mice. Whether these results can be extrapolated to other species or other conditions has to be carefully considered.

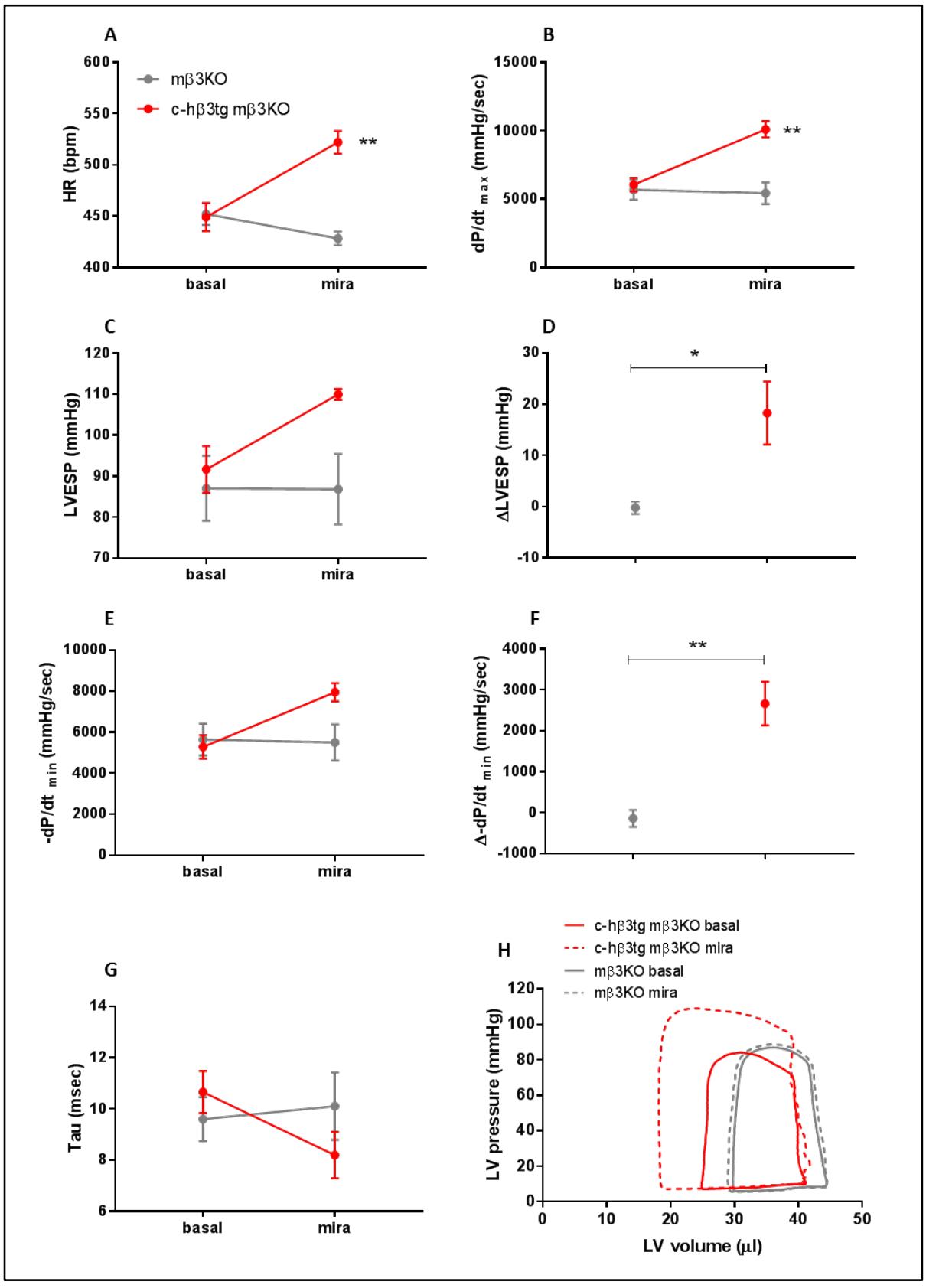
A
mβ3KO
c-hβ3tg mβ3KO
HR (bpm)
600
550
500
450
400
basal
mira
**
B
dP/dt max (mmHg/sec)
15000
10000
5000
0
basal
mira
**
C
LVESP (mmHg)
120
110
100
90
80
70
basal
mira
D
ΔLVESP (mmHg)
30
20
10
0
-10
*
E
-dP/dt min (mmHg/sec)
10000
8000
6000
4000
2000
0
basal
mira
F
Δ-dP/dt min (mmHg/sec)
4000
3000
2000
1000
0
-1000
**
G
Tau (msec)
14
12
10
8
6
basal
mira
H
c-hβ3tg mβ3KO basal
c-hβ3tg mβ3KO mira
mβ3KO basal
mβ3KO mira
LV pressure (mmHg)
120
100
80
60
40
20
0
0
10
20
30
40
50
LV volume (µl)

Figure 5: The human beta3-adrenergic receptor in cardiomyocytes of c-hβ3tg mice is functional and its stimulation generates a positive inotropic and chronotropic effect

In vivo assessment of LV function in c-hβ3tg mβ3KO mice (red, n=3) and mβ3KO control littermates mice (grey, n=3) in basal conditions and in response to the β3AR agonist mirabegron (1µg/kg). (**A**) Increase in the chronotropic response was observed in the effect on heart rate (HR). (**B**) Increase in systolic function was observed in the maximal derivative of LV pressure (dP/dt_{max}) and (**C**, **D**) the left ventricular end systolic pressure (LVESP). (**E**, **F**) An increase in the diastolic function was observed in the minimal derivative of LV pressure (dP/dt_{min}) and (**G**) the time constant of isovolumic relaxation (Tau). (**H**) Representative pressure–volume loops show that in transgenic mice the loop is shifted upward and to the left after mirabegron administration indicating enhanced contractility. Data are means ± SEM. Two-way ANOVA, **P<0.01 and t test (for increase plots), *P<0.05, **P<0.01.

4.1.1.2 Generation of a mouse model with constitutive expression of the human β3-adrenergic receptor in endothelial cells

Mice with endothelial specific expression of the hβ3AR (e-hβ3tg) were achieved by crossbreeding the hβ3AR transgenic mouse line (*ADRB3*$^{tg/tg}$) with a mouse with Cre expression under the control of the Tie2 promoter (*Tie2*$^{Cre/+}$). The endothelial-specific *Tie2-Cre* line is active from day 7.5 of embryonic development onwards in vascular endothelium and endocardium *(146)*. We first evaluate the expression of the transgene in embryos (Fig. 6A). A clear expression of the EGFP reporter gene in the vasculature of fresh embryos was observed using confocal microscopy imaging. In adult mice, the presence of EGFP in the heart and lungs was observed by immunoblot analysis (Fig. 6B). Immunostaining analysis in aortas confirmed that the transgene was expressed exclusively in endothelial cells (Fig. 6C).

We then explored the consequences of the expression of hβ3AR in the phenotype of these transgenic animals. To better dissect the function of the β3AR in endothelial cells, we crossbred the e-hβ3tg mice with mice lacking the β3AR (mβ3KO). The resulting mice (e-hβ3tg mβ3KO) had an endothelial-restricted expression of the β3AR with no β3AR expression in any other cell of the body. We first examined the systolic arterial pressure and pulse in conscious mice under basal conditions using a noninvasive automated tail-cuff system (Fig. 7A). No differences were found between e-hβ3tg mβ3KO and mβ3KO mice indicating that systolic arterial pressure and pulse was not altered by the expression of the hβ3AR in endothelial cells. To assess the effect of the stimulation of the β3AR in endothelial cells, we performed ex vivo experiments with aortic rings from e-hβ3tg mβ3KO mice and mβ3KO mice as controls. Using a wire myograph system, we observed that after induced contraction with U46619, aortic rings from transgenic mice showed a vasodilator response to increasing doses of the β3AR specific agonist mirabegron while mβ3KO rings showed a marginal effect. Vasodilation properties of β3AR agonists have been linked to the increase in NO production

(158). We further investigated the mechanisms implicated in the vasodilation response due to β3AR stimulation incubating the aortic rings with the NOS inhibitor L-NAME. We found that the relaxation provided by mirabegron was abolished when NOS was inhibited suggesting a coupling of the hβ3AR with NOS in the endothelial cells of the e-hβ3tg mice (Fig. 7B).

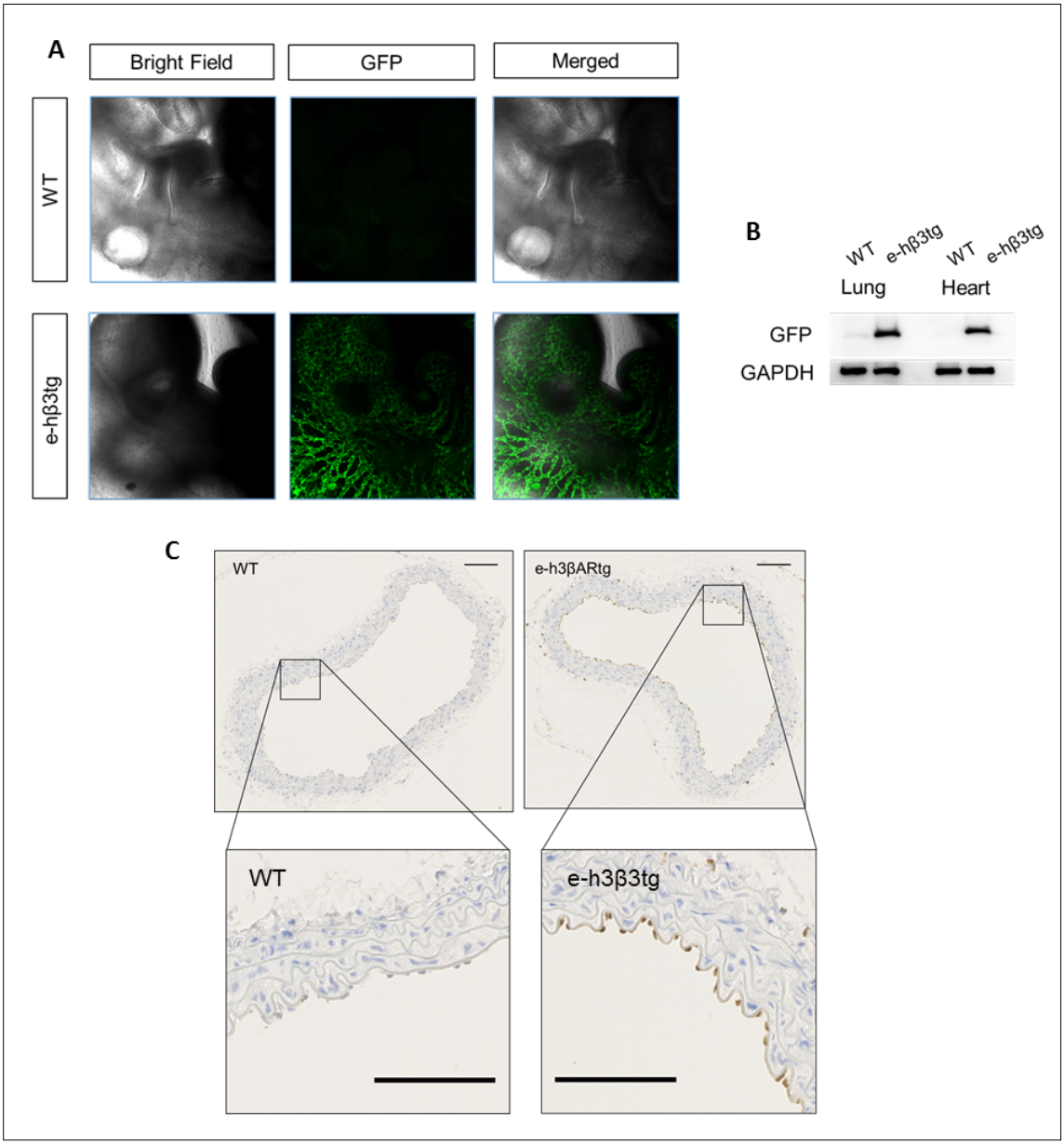

Figure 6: Transgenic mice with endothelial specific expression of the human β3AR efficiently express the transgene in endothelial cells

(**A**) Confocal microscopy images of embryos at 9.5 days from *Tie2*$^{+/+}$;*ADRB3*$^{tg/tg}$ (WT) and *Tie2*$^{Cre/+}$;*ADRB3*$^{tg/tg}$ (e-hβ3tg) mice showing the presence of GFP signal restricted to the vasculature during embryonic development. (**B**) GFP is also present in different tissues of adult e-hβ3tg mice. Immunoblot analysis for GFP in lungs and cardiac tissue of adult mice. (**C**). Immunostaining for GFP in aortas with restricted signal in endothelial cells in e-hβ3tg mice. Scale bar, 0.1µm.

All these data demonstrate that the recombination strategy by LoxP-Cre system using a *Tie2-Cre* line successfully generates transgenic mice that express the human β3AR protein in endothelial cells. Despite being a human protein, this receptor is also functional in the mouse endothelial cells since it mediates a vasodilator response. The correct coupling with NOS indicates that the hβ3AR is functional and undergoes the correct processing necessary for coupling with other proteins to generate an intracellular response similar to was has been described in the literature.

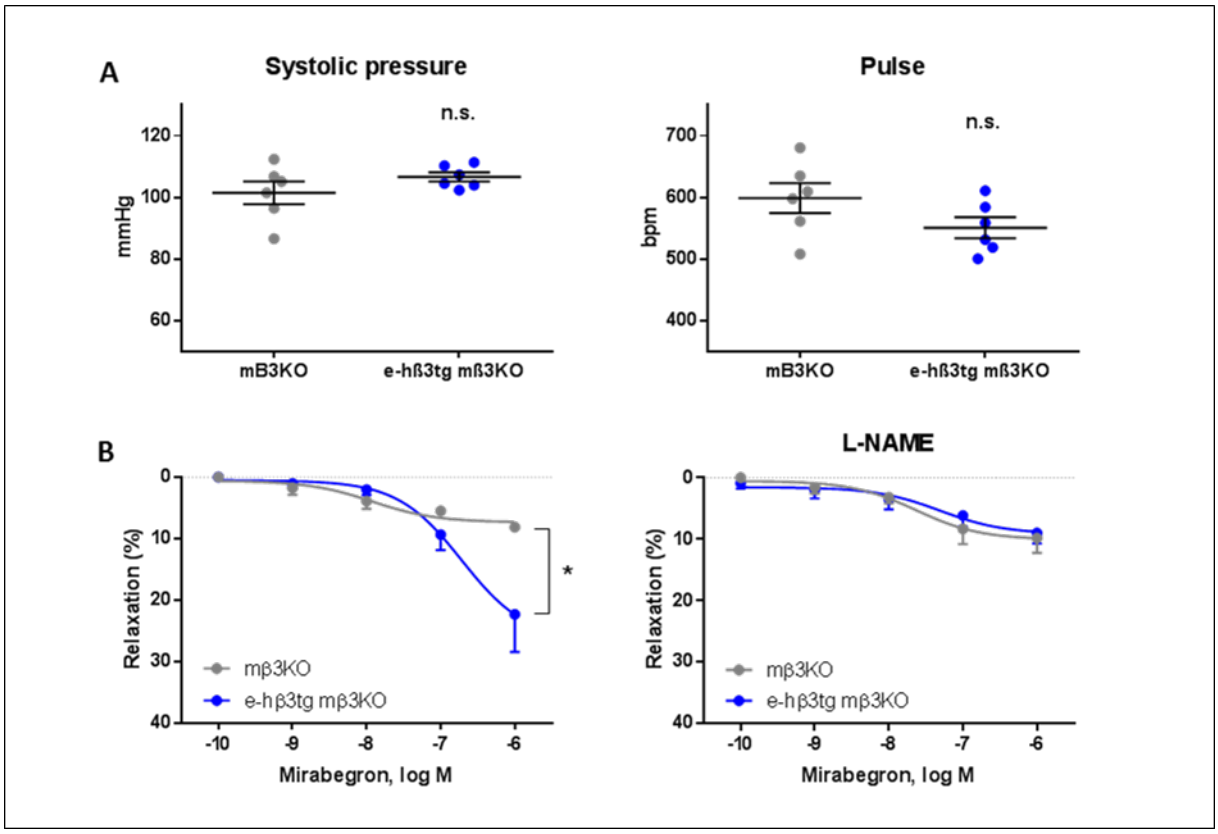

Figure 7: The hβ3AR in endothelial cells of e-hβ3tg mice is functional

(**A**) hB3AR in endothelial cells does not alter basal vascular tone. Arterial systolic pressure and pulse was measured using a noninvasive automated tail-cuff system in conscious mice lacking β3AR (mβ3KO) and with endothelial-restricted expression of the β3AR (e-hβ3tg mβ3KO) (n=6). Data are means ± SEM. NS, not significant. (**B**) Specific stimulation of the hβ3AR induces vasodilation through NO. Thoracic aorta segments from mice lacking β3AR (mβ3KO) (n=5) and with endothelial restricted expression of the β3AR (e-hβ3tg mβ3KO) (n=7-9) were mounted on a wire myograph to examine dilation at increasing doses of the β3AR agonist mirabegron in the absence or presence of the nitric oxide synthase inhibitor L-NAME 10^{-4}M. Data are presented as the percentage of relaxation after contraction induced by U46619 10^{-7}M. Data are means ± SEM. Two-way ANOVA, *P<0.05.

4.1.2 Expression of the human β3-adrenergic receptor in cardiomyocytes by recombinant adeno-associated virus based gene therapy

Mice with constitutive expression of a transgene is a powerful tool to explore the role of a given protein. However, mice's embryonic development is under the influence of this protein and unwanted consequences may appear in adults. Moreover, these models have a poor translational impact when the protein is studied as therapeutic tool. For this reason, we generated recombinant adeno-associated virus (rAAV) encoding the hβ3AR gene under the control of a truncated chicken cardiac troponin-T (cTnT) promoter and strengthened by the enhancer Cmr4 (Fig. 8A). In order to able track in vivo the transduction of the mice, we placed a luciferase reporter gene after the hβ3AR gene. Expression of the luciferase can be assessed in vivo after administration of D-luciferin using an In Vivo Imaging System (IVIS). To avoid fusion of both proteins, we placed an IRES sequence between the two genes. A polyA sequence was added at the end to confer stability to the mRNA. The genetic construction was flanked ITR sequences for AAV machinery recognition. As a control, we also generated a recombinant adeno-associated virus encoding EGFP followed by the luciferase gene (Fig. 8A).

4.1.2.1.1 AAV9-mediated gene delivery distribution

We used the already mentioned genetic constructions for rAAV (Fig. 8A) to generate AAVs serotype 9. This serotype has been demonstrated to efficiently transduce cardiac tissue in mice *(159)*. After IV injection (femoral vein) of $3x10^{11}$ viral genomes in C57Bl6J wild type mice, we allowed expression of the transgene for 2 weeks. After intraperitoneal administration of D-luciferin, we checked luminescence signal in an IVIS. Animals correctly transduced showed a strong signal in the cranial part of the abdomen (Fig. 8B). In order to verify the source of the luminescent signal, mice were euthanized and organs were excised and incubated in D-luciferin. Among all the organs only liver and heart showed luminescence with a predominant signal in the heart demonstrating the cardiac specificity of the AAV9 combined with the cTnT promoter (Fig. 8C). A closer look to the cardiac tissue revealed a mosaic pattern of transduction by the AAV9 in cardiac myocytes as already demonstrated by others *(160)* (Fig. 8D).

Therefore, we found that AAV9 is a powerful tool for gene delivery. The combination of AAV9 and the cTnT promoter showed successful results in targeting the gene expression in cardiac myocytes as already seen by others *(160)*.

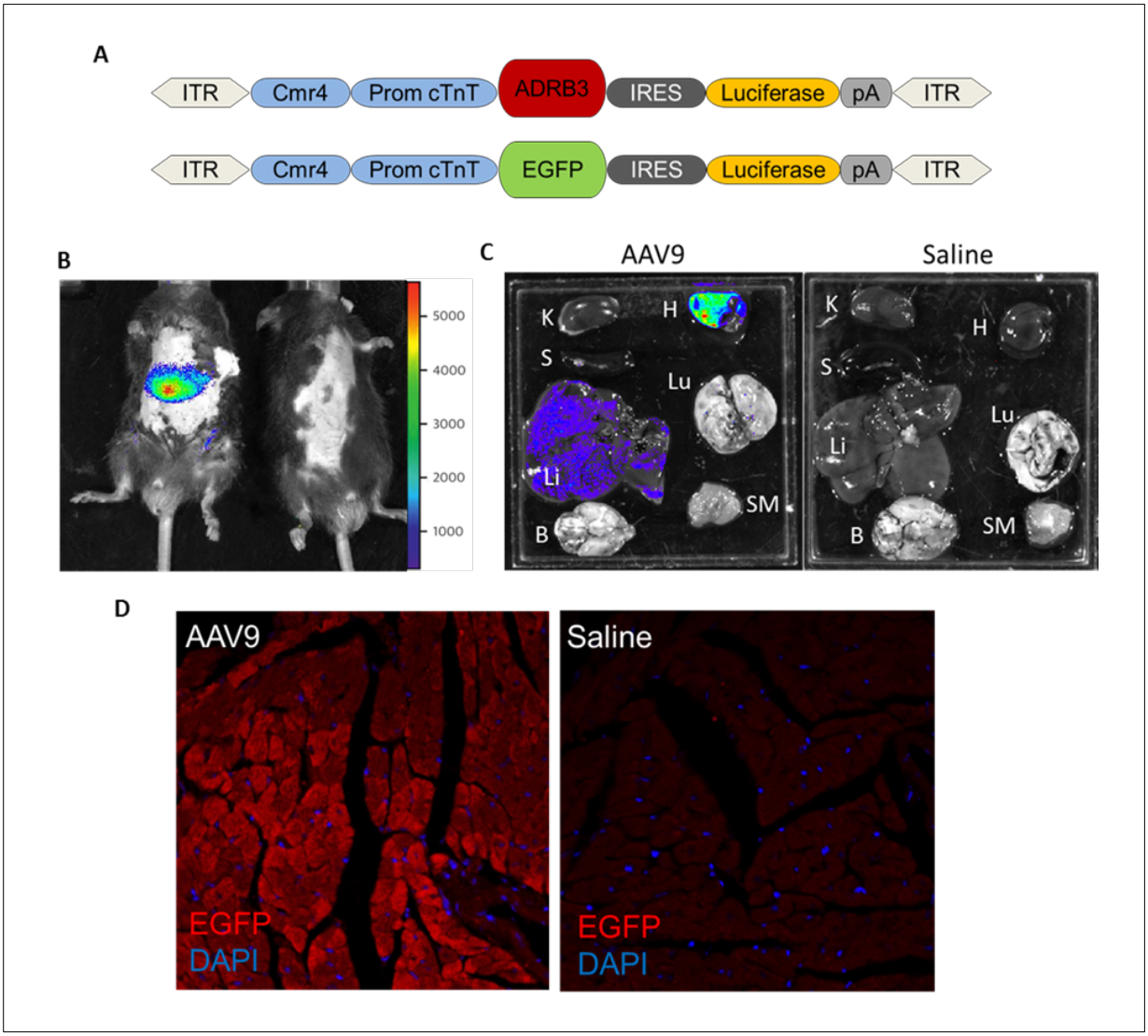

Figure 8: Adeno-associated virus serotype 9 (AAV9) efficiently transduce cardiac tissue in mice

(**A**) Schematic representation of the genetic constructions for adeno-associated virus (AAV) vectors encoding hβ3AR and control EGFP. ITR, recognition site for AVV packaging. Cmr4, enhancer sequence. Prom cTnT, Troponin T promoter sequence for cardiomyocyte specific expression. ADRB3, c-DNA sequence of the human β3AR receptor. EGFP, enhanced Green Fluorescent Protein sequence. IRES, Internal Ribosome Entry Site. Luciferase, firefly luciferase sequence. pA, simian virus 40 polyadenylation signal. (**B**) In vivo bioluminescence images showing luciferase activity in C57Bl6J mice obtained 2 weeks following intravenous (femoral vein) AAV9 ($3x10^{11}$ viral genomes/mouse) administration (left) or saline (right). (**C**) Ex vivo bioluminescence images from organs immersed in D-luciferin solution of mice transduced with AAV9 (left) or saline (right). K, kidney. S, spleen. Li, liver. B, brain. H, heart. Lu, lungs. SM, skeletal muscle. Luciferase activity was predominantly observed in the heart and low activity was observed in the liver. (**D**) Fluorescence microscopy of heart cryosections from mice transduced with AAV9-EGFP (left) or saline (right) showing the mosaic cellular distribution of the transgene expression.

4.1.2.1.2 AAV9-mediated hB3AR gene expression, protein synthesis and protein functionality

Once we confirmed that the AAV9 correctly transduced cardiac myocytes in vivo, we then evaluated the efficacy of the AAV9-hβ3AR to induce expression of the hβ3AR. We first checked gene expression of the hβ3AR. Mice transduced with AAV9-hβ3AR for 4 weeks were sacrificed and the presence of hβ3AR mRNA in isolated cardiomyocytes was assessed by RT-PCR. We designed specific primers in order to discriminate human β3AR and mouse β3AR cDNA. Products of the RT-PCR to detect hβ3AR mRNA are shown in Fig. 9A. Then, we verified the presence of hβ3AR protein in cardiac myocytes by immunostaining (Fig. 9B). The receptor was localized in the sarcolemma of the myocytes meaning a correct posttranslational modification and processing necessary for membrane insertion. Functionality of the protein was evaluated by two different approaches. It has been demonstrated that β3AR activates sGC increasing the levels of cGMP *(113)*. In ex vivo experiments, hearts from mβ3KO mice transduced with the AAV9-hβ3AR showed increased production of cGMP when they were stimulated with the β3AR specific agonist BRL 34377 compared to controls. In in vivo experiments, we evaluated invasively the LV function in anesthetized mice. We found a differential response to increasing doses of BRL in WT mice transduced with AAV9-hβ3AR compared to WT controls mice transduced with AAV9-EGFP. AAV9-hβ3AR mice had a higher increase in dP/dt_{max} (Fig. 9D) and dP/dt_{min} (Fig. 9F) and a higher heart rate (Fig. 9G). Differences in LVESP were not statistically significant but had a tendency to be higher in AAV9-hβ3AR mice (Fig. 9E). Therefore, we can conclude that hβ3AR increases cardiac contractility in WT mice supporting the results obtained in c-hβ3tg mice.

These data confirm that AAV9 mediated gene therapy is an efficient tool to express in vivo the hβ3AR in cardiac myocytes of mice. The resulting human protein is correctly localized in the plasma membrane of mouse cardiac myocytes and couples correctly with other proteins generating a physiological change in cardiac contractility.

To summarize, we have developed transgenic mice expressing a functional human beta3 adrenergic receptor in cardiac myocytes and in endothelial cells. Crossbreeding these transgenic mice with β3KO mice, we have generated mice with restricted expression of the β3AR in a specific cell type of the body. These mice allow us to explore the role of the β3AR precisely in cardiomyocytes or in endothelial cells without the influence of the β3AR response in other cell types. In addition, we have developed a tool to express the hβ3AR in adult WT mice. This AAV9-hβ3AR could be used as therapeutic approach in WT mice, also known as gene therapy.

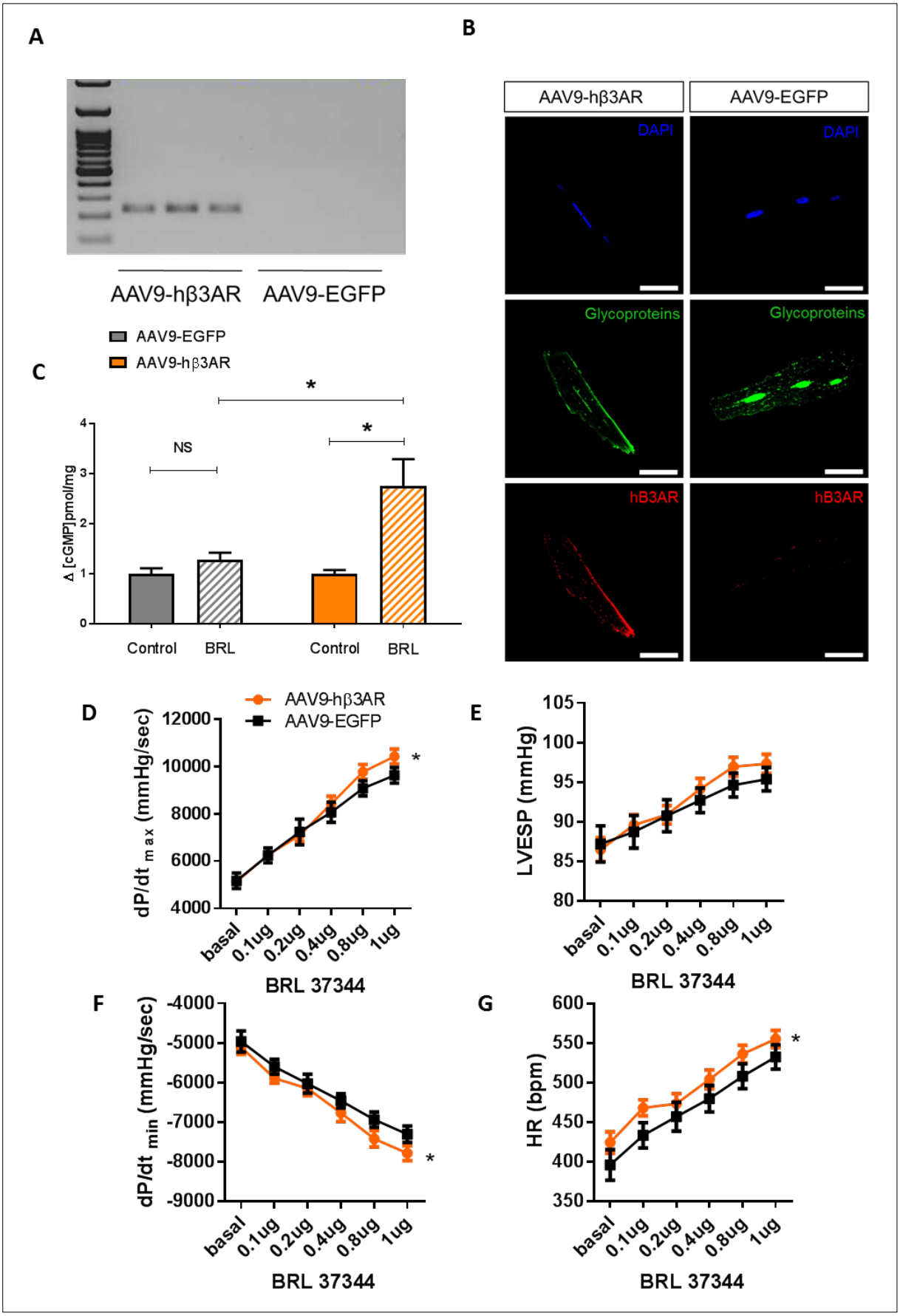
A
AAV9-hβ3AR
AAV9-EGFP
B
AAV9-hβ3AR
AAV9-EGFP
DAPI
Glycoproteins
hB3AR
C
AAV9-EGFP
AAV9-hβ3AR
Δ [cGMP]pmol/mg
NS
*
Control
BRL
D
dP/dt max (mmHg/sec)
basal
0.1ug
0.2ug
0.4ug
0.8ug
1ug
BRL 37344
E
LVESP (mmHg)
F
dP/dt min (mmHg/sec)
G
HR (bpm)

Figure 9: Mice transduced with AAV9-hβ3AR express a functional beta3-adrenergic receptor in cardiomyocytes

(**A**) AAV9-hβ3AR transduced mice show ADRB3 gene expression. RT-PCR products for ADR3B3 from cardiomyocytes of mice transduced with AAV9-hβ3AR or AAV9-EGFP were separated in an agarose gel. The probe was design to discriminate between human and mouse β3AR cDNA sequence. (**B**) Immunostaining in adult mouse ventricular myocytes from a AAV9-hβ3AR transduced mouse (left) or a control AAV9-EGFP transduced mouse (right); hβ3AR (red) is found at the sarcolemma of AAV9-hβ3AR transduced cardiomyocytes; Lectin staining for glycoproteins in membranes (green) is shown for comparison. Scale bar, 50µm. (**C**) Hearts from AAV9-hβ3AR mice show a higher increase in cGMP production when stimulated with the β3AR agonist BRL37344: Hearts from mβ3KO mice transduced with AAV9-hβ3AR or AAV9-EGFP were perfused ex vivo using a buffer with BRL (0.1µM) or without (Control). To avoid cGMP degradation IBMX (400µM) was added to the buffer. Increases in accumulated cGMP level compared to each control are shown (n=3). (**D**, **E**, **F**, **G**) In vivo assessment of LV function in mice transduced with AAV9-hβ3AR (orange, n=9) or AAV9-EGFP (black, n=10) in basal conditions and in response to increasing doses of the β3AR agonist BRL 37344 showing an increase in the chronotropic response (heart rate, HR), an increased systolic function by maximal derivative of LV pressure (dP/dt_{max}) and left ventricular end systolic pressure (LVESP) and an increased diastolic function by the minimal derivative of LV pressure (dP/dt_{min}). Data are means ± SEM. Two-way ANOVA, *P<0.05

4.2 Role of the human β3-adrenergic receptor in cardiac ischemia/reperfusion injury

Different groups including ours have demonstrated the beneficial effects of a IV single dose of a β3AR agonist before reperfusion in cardiac ischemia/reperfusion injury *(134, 136)*. This therapy results in a reduction of the infarct size. The investigated molecular mechanisms have implicated the increase of the NO production as the leading cause of the cardioprotective effect. However, the NO production in cardiac tissue by β3AR stimulation has been demonstrated in both endothelial cells *(139, 158)* and cardiac myocytes *(113)*. In this part of the thesis, we will dissect the cellular origin of the cardioprotection afforded by β3AR stimulation in IR injury.

4.2.1 Cell type-specific expression of the β3-adrenergic receptor show different protective effect in ischemia/reperfusion injury

To determine the contribution of the β3AR from cardiomyocytes or endothelial cells in attenuating myocardial injury from myocardial IR, we generated mice with restricted expression of the β3AR in cardiomyocytes (c-hβ3tg mβ3KO) or in endothelial cells (e-hβ3tg mβ3KO). These mice were the consequence of crossbreeding β3KO mice and transgenic mice with cardiomyocyte or endothelial expression of the hβ3AR. In these resulting mouse lines, litters were composed by hβ3tg mβ3KO transgenic mice and β3KO littermates (mβ3KO). Transgenic mice and control littermates were subjected to 45 minutes of left coronary artery occlusion, followed by 24 hours of reperfusion. At this time, myocardial injury was assessed by determining infarct size (IS) using 2,3,5-triphenyltetrazolium chloride (TTC). To normalized myocardial injury, left ventricular (LV) area at risk (AAR) was determined by Evans blue staining prior to TTC staining. This protocol is summarized in Fig. 10A. The AAR normalized to the total LV was similar in all groups (Fig. 10B, E). The e-hβ3tg mβ3KO mice revealed a similar IS normalized to AAR (39.9 ± 4.5%) compared to controls (46.3 ± 6.3%) (Fig. 10C). Representative mid-ventricular cross-sections of e-hβ3tg mβ3KO and mβ3KO littermates are shown in Fig. 10D. Mice with cardiac restricted expression of the β3AR displayed a reduced IS (33.6 ± 4.1) compared to mβ3KO littermates (49.8 ± 4.2), a 33% reduction (Fig. 10F). Representative mid-ventricular cross-sections of c-hβ3tg mβ3KO and mβ3KO littermates are shown in Fig. 10G. This results show that restoration of the expression of β3AR in cardiac myocytes but not in endothelial cells was able to reduce infarct size.

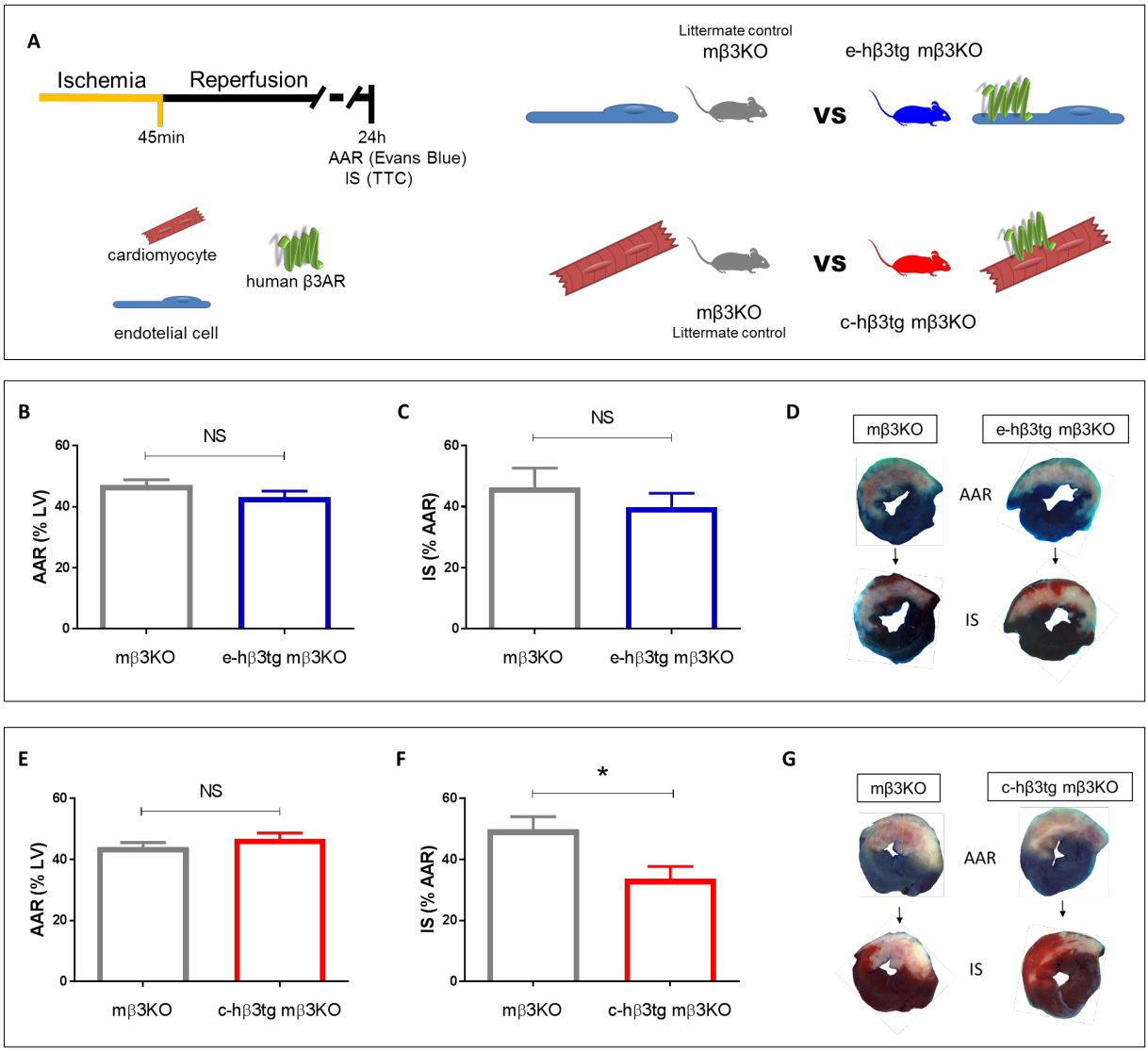

Figure 10: β3-adrenergic receptor expression in cardiomyocytes but not endothelial cells reduces infarct size

(**A**) Experimental protocol. Mice were subjected to left coronary artery occlusion for 45 min followed by 24 h of reperfusion. Myocardial area-at-risk (AAR) and myocardial infarct size (IS) were determined at 24 h of reperfusion by IV injection of Evans Blue and incubation with triphenyltetrazolium chloride (TTC) of the cardiac slices respectively. Mice with endothelium-restricted expression of the β3AR (e-hβ3tg mβ3KO; blue) were achieved by expression of the human β3AR with a Cre-Lox system in endothelial cells of β3KO mice. Mice with cardiomyocyte-restricted expression of the β3AR (c-hβ3tg mβ3KO; red) were achieved by expression of the human β3AR with a Cre-Lox system in cardiac myocytes of β3KO mice. β3KO littermates (mβ3KO in grey) were used as controls. (**B**, **C**) Histological evaluation of left ventricle (LV) AAR and IS in e-hβ3tg mβ3KO mice with endothelium-restricted expression the β3AR (n=9; blue) and mβ3KO littermate controls (n=7; grey) subjected to IR. (**E**, **F**) Histological evaluation of left ventricle (LV) AAR and IS in c-hβ3tg mβ3KO mice with cardiomyocyte-restricted expression the β3AR (n=8; red) and mβ3KO littermate controls (n=7; grey) subjected to IR. (**D**, **G**) Representative images of LV slices showing AAR (negative for Evans Blue) in upper panels and extent of necrosis (TTC-negative area) in lower panels. Data are means ± SEM. t test, *P=0.0176. NS, not significant.

4.2.2 Cell type-specific stimulation of the β3-adrenergic receptor with mirabegron show different protective effect in ischemia/reperfusion injury

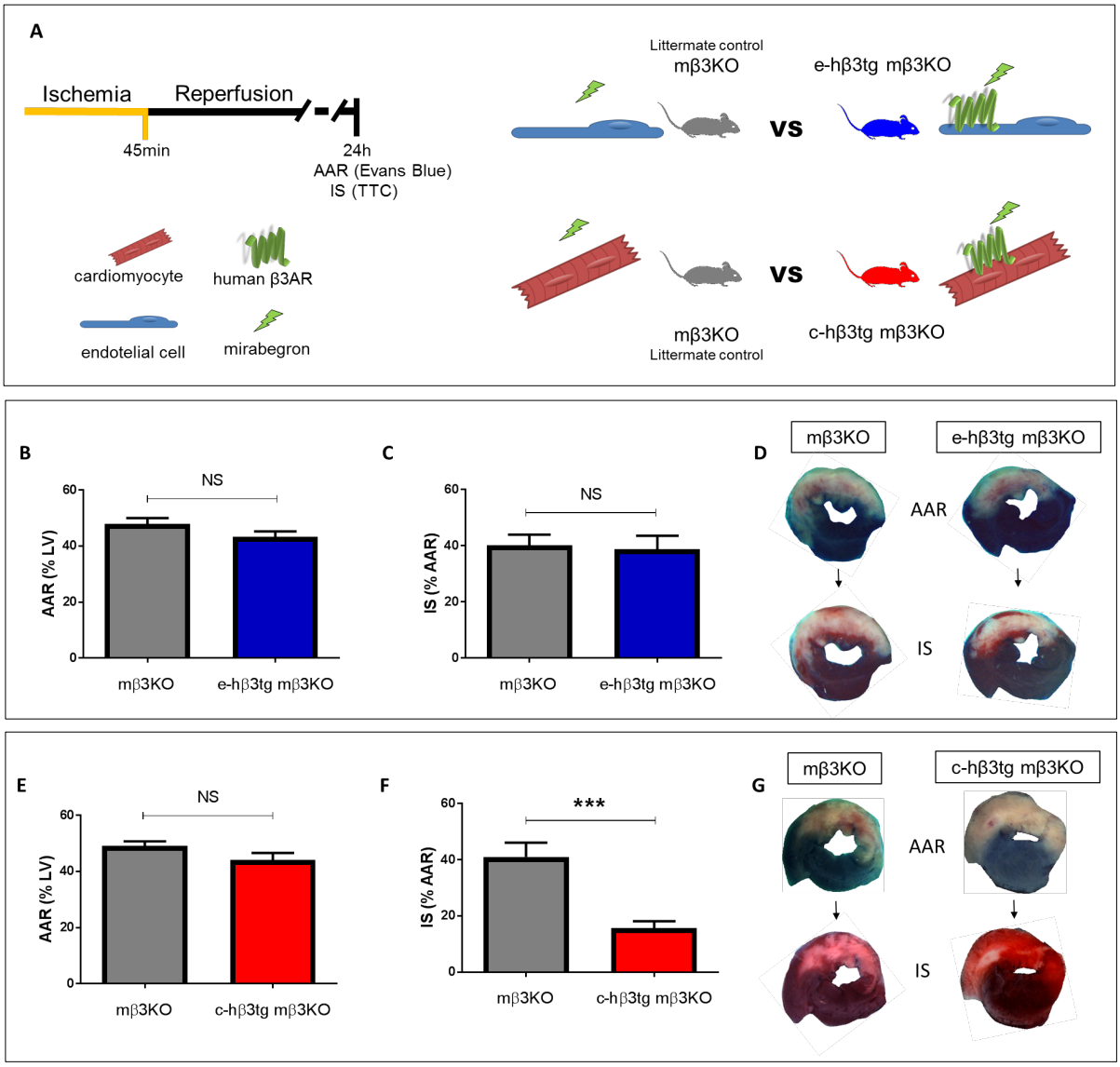

Figure 11: β3-adrenergic receptor stimulation with mirabegron in cardiomyocytes but not endothelial cells reduces infarct size

(**A**) Experimental protocol. Mice were subjected to left coronary artery occlusion for 45 min followed by 24 h of reperfusion. The β3AR specific agonist mirabegron (1µg/kg) was injected IV (femoral vein) 10 min before reperfusion. Myocardial area-at-risk (AAR) and myocardial infarct size (IS) were determined at 24 h of reperfusion by IV injection of Evans Blue and incubation with triphenyltetrazolium chloride (TTC) of the cardiac slices respectively. Cell specific stimulation of the β3AR was achieved by administration of mirabegron in mice with cardiomyocyte (c-hβ3tg mβ3KO; red) or endothelial cell (e-hβ3tg mβ3KO; blue) restricted expression of the β3AR. β3KO littermates (mβ3KO; grey) were used as controls. (**B**, **C**) Histological evaluation of left ventricle (LV) AAR and IS in e-hβ3tg mβ3KO mice with endothelium-restricted expression the β3AR (n=10; blue) and mβ3KO littermate controls (n=10; grey) subjected to IR. (**E**, **F**) Histological evaluation of left ventricle (LV) AAR and IS in c-hβ3tg mβ3KO mice with cardiomyocyte-restricted expression the β3AR (n=8; red) and mβ3KO littermate controls (n=7; grey) subjected to IR. (**D**, **G**) Representative images of LV slices showing AAR (negative for

Evans Blue) in upper panels and extent of necrosis (TTC-negative area) in lower panels. Data are means ± SEM. t test, ***P=0.0009. NS, not significant.

Next, we explored the effect of the selective stimulation of the β3AR from cardiomyocytes or endothelial cells in reducing myocardial injury from myocardial IR. To do so, we used mice with restricted expression of the β3AR in cardiomyocytes (c-hβ3tg mβ3KO) or in endothelial cells (e-hβ3tg mβ3KO). After administration of one single bolus of the β3AR selective agonist mirabegron (1µg/kg) through the femoral vein 10 minutes before reperfusion, we were able to stimulate selectively the β3AR in cardiac myocytes or endothelial cells. Transgenic mice and control littermates were subjected to 45 minutes of left coronary artery occlusion, followed by 24 hours of reperfusion. IS and AAR were evaluated as previously. The protocol is summarized in Fig. 11A. The AAR normalized to the total LV was similar in all groups (Fig. 11B, E). The e-hβ3tg mβ3KO mice revealed a similar IS normalized to AAR (38.8 ± 4.8%) compared to controls (40.2 ± 3.8%) (Fig. 11C). Representative mid-ventricular cross-sections of e-hβ3tg mβ3KO and mβ3KO littermates are shown in Fig. 10D. Mice with specific stimulation the β3AR in cardiac myocytes displayed a reduced IS (15.7 ± 2.4) compared to mβ3KO littermates (41.0 ± 5.1%), a 62% reduction (Fig. 11F). The percentage of reduction was greater than with just restoration of the receptor, 33% reduction (Fig. 10F). Representative mid-ventricular cross-sections of c-hβ3tg mβ3KO and mβ3KO littermates are shown in Fig. 11G. This results show that specific stimulation of the β3AR in cardiac myocytes but not in endothelial cells reduces infarct size.

4.2.3 β3-adrenergic receptor protects isolated adult mouse cardiac myocytes from hypoxia/reoxygenation injury

In order to confirm these results we isolated cardiomyocytes from adult c-hβ3tg mβ3KO mice and from mβ3KO control littermates. To simulate in vivo ischemic conditions, cells were platted and incubated for 1 hour under hypoxic conditions (1% O_2) in a buffer with low pH (6.8) and sodium lactate. Then, cells were subjected to reoxygenation by addition of a normoxic buffer with physiological pH (7.38) and glucose and containing mirabegron (1µM). The amount of dead cells, quantified by propidium iodide internalization with a fluorescence microscope, was significantly lower in myocytes expressing the β3AR than in control myocytes at 15, 30, 45 and 60 min after reoxygenation (Fig. 12A). Representative images of platted cardiomyocytes at 60 min of reoxygenation are shown in Fig. 12B. This experiment further confirms the protective effect of β3AR stimulation in cardiac myocytes.

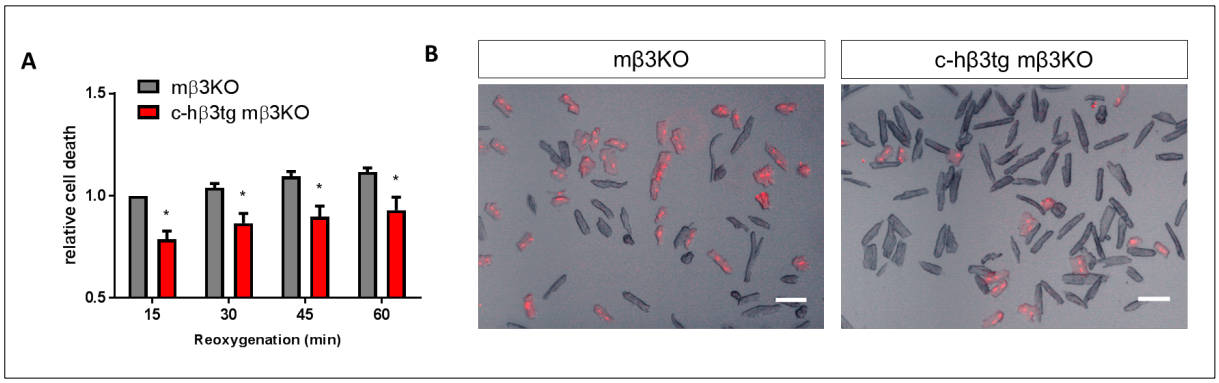

Figure 12: β3-adrenergic receptor stimulation protects isolated adult mouse cardiac myocytes from hypoxia/reoxygenation injury

(**A**) Cell death quantification of isolated adult mouse cardiac myocytes from mβ3KO mice (n=4, grey) and from c-hβ3tg mβ3KO mice expressing the human β3AR (n=4, red) subjected to 1 hour hypoxia (1% O_2) and 1 hour of reoxygenation. Cell death was assessed by propidium iodide (PI) internalization every 15 min after the beginning of reoxygenation. Mirabegron (1µM) was added at the time reoxygenation. Data are means ± SEM. Two-way ANOVA (*P<0.05). (**B**) Representative images of isolated cardiomyocytes after reoxygenation showing PI-negative rod-shaped fresh cardiomyocytes and PI-positive (red) dead cardiomyocytes from mβ3KO mice (left panel) and from c-hβ3tg mβ3KO mice (right panel). Transgenic cells presented lower death rate. Scale bar, 100µm.

4.2.4 Cardiomyocyte specific overexpression of β3-adrenergic receptor maximizes β3-adrenergic receptor stimulation protective response in ischemia/reperfusion injury

In normal conditions, β3AR only represents 3% of the total amount of the cardiac βARs *(101)*. Even if its expression is low, β3AR stimulation protects against cardiac ischemia reperfusion injury. So far, only cardiomyocyte's β3AR have shown protective effects in myocardial IR injury. We next studied the effect of the β3AR overexpression in cardiomyocytes and whether the combination of stimulation and overexpression has a cardioprotective additive effect in myocardial IR injury. For that purpose we used c-hβ3tg mice with cardiomyocyte overexpression of the β3AR (human and mouse β3AR) and WT littermates with regular expression of the β3AR. Transgenic mice and WT control littermates were subjected to 45 minutes of left coronary artery occlusion, followed by 24 hours of reperfusion. IS and AAR were evaluated as previously. Ten minutes before reperfusion mice were randomized to receive a single dose of mirabegron (1µg/kg) through the femoral vein or vehicle. The protocol is summarized in Fig. 13A. The AAR normalized to the total LV was similar in transgenic mice compared to controls (Fig. 13B, E). Mice overexpressing the β3AR showed a 56% reduction in IS normalized to AAR (20.0 ± 2.3%) compared to WT controls with normal levels of β3AR (45.1 ± 3.4%) (Fig. 13C).

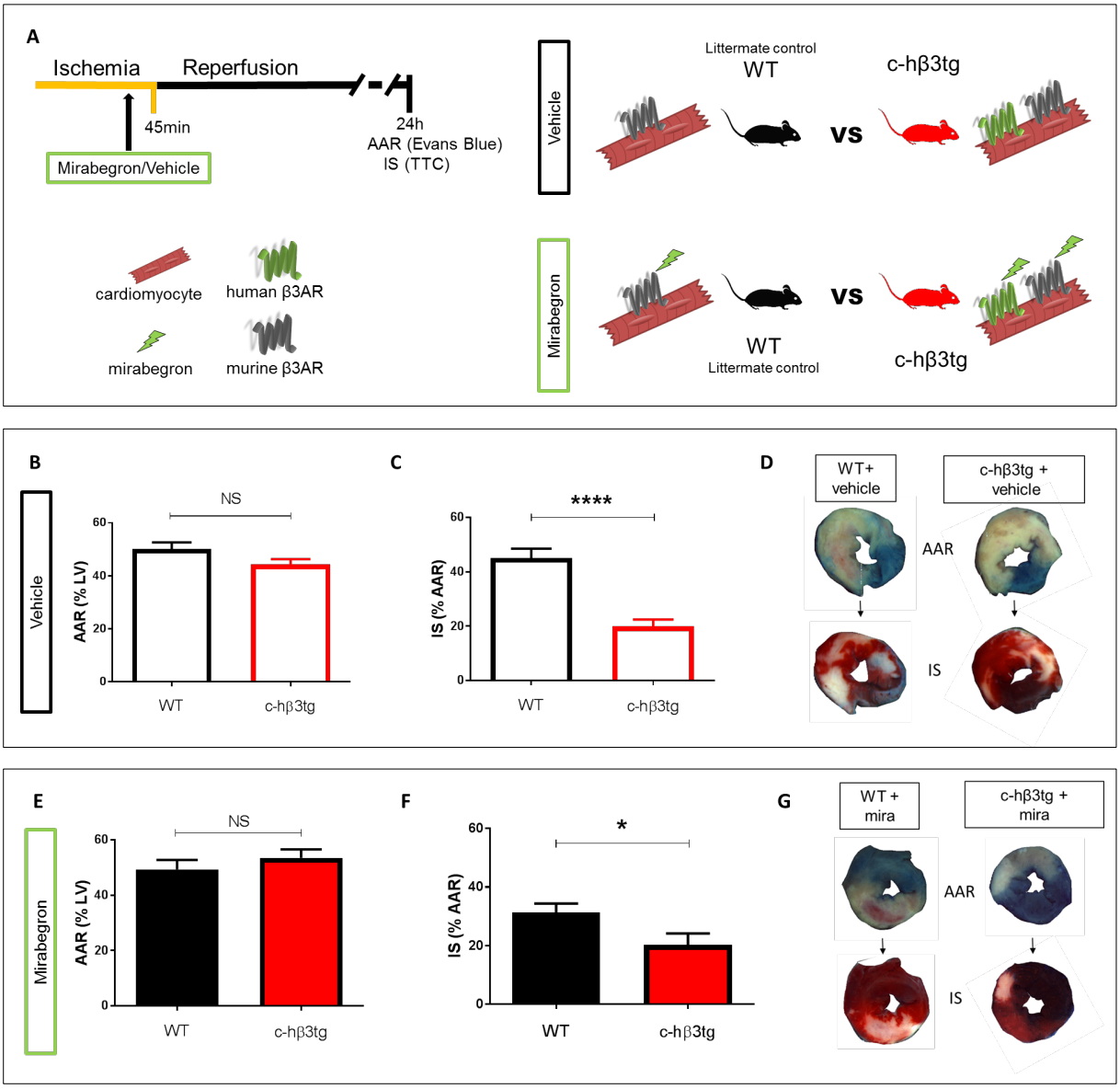

Figure 13: β3-adrenergic receptor overexpression in cardiomyocytes reduces infarct size and maximizes the cardioprotective effect of the beta3-adrenergic receptor stimulation in ischemia/reperfusion injury

(**A**) Experimental protocol. Mice with overexpression of the β3AR in cardiomyocytes (c-hβ3tg) and their control littermates (WT) were subjected to left coronary artery occlusion for 45 min followed by 24 h of reperfusion. β3AR overexpression was achieved by human receptor expression (green) on top of endogenous murine receptor expression (grey). The β3AR specific agonist mirabegron (1µg/kg) or vehicle was injected IV (femoral vein) 10 min before reperfusion. Myocardial area-at-risk (AAR) and myocardial infarct size (IS) were determined at 24 h of reperfusion by IV injection of Evans Blue and incubation with triphenyltetrazolium chloride (TTC) of the cardiac slices respectively. (**B**, **C**) Histological evaluation of left ventricle (LV) AAR and IS in c-hβ3tg mice (n=6; red) and WT littermate controls (n=6; black) subjected to IR. (**E**, **F**) Histological evaluation of left ventricle (LV) AAR and IS in c-hβ3tg mice (n=6; red) and WT littermate controls (n=6; black) with a single dose of mirabegron before reperfusion. (**D**, **G**) Representative images of LV slices showing AAR (negative for Evans Blue) in upper panels and extent of necrosis (TTC-negative area) in lower panels. Data are means ± SEM. t test, *P=0.0497, ****P<0.0001. NS, not significant.

Transgenic animals receiving mirabegron displayed a 35% decrease IS (20.3 ± 3.7%) compared to WT controls also receiving mirabegron (31.3 ± 3.1%) (Fig. 13F). Representative mid-ventricular cross-sections of transgenic mice and WT littermates are shown in Fig. 13D and G. Confirming previous results *(136)*, WT mice treated with the β3AR agonist presented smaller infarcts (31.3 ± 3.1%) that non treated WT mice (45.1 ± 3.4%). Altogether demonstrates that the overexpression of the β3AR in cardiac myocytes can reduce IS and more importantly that an increased number of β3ARs in the cardiac myocytes maximizes the protection provided by the β3AR agonist bolus before reperfusion in myocardial IR injury.

To summarize, we have demonstrated that the cardioprotective effect of the β3AR agonist bolus before reperfusion comes from its effect on the receptor in the cardiac myocyte and not in the endothelial cell. Moreover, this cardioprotective effect can be maximized when the β3AR is overexpressed.

4.3 Role of the human β3-adrenergic receptor in heart failure

The role of the β3AR in cardiac heart failure is controversial due to the multiple animal species and models used. Moreover, β3AR is poorly expressed in cardiac tissue in normal condition. Therefore transgenic animals overexpressing the human receptor are a powerful tool to shed light on the role of this receptor in heart failure.

4.3.1 Overexpression of the β3-adrenergic receptor in neonatal rat cardiac myocytes

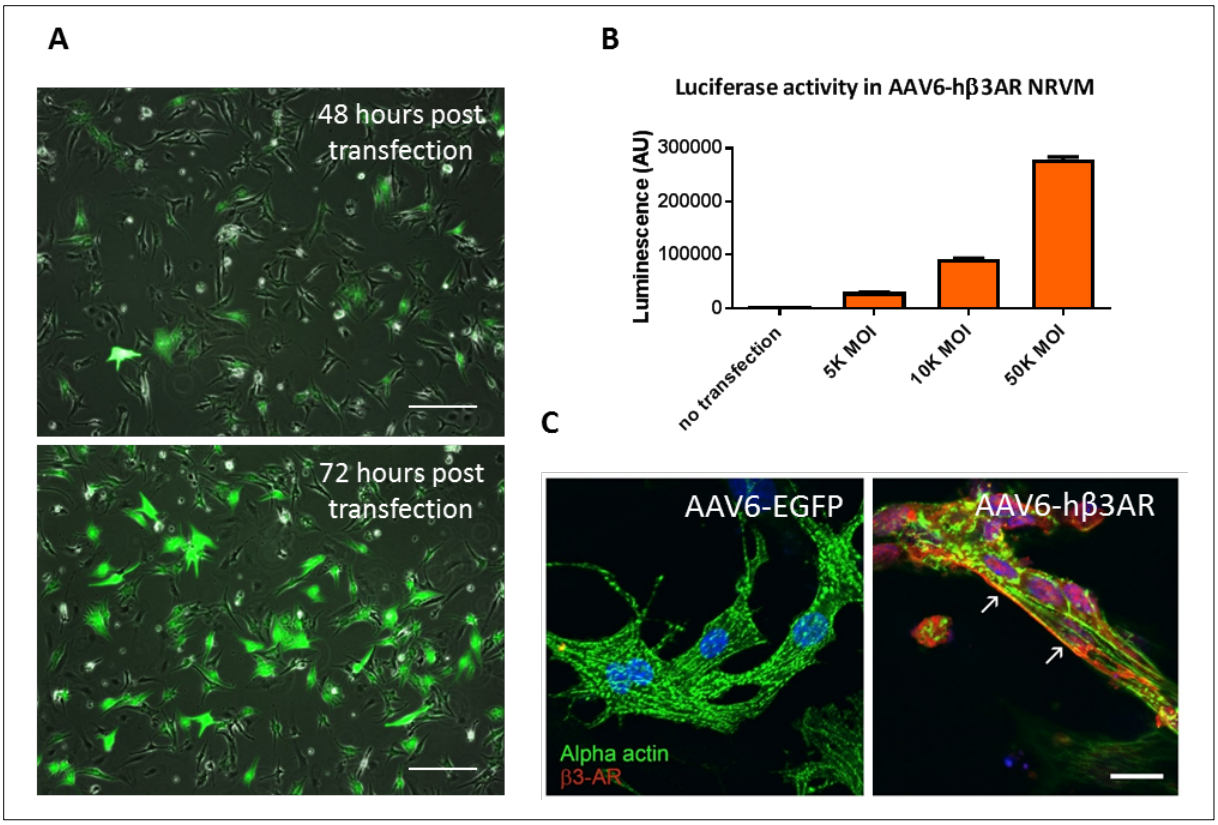

Figure 14: Adeno-associated virus serotype 6 efficiently transduce neonatal rat ventricular myocytes in culture

(**A**) Representative images of neonatal rat ventricular myocytes (NRVM) transfected with EGFP adeno-associated virus serotype 6 at 10K MOI for 48 hours (left panel) and 72 hours (right panel). EGPF signal is evident in most of the cells after 72 hours of transduction. Scale bar, 100µm. (**B**) Luciferase activity quantification in NRVM transduced for 72 hours with hβ3AR-luciferase adeno-associated virus serotype 6 at 5K, 10K and 50K MOI. 10K MOI is sufficient to correctly transduce NRVM. Data are means ± SEM from two independent experiments. (**C**) Immunostaining for α-actin (green) and hβ3AR (red) in NRVM transduced for 72 hours with control (AAV6-EGFP) or human β3AR adeno-associated virus (AAV6-hβ3AR), showing membrane localization of the hβ3AR and no signal in control cells. Scale bar, 20 µm.

Starting at a cellular level, we examined the consequences of overexpressing the β3AR in neonatal rat ventricular myocytes (NRVM). We first generated adeno-associated virus serotype 6 using the genetic construction seen before (Fig. 8A). We next checked AAV6 efficiency to transduce NRVM in culture at 48 and 72 hours using the AAV6-EGFP control virus. Small amount of cells expressed the EGFP transgene at 48 hours (Fig. 14A upper panel) and expression was more evident at 72 hours after infection (Fig. 14A lower panel). Since these vectors are DNA single stranded virus, the time for expression of the transgene is longer than for other vector like adenovirus. Luminescence activity of the reporter protein luciferase was used to define the dose of AAV6 used in the following experiments (Fig. 14B). We found that 10K MOI (multiplicity of infection) was adequate for a correct transduction. NRVMs transduced for 72 hours with 10K MOI of AAV6-hβ3AR were immunostained to check the correct protein expression of the hβ3AR (Fig. 14C). The receptor was present in the cell membrane of the myocytes indicating a correct processing and membrane insertion.

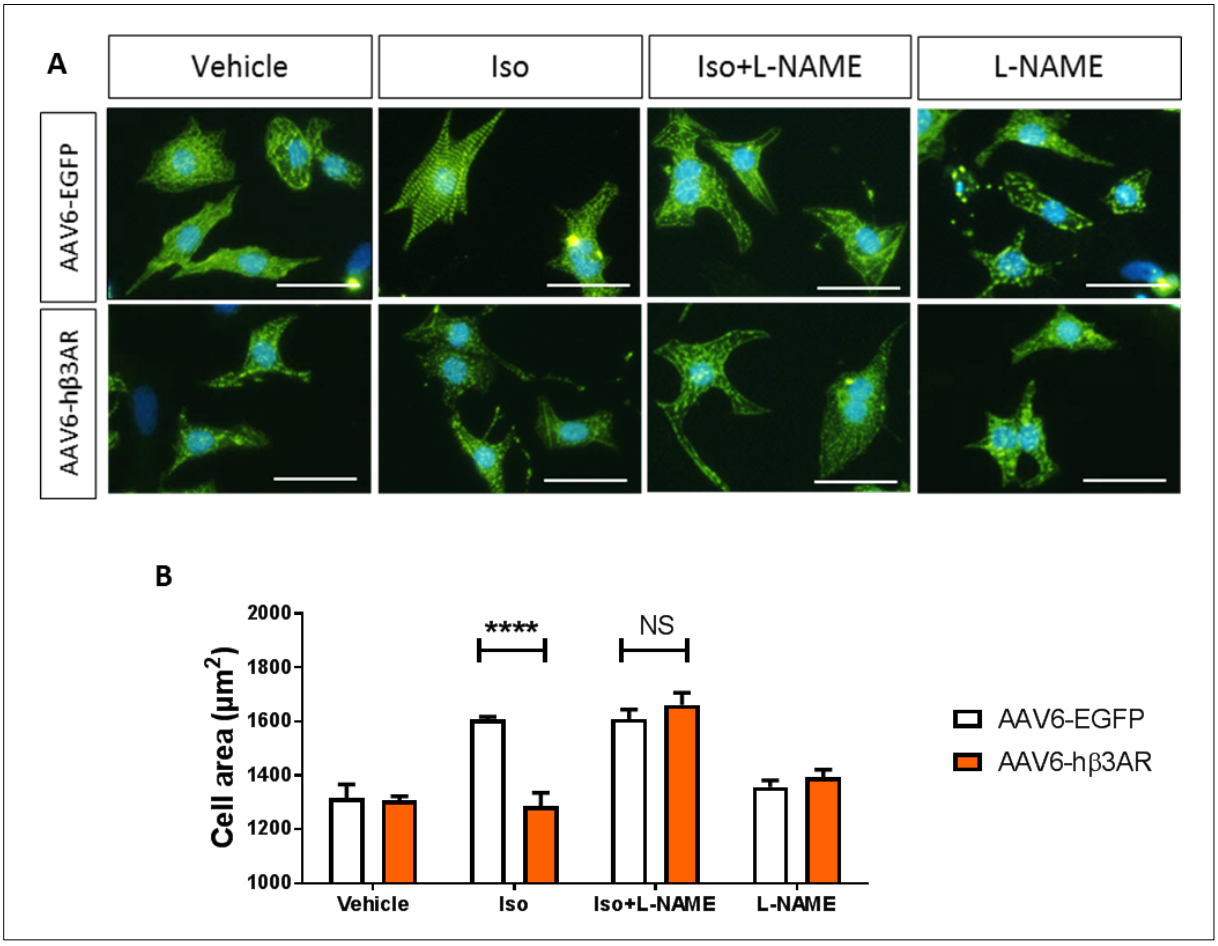

Figure 15: Beta3-adrenergic receptor overexpression protects neonatal rat ventricular myocytes from isoproterenol-induced hypertrophy through NOS dependent mechanism

(**A**) Representative images of neonatal rat ventricular myocytes (NRVM) transduced with control (AAV6-EGFP) or human β3AR adeno-associated virus (AAV6-hβ3AR) for 72h and incubated for 24h with isoproterenol (Iso, 10µM), L-NAME (100µM) or both. Nucleus is stained in blue with DAPI and α-actin is stained in green to differentiate myocytes from other cells. Scale bar, 60 µm. (**B**) Size assessment of NRVM treated as above (40 cells/condition in each preparation; 3 independent preparations). The hypertrophic response to Iso is blunted in hβ3AR myocytes and NOS inhibition by L-NAME restores the hypertrophy. Data are means ± SEM. Two-way ANOVA with Tukey's multiple comparisons test. (****P<0.0001). NS, not significant.

We next evaluated the effect of β3AR overexpression in catecholamine-induced hypertrophy. NRVMs were first transduced for 72 hours and then incubated for 24 hours with isoproterenol 10µM. Myocytes were fixed and immunostained for α-actin to visualize the total shape and to differentiate them from fibroblasts (Fig. 15A). Cell size was increased in AAV6-EGFP transduced cells after 24 hours of isoproterenol incubation. AAV6-hβ3AR myocytes in contrast maintained size showing a protection against hypertrophy. When incubated with the NOS inhibitor L-NAME, AAV6-hβ3AR myocytes showed an increased size. The cardioprotection afforded by β3AR overexpression was abolished by L-NAME indicating a NO dependent protective pathway (Fig. 15B) as already describe by others *(113)*.

NRVMs spontaneously beat in culture. Isoproterenol induces an increase in the frequency of contraction that can be assessed by simple visual evaluation. After transduction with AAV6-hβ3AR and control AAV6-EGFP, myocytes were incubated with isoproterenol 10µM. Control myocytes showed an increase in beating frequency that was maintained over the days (Fig. 16A). β3AR myocytes also showed an increase in the beating frequency immediately after isoproterenol addition but the frequency strongly decreased at day 4 and 5 after the start of the treatment (Fig. 16A). This could be explained by a time dependent increase in the levels of hβ3AR expression. In addition, increase in contractility due to isoproterenol incubation could promote enhanced activation of the TnT promoter used in the AAV genetic constructions and therefore enhancing the expression of the hβ3AR. When coincubated with L-NAME, β3AR myocytes followed the same trend as before suggesting a NO independent mechanism for this decrease in beating frequency (Fig. 16B).

The antihypertrophic effect and the reduction in beating frequency in NRVM were indicative of cardioprotective characteristics of the β3AR during overexposure to catecholamine. The increase in catecholamines' production is a main feature of heart failure therefore we hypothesized that overexpression of the β3AR in cardiac myocytes could result in protection in in vivo models of heart failure. Following this hypothesis, we moved to in vivo experiments using a pressure overload heart failure model in transgenic mice overexpressing the β3AR in cardiomyocytes.

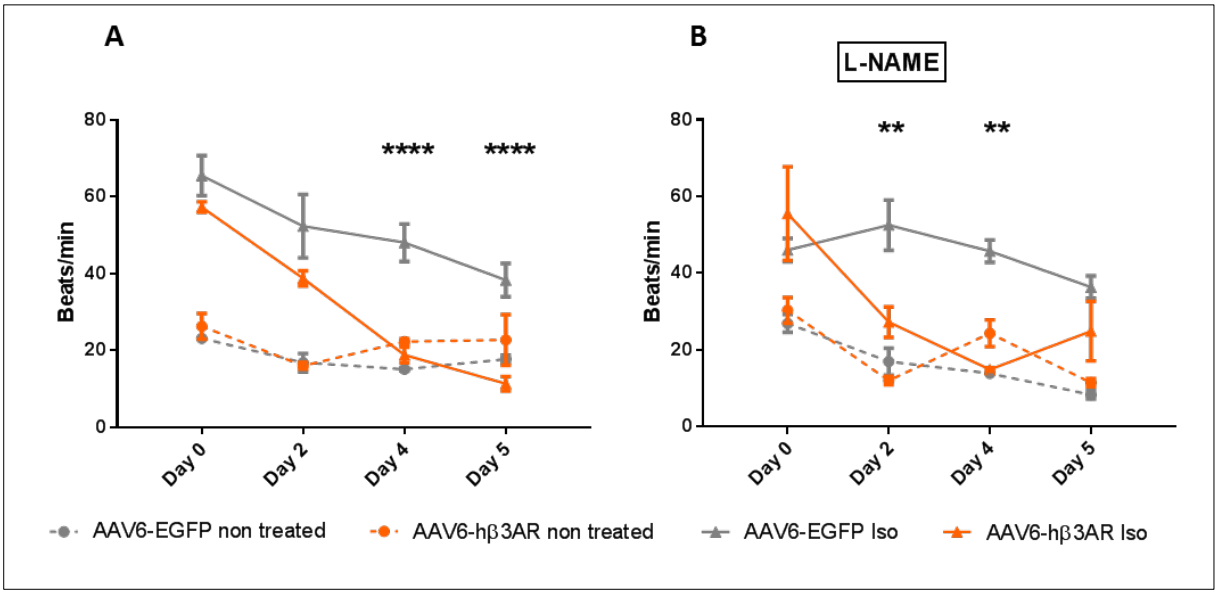

Figure 16: Beta3-adrenergic receptor overexpression reduces positive chronotropic response to isoproterenol in cultured neonatal rat ventricular myocytes through NOS independent mechanism

(**A**) Beating rate in neonatal rat ventricular myocytes (NRVM) was counted in 10 different positions of 6 independent wells per condition immediately after isoproterenol (Iso, 10µM) addition (day 0) and 3, 4 and 5 days later. 72 hours before Iso stimulation NRVM were transduced with control (AAV6-EGFP) or human β3AR adeno-associated virus (AAV6-hβ3AR). hβ3AR myocytes presented a decrease in the beating rate after prolonged Iso stimulation. (**B**) Effect of NOS inhibition by cotreatment with L-NAME (100µmol/l). The decrease in the beating rate by hβ3AR overexpression is maintained in the presence of L-NAME suggesting a NOS independent pathway. Data are means ± SEM. Two-way ANOVA with Sidak's multiple comparisons test. (**P<0.01, ****P<0.0001 in AAV6-EGFP Iso vs AAV6-hβ3AR Iso).

4.3.2 β3-adrenergic receptor overexpression prevents heart failure in a model of pressure overload

To test if β3AR has a cardioprotective effect in vivo in response to sustained pressure overload, mice with cardiomyocyte overexpression of the β3AR (c-hβ3tg) and WT control littermates were subjected to transaortic constriction and followed by echocardiography for 12 weeks (Fig. 17A). WT control displayed a severe reduction in left ventricular ejection fraction (30% LVEF) (Fig. 17C) and a massive increase in cardiac mass (2.1 fold increase) (Fig. 17D, E) after TAC surgery. Systolic and diastolic left ventricular volumes were also dramatically increased (Fig. 17F, G). In contrast, transgenic mice maintained LVEF, displayed less increase in LV mass (1.6 fold increase) and showed no signs of LV dilation (Fig.17B). The clear increase in LVEF at week 1 after TAC in transgenic mice support the idea of a positive inotropic effect mediated by the hβ3AR. This is also accompanied by a reduction in systolic and diastolic volumes and an increase in cardiac mass suggesting a concentric hypertrophy characteristic of an adaptive remodeling.

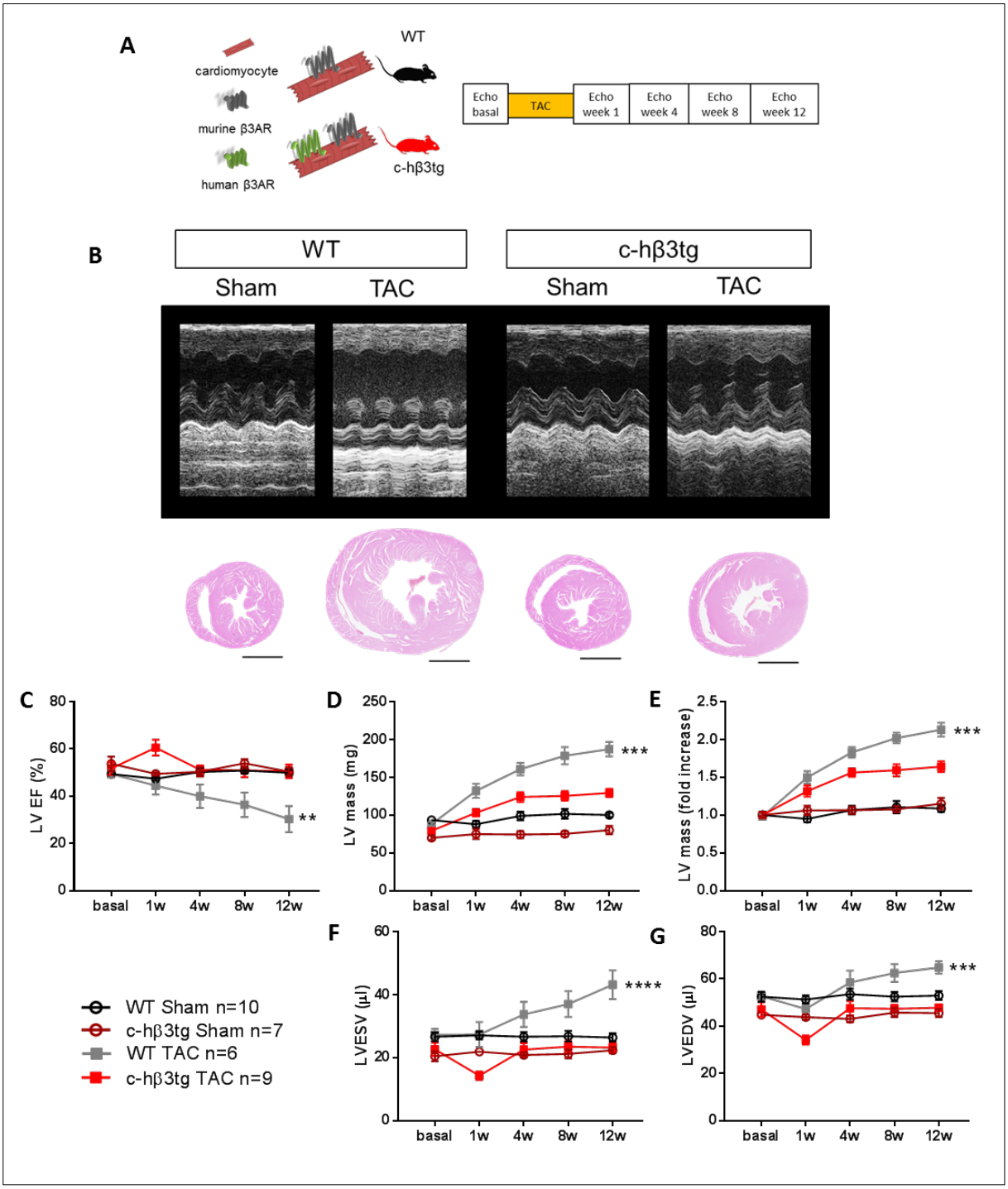

Figure 17: Beta3-adrenergic receptor overexpression in cardiomyocytes preserves cardiac function and protects against cardiac hypertrophy and ventricular dilation

(**A**) Mice with cardiomyocyte specific overexpression of the β3AR (c-hβ3tg) and littermate control (WT) were subjected to transaortic constriction surgery (TAC) or sham surgery and were followed for 12 weeks. (**B**) Representative left ventricle M-mode echocardiograms (Upper) and heart sections (Lower) 12 weeks after surgery. Scale bar 2 mm. (**C**, **D**, **E**, **F**, **G**) Echocardiographic evaluation of left ventricular ejection fraction (LVEF), left ventricular mass and left ventricular internal volumes in systole (LVESV) and diastole (LVEDV). c-hβ3tg mice maintained a normal ejection fraction and left ventricular volumes and showed less cardiac hypertrophy induced by TAC surgery than WT controls. In graphs, data are means ± SEM. Two-way ANOVA, **P<0.01, ***P<0.001, ****P<0.0001 compared to c-hβ3tg TAC.

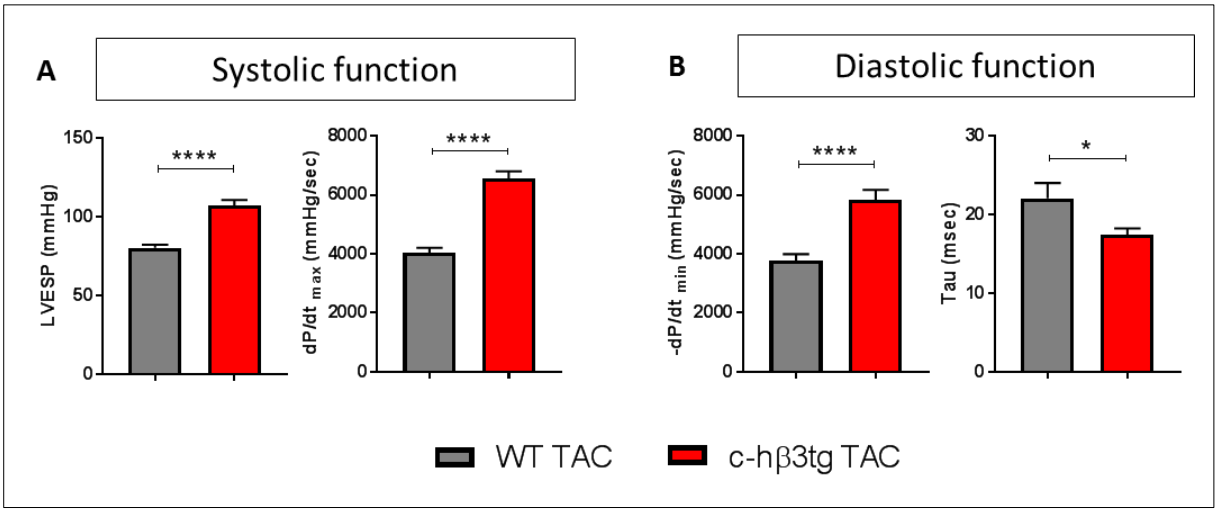

Figure 18: Beta3-adrenergic receptor overexpression in cardiomyocytes protects against systolic and diastolic dysfunction

Mice with cardiomyocyte specific overexpression of the β3AR (c-hβ3tg) and littermate control (WT) were subjected to TAC surgery. Hemodynamics parameters were measured invasively 12 weeks after surgery using a Millar catheter. (**A**) Systolic function was determined by left ventricular end systolic pressure (LVESP) and maximal derivative of LV pressure (dP/dt_{max}) measurements. c-hβ3tg mice showed increased LVESP and dP/dt_{max} confirming a better systolic function. (**B**) Diastolic function was determined by minimal derivative of LV pressure (LV dP/dt_{min}) and the time constant of isovolumic relaxation (Tau). c-hβ3tg mice showed increased LV dP/dt_{min} and decreased Tau confirming a better diastolic function. Data are means ± SEM. n=7-9. t test, *P<0.05, ****P<0.0001.

LV function was evaluated invasively 12 weeks after TAC surgery using a Millar catheter. Hemodynamic parameters revealed a better systolic function in transgenic mice with increased left ventricular end systolic pressure (LVESP) and increased dP/dt_{max} (Fig. 18A). Diastolic function was evaluated by dP/dt_{min} and the time constant of isovolumic relaxation (Tau). c-hβ3tg mice showed higher $-dP/dt_{min}$ and faster Tau. (Fig. 18B) revealing a better diastolic function.

At sacrifice, heart weight of transgenic animals was also diminished compared to WT TAC animals (Fig. 19D) confirming echocardiographic findings. Lung weight and lung water content was assessed as a sign of congestive heart failure. WT TAC mice showed increased lung weight and lung water content suggesting pulmonary remodeling and edema. On the contrary, transgenic mice did not display any sign of congestive heart failure. In the histological analysis of heart sections (Fig. 19A), transgenic mice showed reduced fibrosis (Fig. 19B), supporting the observed better diastolic function (Fig. 18B) and reduced myocyte hypertrophy (Fig. 19C) compared to WT TAC group. Therefore, mice overexpressing the β3AR did not developed maladaptive cardiac remodeling leading to diastolic and systolic dysfunction and consequently, they were protected against heart failure.

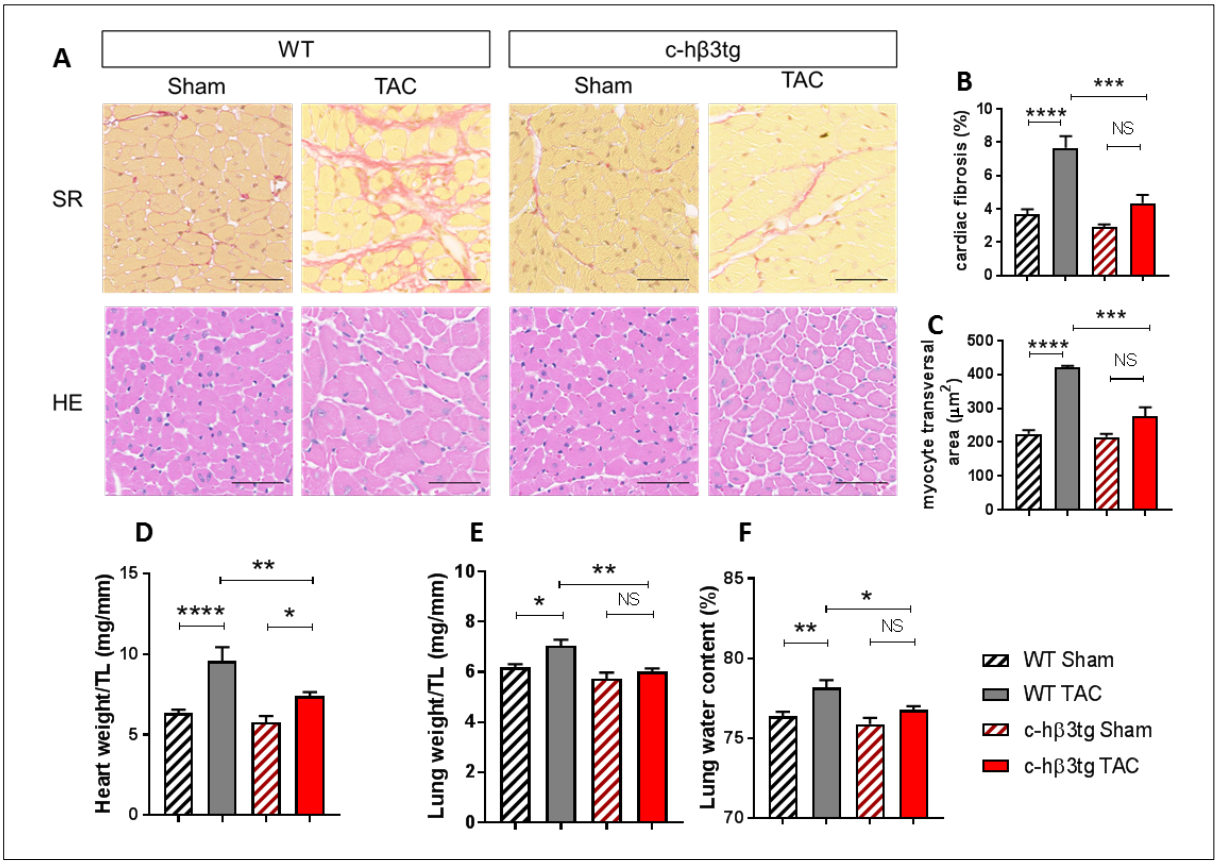

Figure 19: Beta3-adrenergic receptor overexpression in cardiomyocytes reduces myocytes hypertrophy, cardiac fibrosis and protects against heart failure

Mice with cardiomyocyte specific overexpression of the β3AR (c-hβ3tg) and littermate control (WT) were subjected to TAC or Sham surgery, 12 weeks after surgery mice were euthanized for necropsies and histological studies. (**A**) Fibrosis and myocyte size in sham and TAC, WT and c-hβ3tg mice. Histological images of heart sections stained with sirius red (SR, first row) and hematoxylin-eosin (HE, second row). TAC surgery increased fibrosis and myocyte size in WT animals. c-hβ3tg mice showed reduced fibrosis and cardiomyocyte size induced by TAC. Scale bar 50µm. (**B**) Quantification of the total area of fibrosis in heart sections. n=6-8. (**C**) Quantification of the cross-sectional area of left ventricular cardiac myocytes. n=3. (**D**) Heart weight normalized to tibia length (TL). c-hβ3tg mice showed less cardiac hypertrophy induced by TAC. n=6-8. (**E**) Lung weight normalized to tibia length (TL). n=6-8. (**F**) Lung water content as a percentage of fresh lung weight. n=6-8. In WT mice TAC surgery induced increase in lung weight by vascular remodeling and pulmonary edema (water content) due to congestive heart failure mice. c-hβ3tg mice were protected against heart failure. In graphs, data are means ± SEM. Two-way ANOVA with Tukey's multiple comparisons test. *P<0.05, **P<0.01, ***P<0.001, ****P<0.0001. NS, not significant.

4.3.3 β3-adrenergic receptor overexpression prevents metabolic switch in heart failure

Healthy hearts predominantly obtain their energy from β oxidation of free fatty acids and in less proportion from glucose metabolism. During heart failure free fatty acids utilization declines and glucose becomes the preferential substrate for energy obtention, this is known as metabolic switch *(161, 162)*. We decided to explore the metabolic profile of control and transgenic mice in HF. Twelve

weeks after surgery, WT and c-hβ3tg underwent a positron emission tomography–computed tomography (PET-CT) to monitor in vivo the cardiac uptake of ^{18}fluorodeoxyglucose ([^{18}F]FDG) (Fig. 20A). We found that overexpression of the β3AR prevented the increase in cardiac glucose uptake observed in heart failure stage (Fig. 20B). In basal conditions (sham), overexpression of the receptor did not alter glucose uptake.

Mitochondria are the powerhouse of the cell transforming different metabolic substrates into energy in the form of ATP molecules. Hence, it is in charge of the metabolic performance of the cell and it is the link between substrate utilization and energy production. It has been described that increased mitochondrial fragmentation causes an enhancement in cardiac glucose metabolism and heart failure *(154)*. Animal model of pressure overload display mitochondrial fragmentation *(163, 164)*. We examined the morphology of mitochondria by transmission electron microscopy (TEM) of

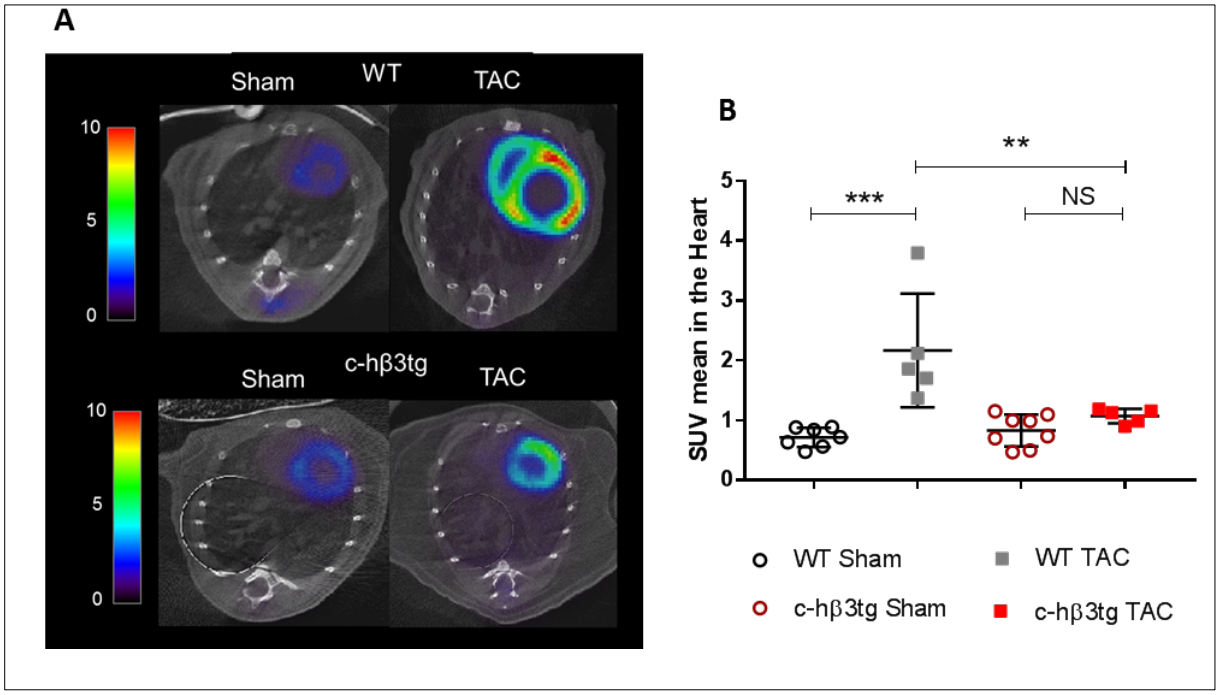

Figure 20: Beta3-adrenergic receptor overexpression prevents cardiac metabolic switch during heart failure

Mice with cardiomyocyte specific overexpression of the β3AR (c-hβ3tg) and littermate control (WT) were subjected to TAC or Sham surgery. PET-CT scans were performed 12 weeks after surgery. (**A**) Representative images of PET-CT thoracic scans after [^{18}F]FDG injections in WT and c-hβ3tg mice. (**B**) Average standardized uptake value (SUV) of [^{18}F]FDG in WT (n=7) and c-hβ3tg (n=8) sham hearts and WT (n=5) and c-hβ3tg (n=5) TAC hearts. TAC induced heart failure is characterized by a metabolic switch where the myocardium increases the glucose uptake as seen in WT TAC animals. c-hβ3tg mice showed no increase in glucose uptake. In graphs, data are means ± SEM. Two-way ANOVA with Tukey's multiple comparisons test. **P<0.01, ***P<0.001. NS, not significant.

WT and c-hβ3tg mice subjected to TAC (Fig. 21A). Smaller mitochondria with disrupted architecture of cristae were found in the cardiac tissue of WT TAC mice. In contrast, transgenic animals presented

bigger mitochondria with normal cristae (Fig. 21A-C). Notably, the proportion of ultra-fragmented mitochondria (<0.25µm^2) was half in transgenic animals compared to controls (Fig. 21D)

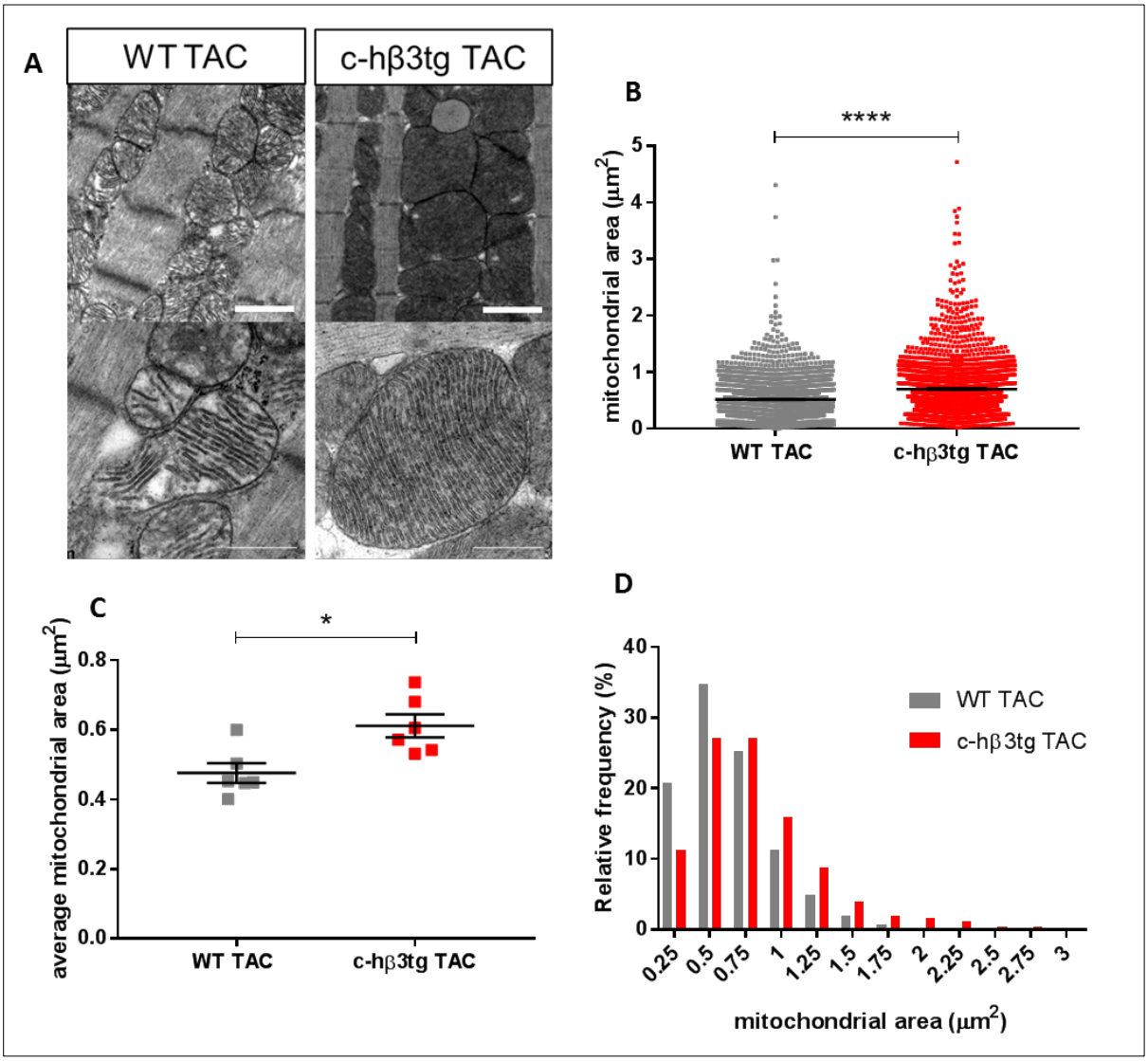

Figure 21: Beta3-adrenergic receptor overexpression prevents mitochondrial fragmentation

Mice with cardiomyocyte specific overexpression of the β3AR (c-hβ3tg TAC) and littermate control (WT TAC) were subjected to TAC surgery. Ultrastructural examination of the cardiac tissue was performed 12 weeks after surgery. (**A**) Representative transmission electron microscopy (TEM) images from WT and c-hβ3tg mice subjected to TAC. (thick scale bar, 1µm; thin scale bar, 500 nm). WT mice showed more fragmented and damaged (disorganized cristae) mitochondria. (**B**) Mitochondrial size represented as surface area of WT TAC (n=2233) and c-hβ3tg TAC (n=2143) mitochondria from cardiac tissue imaged by TEM. (**C**) Median mitochondrial size per mouse in cardiac tissue from WT TAC (n=6) and c-hβ3tg TAC (n=6) mice. (**D**) Frequency distributions of mitochondrial area from WT TAC (n=2233) and c-hβ3tg TAC (n=2143) mitochondria. The percentage of ultra-fragmented mitochondria was higher in WT cardiac tissue. In graphs, data are means ± SEM. t test, *P <0.05 and Wilcoxon-Mann–Whitney test, ****P <0.0001.

Increasing fatty acids utilization has been demonstrated to attenuate mitochondrial fragmentation in the failing heart and protect against cardiac dysfunction *(163)*. Interestingly, we

found that activation of the β3AR enhanced free fatty acid utilization in isolated adult cardiac myocytes from transgenic mice assessed by oxygen consumption rate (Fig. 22A). Using β3KO myocytes as control, we ensured that this response was specific for β3AR. Notably, glucose utilization evaluated by extracellular acidification rate was not differentially increased by β3AR activation (Fig. 22B).

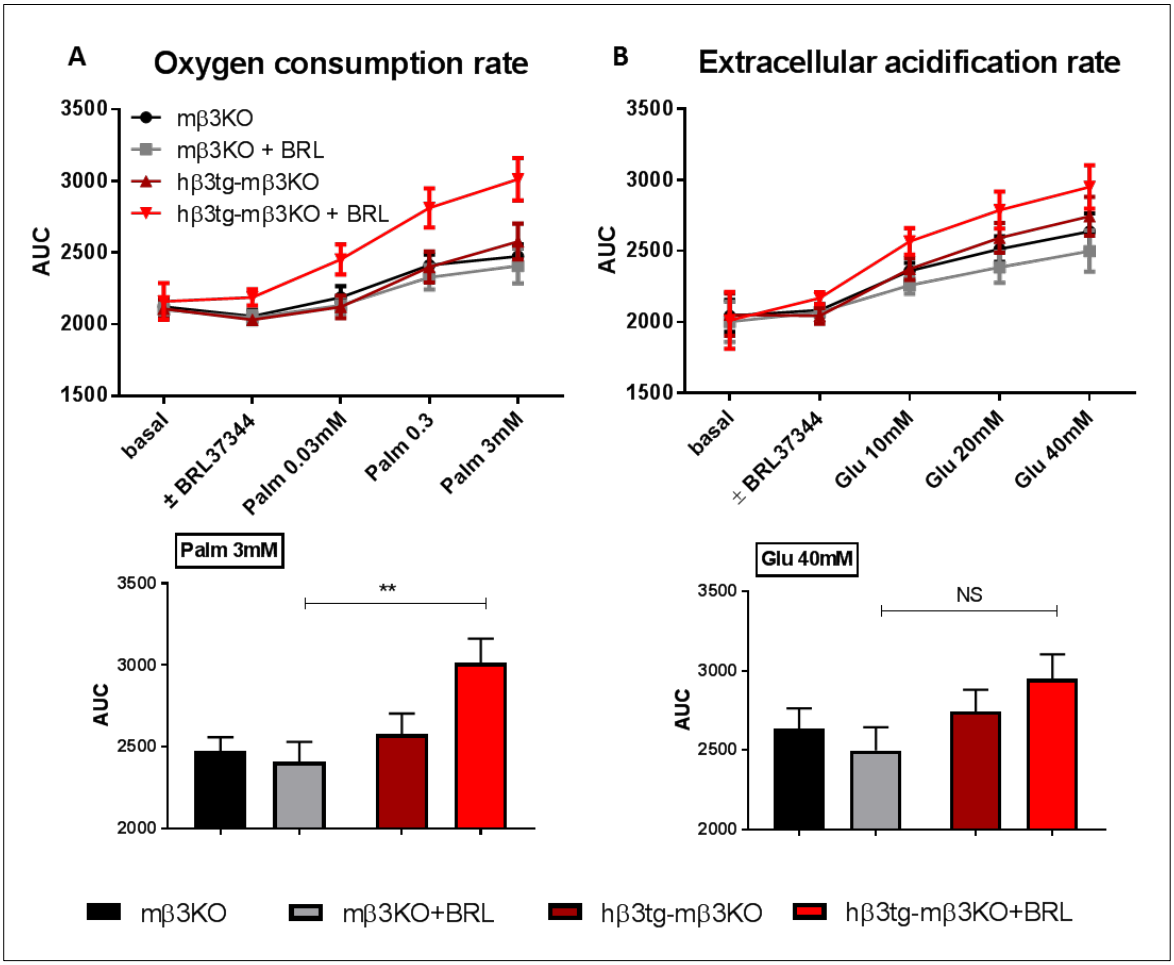

Figure 22: **Beta3-adrenergic receptor stimulation increases free fatty acids utilization in cardiomyocytes**

Cardiomyocytes were isolated from healthy adult mβ3KO mice and c-hβ3tg mβ3KO mice expressing the human β3AR. After plating, cardiomyocyte's metabolic changes in response of increasing doses of substrate were measured. (**A**) Oxygen consumption rate analyzed by Seahorse Bioscience XF96 Flux Analyzer in response of increasing doses of the free fatty acid palmitate (Palm) in the presence or absence of the β3AR agonist BRL37344 1µM (n=8). β3AR stimulation by BRL significantly increases fatty acid oxidation measured as increase in oxygen consumption rate. Measurements for the highest concentration of palmitate 3mM are represented as bars (lower panel). Two-way ANOVA, **P<0.01. (**B**) Extracellular acidification rate analyzed by Seahorse Bioscience XF96 Flux Analyzer in response of increasing doses of glucose (Glu) in the presence or absence of the β3AR agonist BRL37344 1µM (n=8). β3AR stimulation by BRL has no statistically significant impact in the glucose utilization measured as the extracellular acidification rate (dependent on the production of lactic acid). Measurements for the highest concentration of glucose 40mM are represented as bars (lower panel). In graphs, data are means ± SEM. Two-way ANOVA **P<0.01. NS, not significant.

4.3.4 β3-adrenergic receptor overexpression in cardiomyocytes by adeno-associated virus-mediated gene therapy protects against heart failure

Gene therapy has been wildly used in mouse models to overexpressed proteins that have demonstrated beneficial effects *(165, 166)*. Recombinant adeno-associated virus are one of the most used vectors for this purpose due its safety, long term transgene expression and flexibility given the different tropisms of its different serotypes. AAVs have been used in animal models *(167, 168)* and also in clinical trials with heart failure patients *(169)*. We used the AAV based gene therapy approach to overexpress the β3AR in cardiac myocytes of adult C57Bl6J mouse. Mice transduced with $3x10^{11}$ viral genomes/mouse of AAV9-hβ3AR or a control AAV9-EGFP were subjected 4 weeks after AAV injection to TAC surgery and followed by echocardiography for 8 weeks (Fig. 23A, B). Similarly to c-hβ3tg mice, AAV9-hβ3AR mice developed neither cardiac dysfunction (Fig. 23C) nor LV dilation (Fig. 23E, F) induced by pressure overload. LV mass was also decreased towards the end of the experiment suggesting a protection against maladaptive remodeling (Fig. 23D). Total heart weight was also reduced after TAC in AAV9-hβ3AR (Fig. 24A). Lung weight and lung water content were not altered in this experiment implying that mice did not reach a decompensated heart failure stage (Fig. 24B, C). Histological analysis revealed less fibrosis in AAV9-hβ3AR transduced mice (Fig. 24D, E) confirming the antifibrotic effect seen in c-hβ3tg mice.

These data support that AAV based gene therapy is an efficient tool to achieve the cardioprotection afforded by β3AR overexpression already seen in transgenic animal constitutively overexpressing the receptor. With this in mind, we used AAV9-hβ3AR as a therapeutic tool in WT mice during different stages of the disease, compensated hypertrophy and heart failure.

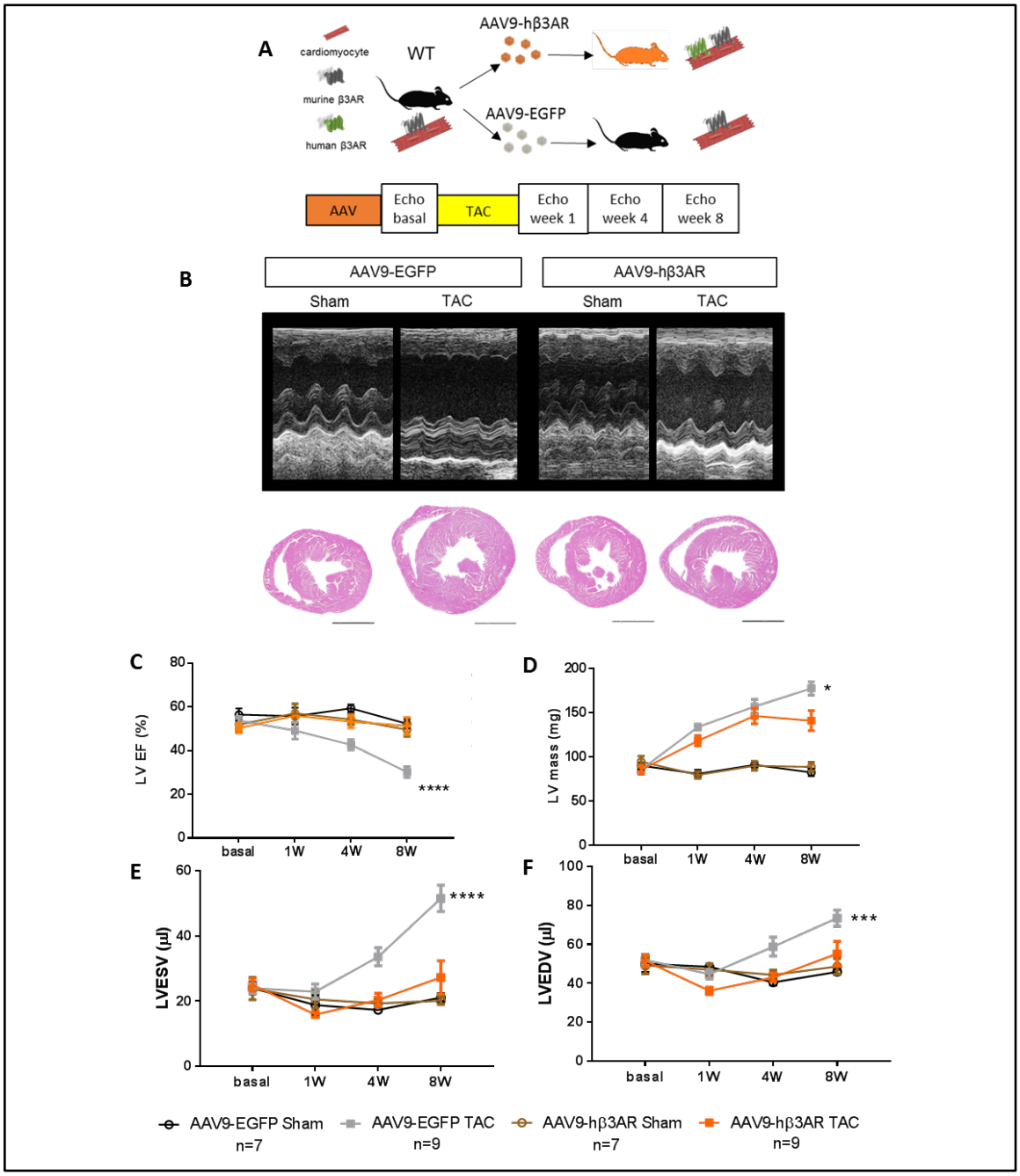

Figure 23: Gene therapy mediated beta3-adrenergic receptor overexpression in cardiomyocytes preserves cardiac function and protects against cardiac hypertrophy and ventricular dilation

(**A**) C57Bl6J WT mice were transduced with $3x10^{11}$ viral genomes/mouse of AAV9-hβ3AR or a control AAV9-EGFP. Four weeks later, mice were subjected to transaortic constriction surgery (TAC) or sham surgery and were followed for 8 weeks. (**B**) Representative left ventricle M-mode echocardiograms (Upper) and heart sections (Lower) 8 weeks after surgery. Scale bar 2mm. (**C, D, E, F**) Echocardiographic evaluation of left ventricular ejection fraction (LVEF), left ventricular mass and left ventricular internal volumes in systole (LVESV) and diastole (LVEDV). AAV9-hβ3AR mice maintained a normal ejection fraction and showed less increase in left ventricular volumes and cardiac mass induced by TAC than AAV9-eGFP control mice. In graphs, data are means ± SEM. Two-way ANOVA, *P<0.05, ***P<0.001, ****P<0.0001 compared to AAV9-hβ3AR TAC.

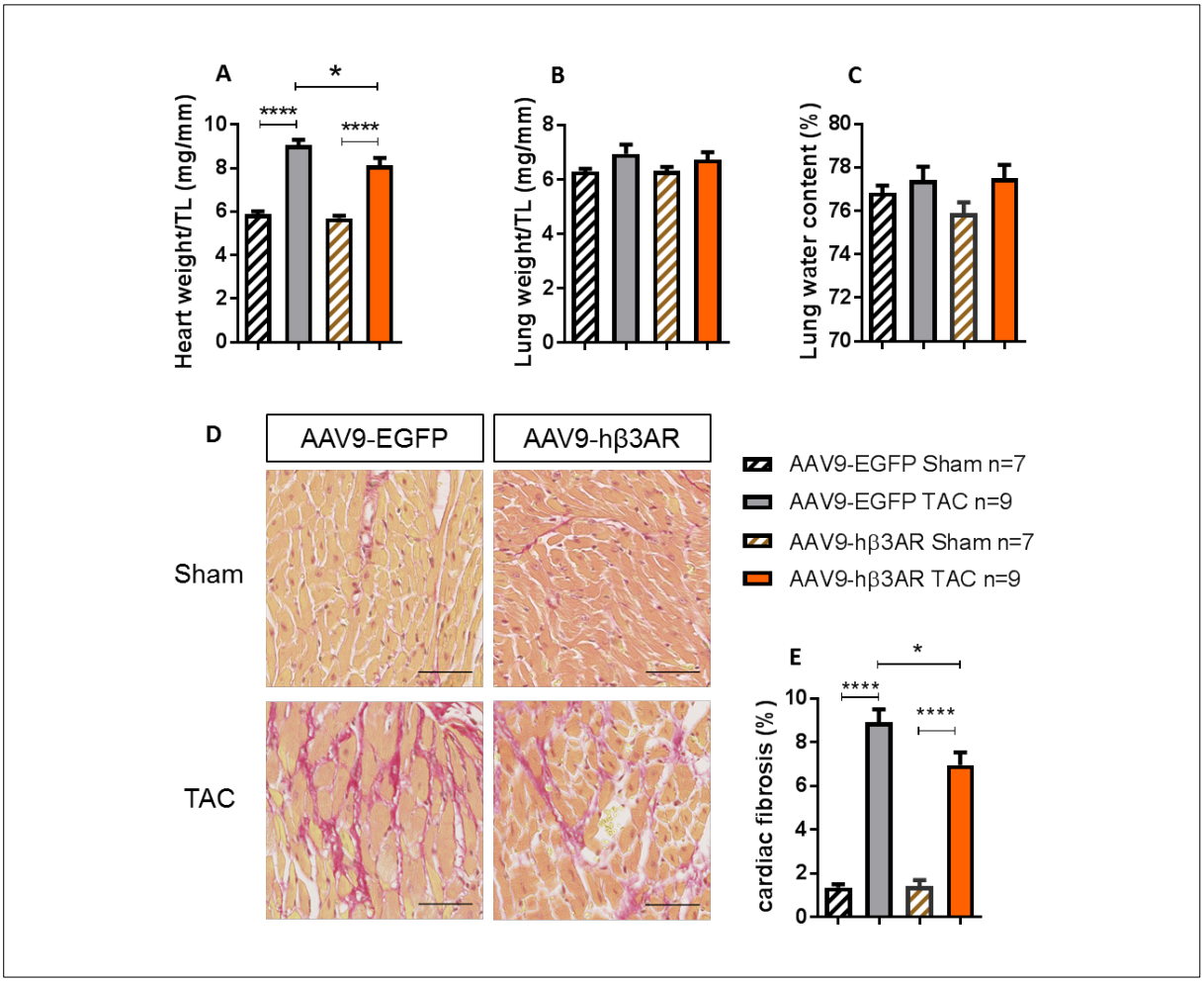

Figure 24: Gene therapy mediated beta3-adrenergic receptor overexpression in cardiomyocytes reduces cardiac remodeling

C57Bl6J WT mice transduced with AAV9-hβ3AR or a control AAV9-EGFP were subjected to TAC or Sham surgery. Eight weeks after surgery mice were euthanized for necropsies and histological studies. (**A**) Heart weight normalized to tibia length (TL). AAV9-hβ3AR mice showed less cardiac hypertrophy induced by TAC. (**B**) Lung weight normalized to tibia length (TL). (**C**) Lung water content as a percentage of fresh lung weight. (**D**) Fibrosis in sham and TAC, AAV9-EGFP and AAV9-hβ3AR mice. Histological images of heart sections stained with sirius red. TAC surgery increased fibrosis in AAV9-EGFP mice. AAV9-hβ3AR mice showed reduced fibrosis induced by TAC. Scale bar 50µm. (**E**) Quantification of the total area of fibrosis in heart sections. n=6-8. In graphs, data are means ± SEM. Two-way ANOVA with Tukey's multiple comparisons test. *P<0.05, ****P<0.0001.

4.3.5 β3-adrenergic receptor gene therapy stops the progression of heart failure

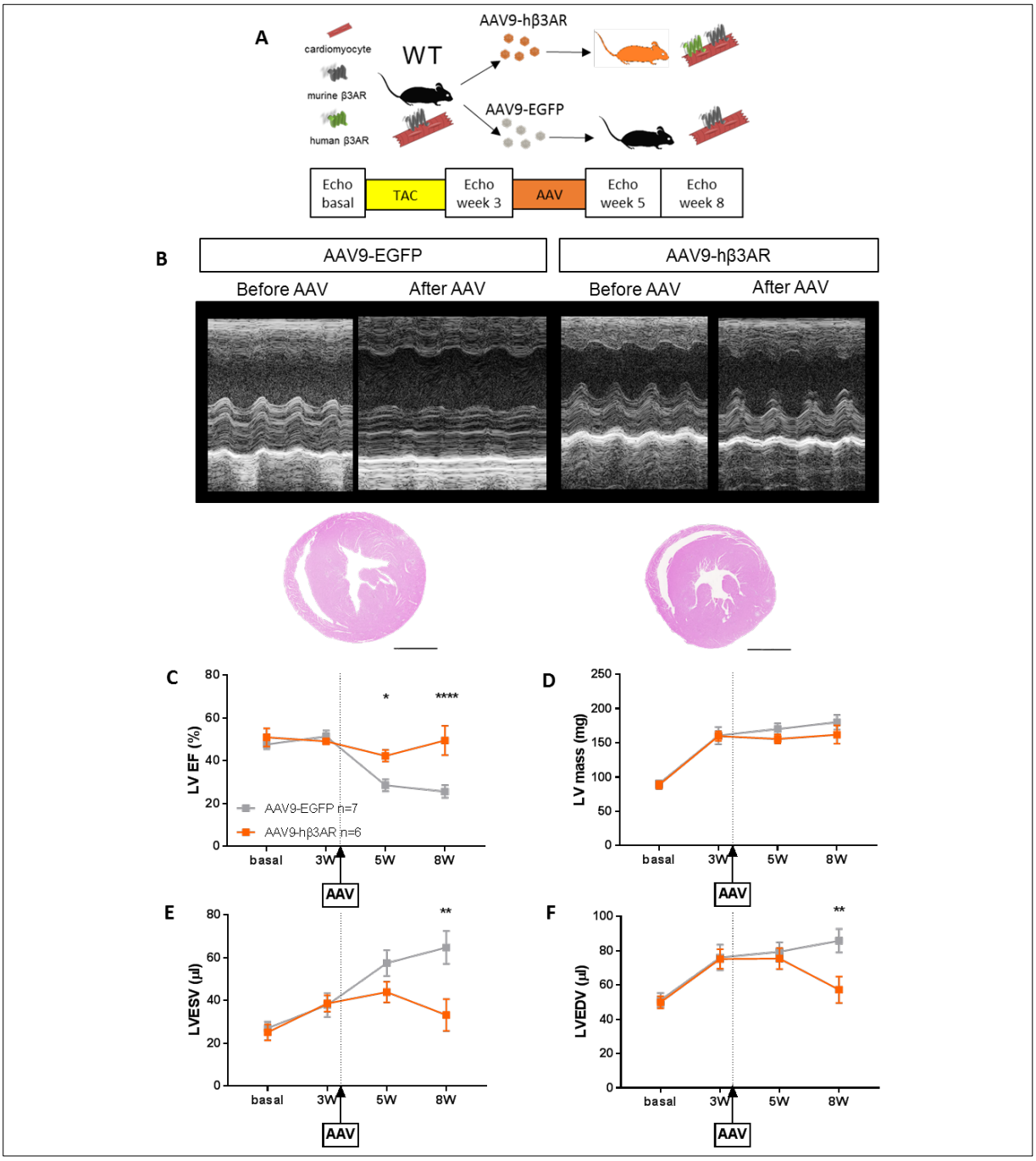

Figure 25: Beta3-adrenergic receptor gene therapy preserves cardiac function and prevents ventricular dilation when administered during compensated cardiac hypertrophy

(**A**) C57Bl6J WT mice were subjected to transaortic constriction surgery (TAC). Three weeks later, mice were transduced with AAV9-hβ3AR (n=6) or a control AAV9-EGFP (n=7). Mice were followed for 5 additional weeks. (**B**) Representative left ventricle M-mode echocardiograms (Upper) and heart sections (Lower) 8 weeks after surgery. Scale bar 2mm. (**C, D, E, F**) Echocardiographic evaluation of left ventricular ejection fraction (LVEF), left ventricular mass and left ventricular internal volumes in systole (LVESV) and diastole (LVEDV). AAV9-hβ3AR mice maintained a normal ejection fraction and showed less increase in left ventricular volumes induced by TAC than AAV9-eGFP control mice. In graphs, data are means ± SEM. Two-way ANOVA with Sidak's multiple comparisons test. , *P<0.05, **P<0.01, ****P<0.0001.

We first explored the effect of overexpressing the β3AR in cardiac myocytes during the compensated hypertrophy stage. C57Bl6J mice were subjected to TAC surgery and allowed to develop cardiac hypertrophy for 3 weeks. At this point, mice were randomized to receive $3x10^{11}$ viral genomes/mouse of AAV9-hβ3AR or control AAV9-EGFP intravenously and were followed for 5 additional weeks (Fig. 25A). AAV9-hβ3AR mice maintained normal LVEF (Fig. 25C) and were protected against ventricular dilation towards the end of the experiement (Fig. 25E, F). Regarding cardiac hypertrophy, AAV9-hβ3AR failed to reduce LV mass (Fig. 25D). This was corroborated by the total heart weight at sacrifice (Fig. 26A). No mice transduced with AAV9-hβ3AR showed an increased lung weight or water content (Fig. 26B, C). Fibrosis showed no changes between groups (Fig. 26D, E). Therefore, overexpression of the β3AR during compensated hypertrophy prevented heart failure but failed to reduce cardiac hypertrophy and fibrosis.

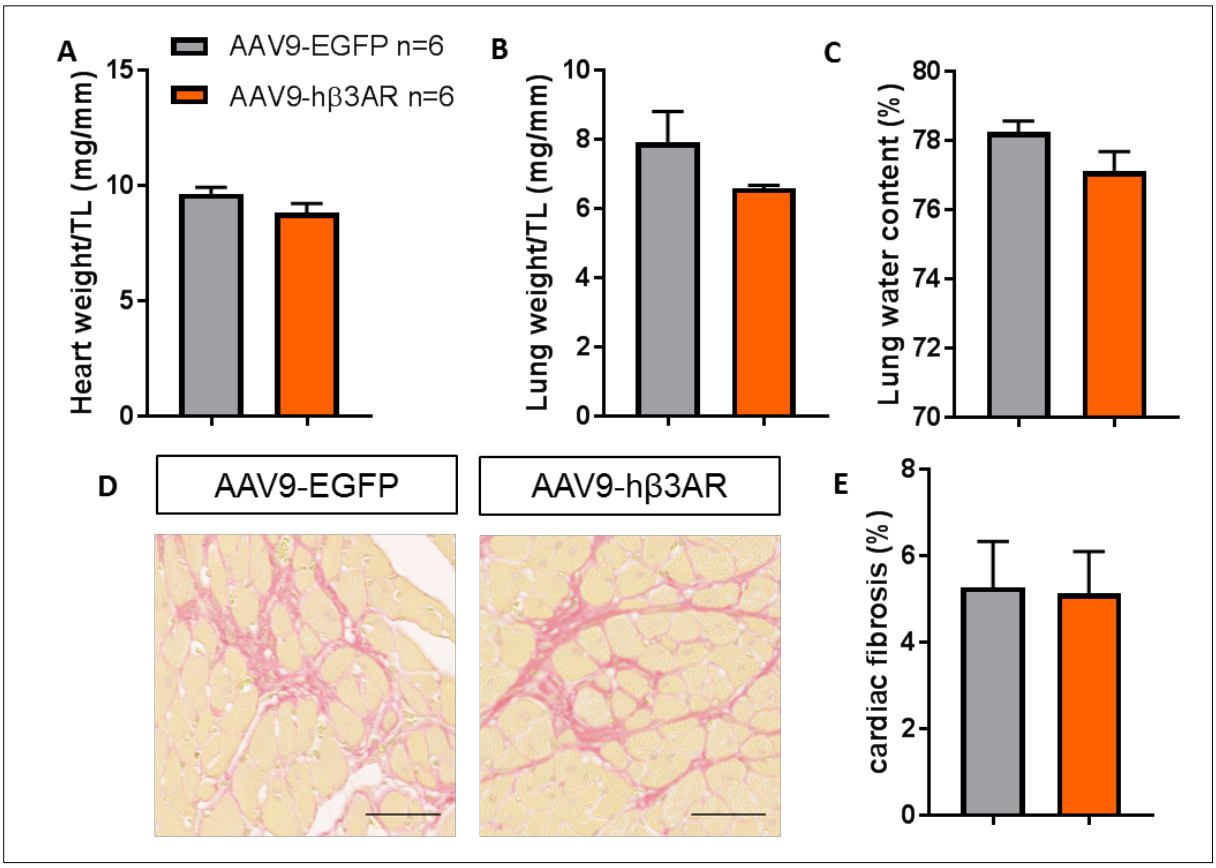

Figure 26: Beta3-adrenergic receptor gene therapy fails to improve cardiac remodeling when cardiac hypertrophy is already established

C57Bl6J WT mice were subjected to transaortic constriction surgery (TAC). Three weeks later, mice were transduced with AAV9-hβ3AR (n=6) or a control AAV9-EGFP (n=6). Eight weeks after surgery mice were euthanized for necropsies and histological studies. (**A**) Heart weight normalized to tibia length (TL). AAV9-hβ3AR failed to decrease cardiac hypertrophy induced by TAC. (**B**) Lung weight normalized to tibia length (TL). (**C**) Lung water content as a percentage of fresh lung weight. (**D**) Fibrosis in sham and TAC, AAV9-EGFP and AAV9-hβ3AR mice. Histological images of heart sections stained with sirius red. AAV9-hβ3AR failed to reduce fibrosis induced by TAC. Scale bar 50μm. (**E**) Quantification of the total area of fibrosis in heart sections. n=6. In graphs, data are means ± SEM.

4.3.6 β3-adrenergic receptor gene therapy reverts heart failure

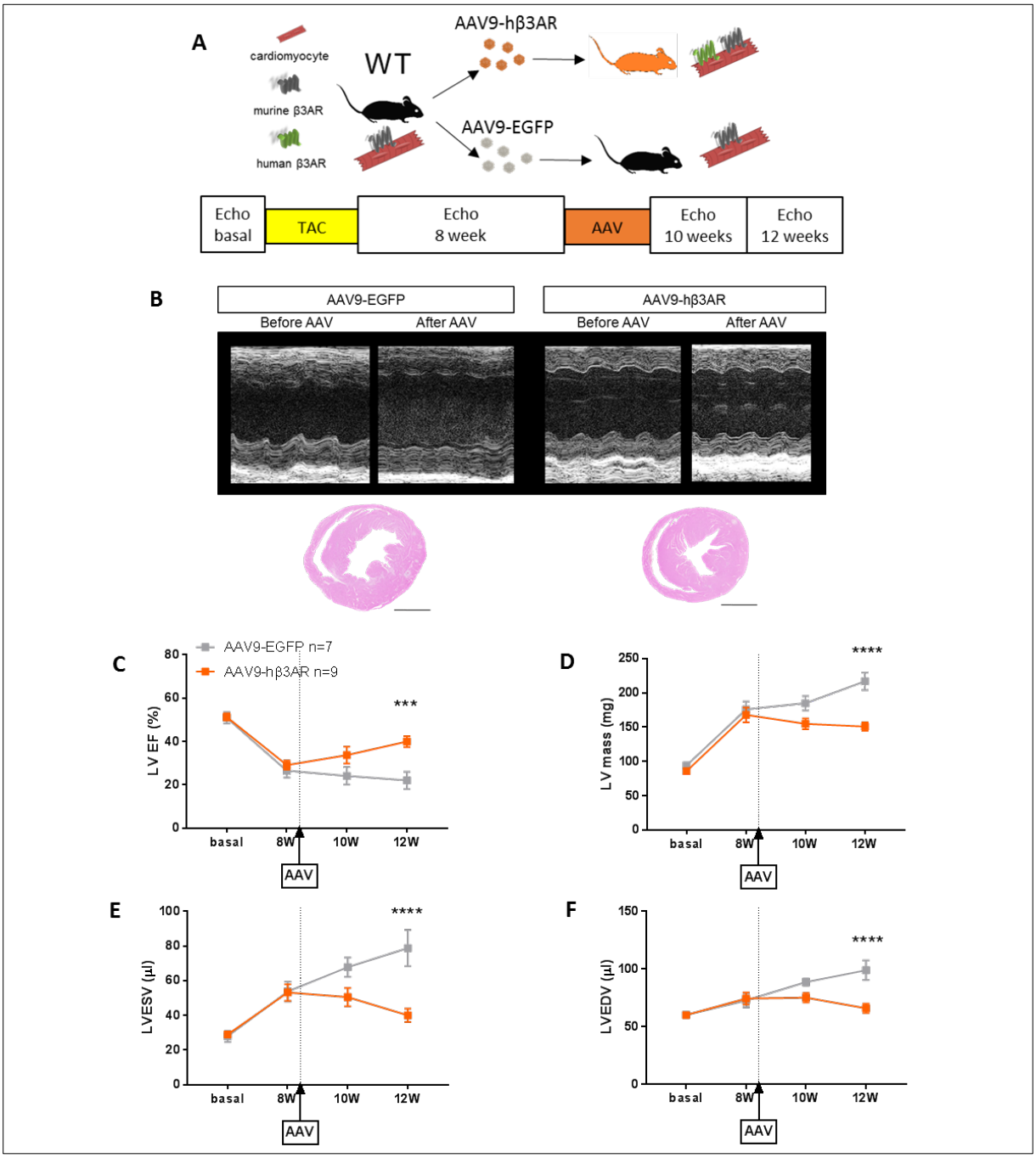

Figure 27: **Beta3-adrenergic receptor gene therapy improves cardiac function and prevents further ventricular dilation in decompensated heart failure**

(**A**) C57Bl6J WT mice were subjected to transaortic constriction surgery (TAC). Eight weeks later, mice were transduced with AAV9-hβ3AR (n=9) or a control AAV9-EGFP (n=7). Mice were followed for 4 additional weeks. (**B**) Representative left ventricle M-mode echocardiograms (Upper) and heart sections (Lower) 12 weeks after surgery. Scale bar 2mm. (**C, D, E, F**) Echocardiographic evaluation of left ventricular ejection fraction (LVEF), left ventricular mass and left ventricular internal volumes in systole (LVESV) and diastole (LVEDV). AAV9-hβ3AR slightly increased ejection fraction and stopped the progression of left ventricular dilation induced by TAC compared to control AAV9-eGFP. In graphs, data are means ± SEM. Two-way ANOVA with Sidak's multiple comparisons test. ***P<0.001, ****P<0.0001.

We next investigated the effect of overexpressing the β3AR in cardiac myocytes during the heart failure stage. C57Bl6J mice were subjected to TAC surgery and were allowed to develop cardiac dysfunction for 8 weeks. At this point, mice presenting less than 40% LVEF were randomized to receive $3x10^{11}$ viral genomes/mouse of AAV9-hβ3AR or control AAV9-EGFP intravenously and were followed for 4 additional weeks (Fig. 27A). Mice receiving AAV9-hβ3AR increased LVEF (Fig. 27C) and were protected against further dilation of the left ventricle (Fig. 27E, F). Regarding cardiac hypertrophy, AAV9-hβ3AR mice maintained LV mass while control mice displayed a notorious increase (Fig. 27D). This was corroborated by the total heart weight at sacrifice (Fig. 28A). Control mice presented a massive increase in lung weight and water content while mice transduced with AAV9-hβ3AR showed normal lungs (Fig. 28B, C). Fibrosis analysis showed no significant changes between groups (Fig. 26D, E). Therefore, overexpression of the β3AR during heart failure is able to revert cardiac dysfunction and prevent cardiac decompensation.

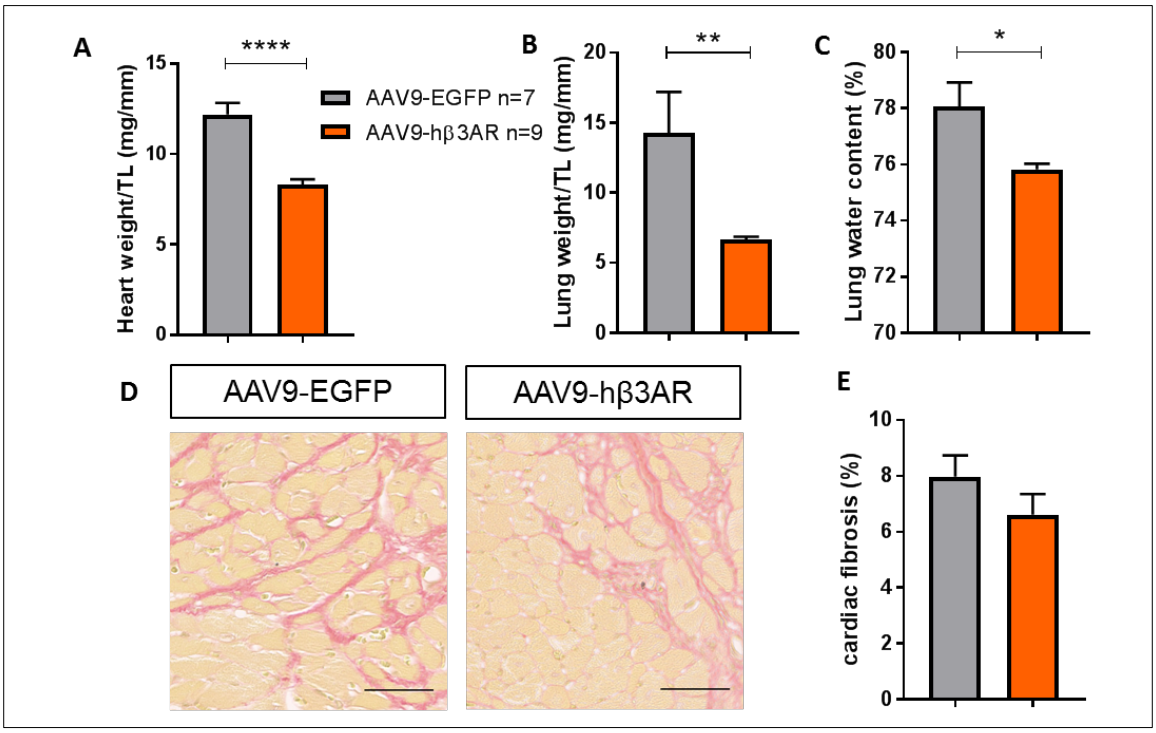

Figure 28: Beta3-adrenergic receptor gene therapy reverts heart failure

C57Bl6J WT mice were subjected to transaortic constriction surgery (TAC). Eight weeks later, mice were transduced with AAV9-hβ3AR (n=9) or a control AAV9-EGFP (n=7). Twelve weeks after surgery mice were euthanized for necropsies and histological studies. (**A**) Heart weight normalized to tibia length (TL). AAV9-hβ3AR mice showed less cardiac hypertrophy induced by TAC. (**B**) Lung weight normalized to tibia length (TL). In control mice presented increased lung weight and pulmonary edema (water content) due to congestive heart failure mice. AAV9-hβ3AR stopped the progression of heart failure. (**C**) Lung water content as a percentage of fresh lung weight. (**D**) Fibrosis in sham and TAC, AAV9-EGFP and AAV9-hβ3AR mice. Histological images of heart sections stained with sirius red. Scale bar 50μm. (**E**) Quantification of the total area of fibrosis in heart sections. n=6-8. In graphs, data are means ± SEM. t test. *P<0.05, **P<0.01, ****P<0.0001.

To summarize, we have demonstrated that overexpression of the β3AR in cardiac myocytes prevents and reverts heart failure. This overexpression is linked to increased FAO, prevention of metabolic switch and mitochondrial structure and size preservation.

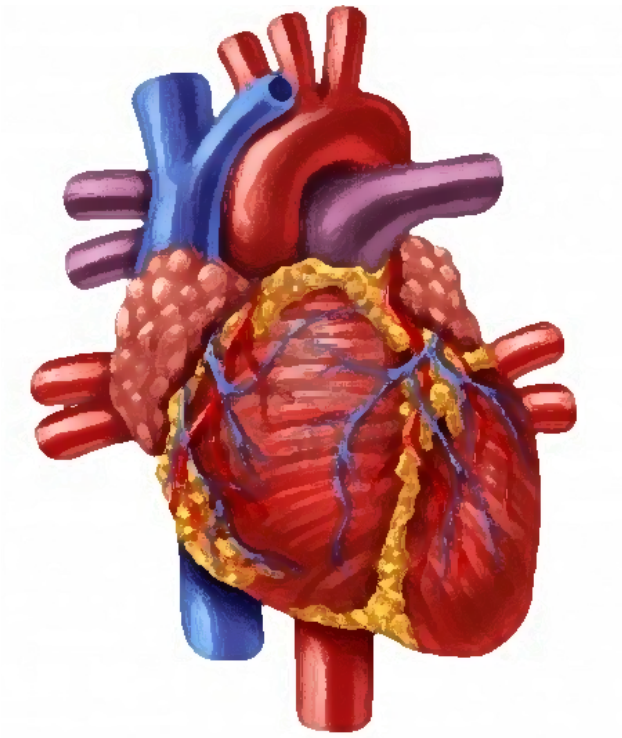

Discussion

5 DISCUSSION

Since its discovery in 1989, the role of the third subtype of the beta-adrenergic receptor family has been extensively discussed. Many groups have studied its implication in the adipose tissue given the strong representation of the β3AR in adipocytes. However recent findings concerning this receptor in the cardiovascular system have increased the interest in the β3AR as a potential target in the treatment of cardiovascular diseases. In order to study the role of this receptor several different animal models have been used. The heterogeneity in the role of this subtype in different species has generated contradictory results. The apparent discrepancies have opened a debate on the implication of the β3AR in the progression of cardiac diseases. Findings in dogs *(126, 170)* and rats *(127)* suggested that β3AR blockage can ameliorate cardiac dysfunction in heart failure and some pharmaceutical companies have shown interested in developing β3AR antagonists. However compelling evidences of a cardioprotective effect of the β3AR stimulation using dog *(171)*, sheep *(140)* and genetically modified mice *(113)* models have led to clinical trials in human patients using β3AR agonists to treat different types of heart failure*(141, 143)*.

This thesis has focused on exploring the role of the β3AR in two key entities of the current state of cardiovascular disease: the ischemia/reperfusion injury and the progression of heart failure.

The role of the β3AR in ischemia/reperfusion injury

Previous studies have demonstrated that β3AR activation protects against ischemia/reperfusion (IR) injury and reduces infarct size *(134, 136)*. The increase in NO production through posttranscriptional modification of eNOS and increase expression of nNOS have been pointed out as responsible for this cardioprotection *(134)*. However the production of NO through the activation of the β3AR has been demonstrated in cardiomyocytes *(109, 113)* and also in coronary endothelial cells *(158)* and both sources of NO have been suggested as actors of the cardioprotective effect of the β3AR stimulation in IR injury. The previous studies that have explored the role of β3AR activation in IR injury have used a pharmacological approach to selectively target the β3AR with two main inconveniences, in one hand several

reports show disagreements with specificity and potency of β3AR agonists *(156, 172, 173)* and on the other hand the pharmacological approach alone does not allow to differentiate the cellular origin of the cardioprotection in vivo. In vitro experiments have been the only way to study the role of this receptor in a particular cell type however these experiments do not replicate the complexity of the in vivo IR injury. In this thesis we have developed genetically engineered mice to be able to precisely target the β3AR activity in one particular cell type in order to understand the cell specific contribution in the cardioprotection afforded by β3AR activation in IR injury. Using β3KO animals in combination with Cre recombinase system, we have generated mice with restricted expression of the β3AR either in endothelial cells or cardiomyocytes. The combination of this restricted expression and the pharmacological stimulation using the specific β3AR agonist mirabegron made it possible to explore the effect of the β3AR in a particular cell type, the cardiac myocyte and the endothelial cell.

It has been demonstrated that β3AR activation in vivo induces hypotension and peripheral vasodilation in different species including mice *(174)*, rats *(173, 175)* and dogs *(176)*. In humans, immunostaining analysis has confirmed the presence of β3AR in coronary microvessels *(98)* and in ex vivo experiments β3AR activation has also demonstrated vasodilatatory effects in human coronary microcirculation *(98, 158)*. Endothelium removal and NOS inhibition strongly decreased the relaxation properties of β3AR agonist in human coronary microarteries and similar results were found in rat thoracic aorta *(177)* suggesting an endothelial NO origin for this vasodilatatory effect. In the present study we show similar results in our transgenic mouse model with restricted expression of the β3AR in the endothelium. Specific endothelial β3AR activation with the selective agonist mirabegron generates vasodilation through NO mediated mechanisms. The beneficial effect on β3AR stimulation in endothelial cells has been demonstrated in a mouse model of myocardial infarction *(139)*. Nebivolol a β1, β2AR antagonist with β3AR agonist properties preserved endothelial NO dependent vasorelaxation effect after myocardial infarction suggesting a protection of the endothelial function mediated by β3AR stimulation. However the only demonstrated direct effect of nevibolol in endothelial cells was the reduction in superoxide production. The possible protective effect of endothelial β3AR activation during myocardial infarction and the increased in endothelial NO production by β3AR agonists have lead to the hypothesis that NO production derived from endothelial β3AR activation could play a role in the cardioprotective effect of the β3AR stimulation in IR injury. One hypothesis is that the NO produced by endothelial cells can diffuse to the cardiac myocytes and provide a protection in these cells and early studies have shown that excreted factors from endothelial cells can

influence cardiac myocytes properties *(178)*. Besides this paracrine effect, another hypothesis is that β3AR activation can reduce endothelial damage induced by IR injury and preserve the endothelial barrier integrity avoiding increased edema, microhemorrhages and cellular infiltration that can cause myocyte death. However, in this study restoration of endothelial β3AR expression in a β3KO background did not show any beneficial effect in IR injury. Confirming these results, targeted stimulation of the β3AR by mirabegron in endothelial cells did not show any impact in infarct size either. Specificity of the human β3AR activation by mirabegron in endothelial cells was previously assessed in myograph in vitro experiments excluding the possibility of a non-functional receptor or a lack of effect of mirabegron. Therefore, we can confirm β3AR activation in endothelial cells is not responsible of the cardioprotection afforded by β3AR stimulation in IR injury.

The protective role of the β3AR in cardiac myocytes has been explored in different in vivo and in vitro models *(113, 133)*. In this study, cardiomyocytes-specific restoration of β3AR expression in a β3KO background resulted in a reduction of the infarct size in an in vivo mouse model of IR injury. This cardioprotective feature was further enhanced when the β3AR was selectively stimulated in cardiac myocytes by mirabegron and isolated cardiac myocytes from these transgenic mice also showed to be protected from hypoxia/reoxygenation injury in vitro. These results confirm initial findings from our group exploring the role of β3AR agonists in hypoxia/reoxygenation in adult isolated cardiac myocytes from WT mice and support the idea of a direct protective action of β3AR stimulation in cardiac myocytes like the delay of the mitochondria permeability transition pore opening *(136)*. Moreover, many authors have linked β3AR with NOS activation and increased NO production in cardiac myocytes *(109, 113, 135)* and NO has been established as a bioactive signaling messenger implicated in many cardioprotective pathways in cardiac myocytes *(179–182)*. Furthermore, β3AR has also been implicated in the stimulation of Na^+-K^+ pump *(140)*. More precisely β3AR protects the β1 subunit of Na^+-K^+ ATPase from inactivation by oxidative S-glutathionylation and maintains the pump activity in high oxidative stress conditions. During ischemia, cardiac myocytes are overloaded with H^+. Oxygenated blood during reperfusion reestablishes a normal extracellular pH and cells release H^+ through H^+-Na^+ pump increasing the intracellular levels of Na^+ that in turn leads to a Ca^{2+} overload in a attempt to decrease Na^+ levels through the Na^+-Ca^{2+} pump *(47)*. We can speculate that activation of the Na^+-K^+ pump by β3AR could help to decrease intracellular excess Na^+ without the fatal consequences of Ca^{2+} overload.

β3AR expression in the heart is low, corresponding only to 2-3% of the total number of cardiac βARs *(101)*. Nevertheless, its activation at the time of reperfusion has clearly shown cardioprotective effects *(134, 136)*. Once we identified the cellular type responsible of the protection afforded by β3AR activation in IR, we explored the potential benefit of overexpressing the β3AR in cardiac myocytes. We found that mice with overexpression of the β3AR in cardiac myocytes showed smaller infarcts compare to mice with regular expression. This result is in line with a previous study suggesting that increased expression of the β3AR in the heart by voluntary exercise protects against IR injury in mice *(135)*. However, whether this enhanced expression resulted in better outcomes in infarct size when β3AR agonist was used at the time of reperfusion was not investigated. Interestingly, in the present study we found that mice overexpressing β3AR in cardiac myocytes showed smaller infarcts than mice with regular expression when the β3AR agonist mirabegron was administered. This result demonstrates that increasing the expression of the receptor in cardiac myocytes in IR injury can maximize the cardioprotection afforded by β3AR agonist therapy.

It has been demonstrated that exercise *(135)*, as well as beta-blockers such as metoprolol *(153, 183, 184)*, can enhance β3AR expression in the heart. This overexpression could result in a reduction of infarct size in patients suffering acute myocardial infarction and could also lead to boost the benefits of using β3AR agonist before reperfusion to reduce IR injury. Therefore, any therapy that enhances β3AR's expression may become a potential recommendation for patients at risk of suffering acute myocardial infarction. Moreover, mirabegron is an FDA approved β3AR agonist *(142)*, clinically indicated for overreactive bladder syndrome and already used in clinical trails for cardiac diseases *(141, 143, 144)*. Our results indicate that mirabegron might have a clinical use in patients with acute myocardial infarction to reduce IR injury when administered before reperfusion although a recent study from our group showed no beneficial effect of mirabegron in the pig model *(185)*. It is important to highlight that in the present study we have explored the role of the human β3AR given the apparent discrepancy of the results generated in other animal models *(126, 127, 170)*.

In summary, this work demonstrates that the cardioprotection afforded by β3AR stimulation in ischemia/reperfusion injury its due to its action in the cardiac myocyte and not in the endothelial cell opening new therapeutic strategies.

The role of the β3AR in heart failure

The beta-adrenergic system plays a mayor role in the progression of HF. In an attempt to maintain cardiac output in a damaged cardiovascular system, increased levels of catecholamines are released to the blood flow. At first, β1AR and β2AR activation by circulating catecholamines increases cardiac function and reduces vascular resistance but these receptors are soon desensitized by GRKs and PKA and are subsequently down regulated. Therefore, the reestablishment of the beta-adrenergic system in HF has been investigated as a way to the increase cardiac function. However, the overexpression of β1AR in cardiac myocytes to increase the inotropic reserves failed to be a successful approach since transgenic mice with higher levels of β1AR developed in basal conditions dilated cardiomyopathy, increased fibrosis and HF at young age *(119)*. Mice with β2AR overexpression in cardiac myocytes showed an enhanced contractility at baseline *(120)* but high levels of the β2AR were found to be deleterious in the TAC mouse model *(123)* suggesting that excessive βAR signaling could be ultimately detrimental to cardiac function.

Regarding the β3AR, its presence in the myocardium is low compared to the other two βARs subtypes *(101)* in physiological conditions but it has been proven to be upregulated in patients with ischemic or dilated cardiomyopathy *(100)*. In transgenic mouse models, β3AR overexpression in cardiac myocytes resulted in reduction of neurohormone-induced hypertrophy *(113)* and a prevention of cardiac fibrosis by a paracrine effect on fibroblasts *(133)*. However, the effect of the β3AR overexpression in HF is still unknown. In this thesis, we demonstrate for the first time that cardiomyocyte specific β3AR overexpression prevents HF using a model of pressure overload maintained until HF stages. β3AR overexpression improved cardiac remodeling and avoided cardiac dysfunction and ventricular size dilation. This cardioprotection is linked to the preservation of cardiac metabolism and mitochondrial viability. Furthermore, we demonstrate that β3AR overexpression by gene transfer using recombinant adeno-associated viral vectors (AAV) can be used as a therapeutic tool to stop the progression of HF in the damaged heart.

We first examined the physiological consequences of the overexpression of the human β3AR (hβ3AR) in our transgenic mouse model. Correct expression of the receptor was assessed

by gene expression evaluation, immunodetection of the reporter protein EGFP and detection of the receptor protein by radioligand binding assay. The functionality of the receptor was evaluated by in vivo stimulation with the β3AR agonist mirabegron. We concluded that stimulation of the hβ3AR expressed in cardiac myocytes produces a positive chronotropic and inotropic effect in vivo as already reported by other authors *(186)*. This experiment was performed in animals lacking the β3AR in all cells except from cardiac myocytes to exclude systemic responses affecting cardiac performance by activation of the β3AR in other compartments like in the vasculature. Confirming this result, a positive inotropic response to the hβ3AR stimulation was also observed in WT mice overexpressing the hβ3AR by AAV gene therapy. Other groups have described opposed results regarding the inotropic effect of the hβ3AR stimulation however the experiments were performed in cardiac tissue ex vivo *(100, 117)*. Interestingly, in another in vivo study, stimulation of the β3AR generated a negative inotropic effect in physiological conditions and a positive inotropic effect in pathological conditions *(140)* suggesting that maybe increased number of this receptor or other variables can affect its coupling.

When subjected to pressure overload by transaortic constriction (TAC), mice overexpressing the hβ3AR in cardiac myocytes (c-hβ3tg) failed to develop HF compared to WT littermates. One of the most important features of this cardioprotection was the duration. Notably, three months after TAC c-hβ3tg mice did not developed neither cardiac dysfunction nor left ventricular dilation and displayed less increase in cardiac mass compared to WT littermates. Decompensated stages of HF were assessed by increased weight of the lungs and fluid buildup in the lungs. Cardiac function was evaluated by non-invasive ultrasound imaging technic revealing a better LVEF in c-hβ3tg mice throughout the entire experiment and these results were confirmed by LV pressure evaluation using an invasive Millar catheter at the end of the experiment. This long term cardioprotective effect of the β3AR can be explained by the lack of phosphorylation sites in the structure of the receptor making it less prompt to desensitization and downregulation *(104)* compared to the other two subtypes of βARs *(80, 81)*.

Features of a compensatory concentric hypertrophy like decreased LV volumes and increased LVEF were evident in c-hβ3tg mice the first week after surgery. These results suggest that mouse endogenous cathecolamines increased after TAC surgery activate the hβ3AR generating a positive inotropic response leading to this concentric hypertrophy. This inotropic response matches with the positive inotropic effect of mirabegron observed in basal

conditions. It has been previously described that the other βAR subtypes β1AR and β2AR have also a positive inotropic effects when they are overexpressed *(118, 119, 120)*. However, the downstream signaling cascade of the β3AR seems to differ from that of the β1AR or the β2AR since the overexpression of these two subtypes generates not only hypertrophy but also myocardial fibrosis, dilated cardiomyopathy and HF *(118, 119, 120)* contrary to the phenotype observed in our c-hβ3tg mice. Moreover, other authors have demonstrated that the overexpression of the hβ3AR in cardiac myocytes produces a downregulation of β1AR and no compensatory changes in β2AR *(114)* ruling out the possibility that the observed increase in contractility is mediated by the other two βAR subtypes.

Adverse cardiac remodeling was also attenuated in c-hβ3tg mice as evaluated by echocardiography and histology. Our results match with a previous study showing that mice lacking the β3AR develop enhanced cardiac hypertrophy with age and present more severe adverse ventricular remodeling when subjected to TAC *(129)*. In addition, another study showed that treatment with BRL 37344, a β3AR agonist, attenuates left ventricular dilation and systolic dysfunction, and partially reduces cardiac hypertrophy induced by TAC in WT mice *(130)*. However, one of the limitation of purely agonist based studies is that the specificity of the β3AR agonists is limited *(156)* and therefore it is difficult to assess the correct dose to maintain β3AR specific stimulation in chronic treatments. In the present study, the genetic approach with the overexpression of the β3AR solves this inconvenience since no drug is needed to observe the specific effect of the receptor. In addition, this genetic approach with cell type specific overexpression shed light about the cellular type responsible of the β3AR-mediated cardioprotection. Until now, it was still unknown what was the cellular type responsible for the protection against HF in the pressure overload model since β3AR is not only present in myocytes but also in coronary endothelial cells in the cardiac tissue *(98–100)*. This study points out the cardiac myocyte as the main responsible of the protection against HF in vivo as suggested by the in vitro experiments performed in NRVM. Regarding fibrosis and hypertrophy, our in vivo results are in line with different studies that explore the antihypertrophic and antifibrotic effect of β3AR using a mouse model with cardiomyocyte specific overexpression *(113, 133)*. However, the present study is the first one that explores the long-term effect of the β3AR in the failing heart.

Previous results in our lab have linked cardiac metabolism and HF *(154)*. Cardiac metabolism is a key player in HF and its correct maintenance is essential for a proper cardiac performance *(187)*. Damage of the cardiac tissue can alter cardiac metabolism and in the same

manner alterations in cardiac metabolism can influence cardiac function. Metabolic intervention has been proven to be a powerful tool to modulate cardiac contractility *(162)*. Free fatty acids (FFA) are the main source of energy in the healthy heart. In HF cardiac metabolism switches from FFA utilization to a preferential use of glucose to obtain energy *(188, 189)*. In TAC failing hearts from WT mice we observed an increase in glucose uptake as already seen by others *(190)*. However, in c-hβ3tg mice we found that switch to glycolytic metabolism was prevented. Mitochondria are the organelles responsible for the metabolism of different substrates and they supply ATP for the high-energy consuming cardiac contraction. Excessive mitochondrial fragmentation is known to impair mitochondrial function and induce metabolic switch to preferential glucose utilization and HF *(154)*. We observed that c-hβ3tg mice had less ultra fragmented mitochondria than controls after TAC and that the ultra structure of their mitochondrion presented more organized cristae suggesting the presence of healthier mitochondria necessary to maintain adequate cardiac metabolism and function in c-hβ3tg mice after TAC.

It has been reported that increase in FFA utilization by the cardiac myocytes has a protective effect in the metabolism and function of the heart. For instance cardiac-specific deletion of acetyl CoA carboxylase 2, an enzyme that blocks FFA entry into the mitochondria, prevents cardiac metabolic switch in the TAC mouse model and attenuates hypertrophy and significantly reduces fibrosis *(190)*. In the same line, a recent study showed that increase in FFA uptake by dietary approach or by increased expression of the FFA translocase CD36 in cardiac myocytes protects the heart against TAC induced HF *(163)*. Interestingly, we found that β3AR activation increases FAO in a FFA dose dependent manner in adult cardiac myocytes suggesting that this could be the mechanism of the cardioprotection afforded by β3AR. Moreover, enhancement in FFA utilization has been linked to decrease in mitochondrial fragmentation in TAC heart failure *(163)* as observed in our model. Supporting the idea of the key role of FAO in the maintenance of cardiac health, other authors have demonstrated that cardiomyocyte specific ablation of the peroxisome proliferator-activated receptor-delta (PPAR-delta), a key regulator of FAO, resulted in cardiac dysfunction, cardiac hypertrophy and congestive HF *(191)*. In humans, it has also been reported that FFA depletion in patients with idiopathic dilated cardiomyopathy aggravates cardiac dysfunction *(192)*.

The cardioprotective effects obtained in the c-hβ3tg transgenic mouse model were confirmed with a different model of overexpression based on adeno-associated virus serotype 9 (AAV9) gene therapy. AAV9 gene therapy was effective in transducing in vivo cardiac

myocytes as already reported by others *(160, 193)* and correct transduction was evaluated four days after viral injection and at the end of every experiment by In Vivo Imaging System using the luminescent signal generated by the reporter protein luciferase after luciferin injection (data not shown). WT mice transduced with AAV9-hβ3AR recapitulated the same features as c-hβ3tg mice with milder protection in cardiac hypertrophy and cardiac fibrosis probably due to a more heterogeneous and weaker overexpression of the receptor but they still displayed a protection against cardiac dysfunction and left ventricular dilation.

Gene therapy gave us the opportunity to explore the role of the overexpression of the hβ3AR as a therapeutic tool. Mice with an established cardiac remodeling at two different stages of HF were transduced with AVV9. Overexpressing the hβ3AR during the compensated phase of cardiac hypertrophy did not reduce the cardiac mass and neither had an impact in cardiac fibrosis suggesting that β3AR can prevent but not reverse hypertrophy or fibrosis. Nevertheless, β3AR was able to prevent ventricular dilation and cardiac dysfunction when overexpressed in hypertrophic hearts. Overexpressing the hβ3AR when cardiac dysfunction was already present improved cardiac function and prevented further dilation of the left ventricle and advanced decompensated stages of HF. However, once again overexpressing the hβ3AR did not show any impact in cardiac fibrosis although a slight trend was observed probably because a second smaller wave of fibrosis was blocked. Interestingly, other authors have observed that cardiomyocyte specific activation of the free fatty acids oxidation pathway by the proliferator-activated receptor alpha (PPAR-alpha) during HF in a mouse TAC model also preserves cardiac function and LV volumes *(194)* and similar results were also found in a porcine model with a pharmacological approach *(195)*.

Our results also match the only in-man trial using mirabegron in chronic HF patients with reduced LVEF, the BEAT-HF trial *(141)*. In this trial stroke volume and LVESV were improved in patients with severe LV dysfunction (LVEF < 40 %) treated with mirabegron compared to placebo group similar to that observed in our experiment where WT mice with cardiac dysfunction (LVEF < 30 %) transduced with AAV9-hβ3AR showed an improvement LVEF and a decrease in LVESV. The authors attribute the beneficial effect of mirabegron to a decrease in oxidative stress by inactivation of NADPH oxidase and subsequent reduction of Na^+-K^+ pump inhibition. However, our study suggests for the first time cardiac metabolism as a key player in the cardioprotection afforded by the β3AR in heart failure.

In summary, this work demonstrates that enhanced expression of β3AR in cardiac myocyte prevents heart failure reducing mitochondrial fragmentation and affecting cardiac metabolism. Furthermore, we demonstrate that β3AR is not only a potential target for the prevention but also for the treatment of heart failure.

Overall, the β3AR has demonstrated to be an important target in two mayor players of cardiovascular diseases, the ischemia/reperfusion injury and the progression of heart failure, opening new strategies for cardiovascular therapies and interventions in the next decade.

LIMITATIONS:

In this thesis, we studied the role of the human β3AR to have a more translational approach. Overexpression of the human receptor in a mouse model may not mimic the exact same properties of the receptor than in humans. Nevertheless, activation of the human receptor by mouse endogenous cathecolamines was proven by signs of concentric hypertrophy during the first week after TAC. The specific molecular pathways involved in the cardioprotection afforded by the β3AR should be further investigated but this doctoral thesis contribute to support the idea of the activation of the β3AR as a therapy for two of the most prevalent problems in clinical cardiology nowadays, IR injury and HF.

Although the human receptor was investigated, animal models of HF are far from the clinical reality since this cardiac condition is influenced by many other factors as diabetes, hypertension, obesity, age, smoking… Similarly, IR model is an open-chest surgery model where the LAD coronary artery is temporally ligated and it is far from recapitulating all the clinical aspects of AMI in patients. However, the observed mechanisms and the use of the FDA approved drug mirabegron to explore the benefits of the hβ3AR activation in this thesis may open new therapeutic avenues for the use of this drug in the clinical arena.

Specific expression of the hβ3AR in different cell type was a powerful tool to elucidate de cellular origin of the β3AR mediated cardioprotection. Nevertheless, studies with specific KO models could also be useful to further confirm our hypothesis adding more information about the role of β3AR.

Concerning HF, because of the apparent discrepancies regarding the beneficial role of the β3AR in HF in different species *(126, 127, 170)* it was important that further studies were

carried out to ensure the cardioprotective role of the β3AR in HF. However β3AR overexpression should be investigated also in other models of HF like myocardial infarction, diabetes or altered mitochondrial dynamics models to ensure its beneficial effect.

The increase in FFA uptake by β3AR overexpression has not been demonstrated in vivo because of the lack of a specific radiomarker. Further experiments should be performed to investigate this hypothesis and assess the activation or the overexpression of different molecules implicated in the FFA uptake and metabolism cascade.

Mitochondrial dynamic profile should be further studied in order to investigate the link between the β3AR and the mitochondrial protection.

In the present study, no specific investigation has been performed regarding the expression levels and the activity of the other βARs subtypes in the different mouse transgenic models.

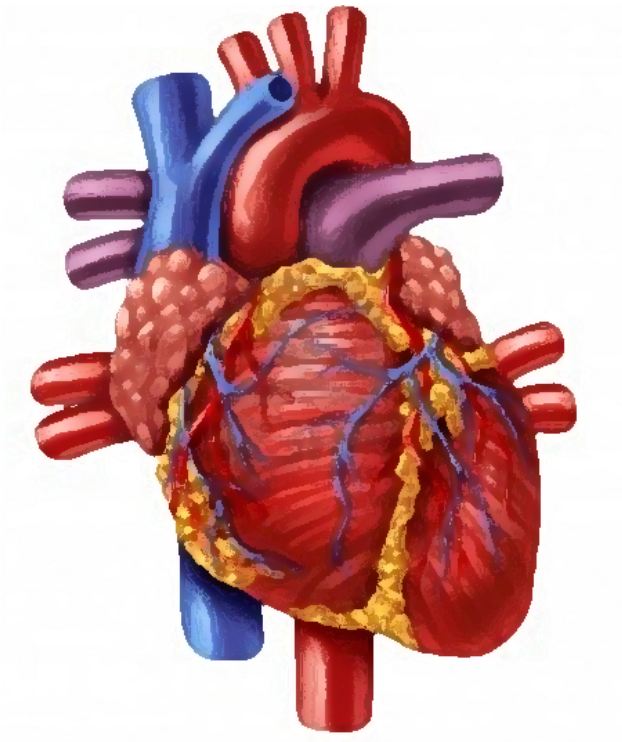

Conclusions

6 CONCLUSIONS

1. In transgenic mice expressing the human β3-adrenergic receptor, its activation in cardiomyocytes generates a positive inotropic and chronotropic response.

2. In transgenic mice expressing the human β3-adrenergic receptor, its activation in endothelial cells generates a vasodilatatory response mediated by nitric oxide synthase activity.

3. Adeno-associated virus serotype 9 mediated gene therapy in mice is an efficient tool to correctly express in vivo a functional human β3-adrenergic receptor in cardiomyocytes.

4. Cardiomyocyte- and not endothelial-specific β3-adrenergic receptor stimulation protects the heart against ischemia/reperfusion injury.

5. Cardiomyocyte-specific β3-adrenergic receptor overexpression protects the heart against ischemia/reperfusion injury and maximizes the cardioprotective effect of the administration of a β3-adrenergic receptor agonist pre-reperfusion.

6. Cardiomyocyte-specific β3-adrenergic receptor overexpression protects against heart failure.

7. Cardiomyocyte-specific β3-adrenergic receptor overexpression increases free fatty acids utilization in cardiomyocyte and also prevents cardiac metabolic switch and reduces mitochondrial fragmentation in heart failure.

8. Gene therapy based cardiomyocyte-specific β3-adrenergic receptor overexpression stops the progression of cardiac damage to further stages of heart failure.

9. Gene therapy based cardiomyocyte-specific β3-adrenergic receptor overexpression reverts heart failure.

CONCLUSIONES

1. En ratones transgénicos que expresan el receptor β3-adrenérgico humano, su activación en cardiomiocitos genera un respuesta inotrópica y cronotrópica positiva.

2. En ratones transgénicos que expresan el receptor β3-adrenérgico humano, su activación en células endoteliales genera un respuesta vasodilatadora mediada por actividad óxido nítrico sintasa.

3.La terapia génica mediada por virus adeno-asociados serotipo 9 es una herramienta eficiente para expresar correctamente in vivo un receptor β3 adrenérgico humano funcional en cardiomiocitos de ratones.

4. La estimulación específica del receptor β3 adrenérgico en cardiomiocitos pero no en células endoteliales protege el corazón frente al daño por isquemia/reperfusión.

5. La sobreexpresión del receptor β3 adrenérgico en cardiomiocitos protege el corazón frente al daño por isquemia/reperfusión y maximiza el efecto cardioprotector de la administración antes de la reperfusión de agonistas del receptor β3 adrenérgico.

6. La sobreexpresión del receptor β3 adrenérgico en cardiomiocitos protege frente a la insuficiencia cardiaca.

7. La sobreexpresión del receptor β3 adrenérgico en cardiomiocitos incrementa la utilización de ácidos grasos libres por el cardiomiocito así como previene el cambio metabólico cardiaco y reduce la fragmentación mitocondrial en la insuficiencia cardiaca.

8. La sobreexpresión del receptor β3 adrenérgico en cardiomiocitos mediante terapia génica frena la progresión del daño cardiaco hacia estados más avanzados de insuficiencia cardiaca.

9. La sobreexpresión del receptor β3 adrenérgico en cardiomiocitos mediante terapia génica revierte la insuficiencia cardiaca.

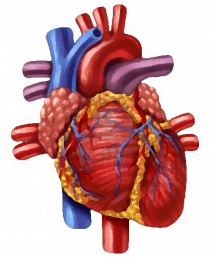

Bibliography

7 BIBLIOGRAPHY

1. A. S. Go, D. Mozaffarian, V. L. Roger, E. J. Benjamin, J. D. Berry, M. J. Blaha, S. Dai, E. S. Ford, C. S. Fox, S. Franco, H. J. Fullerton, C. Gillespie, S. M. Hailpern, J. A. Heit, V. J. Howard, M. D. Huffman, S. E. Judd, B. M. Kissela, S. J. Kittner, D. T. Lackland, J. H. Lichtman, L. D. Lisabeth, R. H. Mackey, D. J. Magid, G. M. Marcus, A. Marelli, D. B. Matchar, D. K. McGuire, E. R. Mohler, C. S. Moy, M. E. Mussolino, R. W. Neumar, G. Nichol, D. K. Pandey, N. P. Paynter, M. J. Reeves, P. D. Sorlie, J. Stein, A. Towfighi, T. N. Turan, S. S. Virani, N. D. Wong, D. Woo, M. B. Turner, American Heart Association Statistics Committee and Stroke Statistics Subcommittee, Heart disease and stroke statistics--2014 update: a report from the American Heart Association. *Circulation* **129**, e28–e292 (2014).

2. J. J. McMurray, M. C. Petrie, D. R. Murdoch, A. P. Davie, Clinical epidemiology of heart failure: public and private health burden., *Eur. Heart J.* **19 Suppl P**, P9-16 (1998).

3. D. Lloyd-Jones, R. J. Adams, T. M. Brown, M. Carnethon, S. Dai, G. De Simone, T. B. Ferguson, E. Ford, K. Furie, C. Gillespie, A. Go, K. Greenlund, N. Haase, S. Hailpern, P. M. Ho, V. Howard, B. Kissela, S. Kittner, D. Lackland, L. Lisabeth, A. Marelli, M. M. McDermott, J. Meigs, D. Mozaffarian, M. Mussolino, G. Nichol, V. L. Roger, W. Rosamond, R. Sacco, P. Sorlie, V. L. Roger, R. Stafford, T. Thom, S. Wasserthiel-Smoller, N. D. Wong, J. Wylie-Rosett, A. H. A. S. C. and S. S. Subcommittee, Heart disease and stroke statistics--2010 update: a report from the American Heart Association., *Circulation* **121**, e46–e215 (2010).

4. D. M. Lloyd-Jones, M. G. Larson, E. P. Leip, A. Beiser, R. B. D'Agostino, W. B. Kannel, J. M. Murabito, R. S. Vasan, E. J. Benjamin, D. Levy, Framingham Heart Study, Lifetime risk for developing congestive heart failure: the Framingham Heart Study. *Circulation* **106**, 3068–72 (2002).

5. E. G. Nabel, E. Braunwald, A Tale of Coronary Artery Disease and Myocardial Infarction. *N. Engl. J. Med.* **366**, 54–63 (2012).

6. Natoinal Institutes of Health, National Institutes of Health, Morbidity & Mortality: 2012 Chart Book on Cardiovascular, Lung, and Blood Diseases. *Natl. Insitutes Heal.* **374**, 1811-1821 (2012).

7. A. P. Ambrosy, G. C. Fonarow, J. Butler, O. Chioncel, S. J. Greene, M. Vaduganathan, S. Nodari, C. S. P. Lam, N. Sato, A. N. Shah, M. Gheorghiade, The Global Health and Economic Burden of Hospitalizations for Heart Failure: Lessons Learned From Hospitalized Heart Failure Registries. *J. Am. Coll. Cardiol.* **63**, 1123–1133 (2014).

8. P. Pazos-López, J. Peteiro-Vázquez, A. Carcía-Campos, L. García-Bueno, J. P. A. de Torres,

A. Castro-Beiras, The causes, consequences, and treatment of left or right heart failure. *Vasc. Health Risk Manag.* **7**, 237–54 (2011).

9. V. L. Burt, J. A. Cutler, M. Higgins, M. J. Horan, D. Labarthe, P. Whelton, C. Brown, E. J. Roccella, Trends in the prevalence, awareness, treatment, and control of hypertension in the adult US population. Data from the health examination surveys, 1960 to 1991. *Hypertens. (Dallas, Tex. 1979)* **26**, 60–9 (1995).

10. L. Bonneux, J. J. Barendregt, K. Meeter, G. J. Bonsel, P. J. van der Maas, Estimating clinical morbidity due to ischemic heart disease and congestive heart failure: the future rise of heart failure. *Am. J. Public Health* **84**, 20–8 (1994).

11. A. L. Bui, T. B. Horwich, G. C. Fonarow, Epidemiology and risk profile of heart failure. *Nat. Rev. Cardiol.* **8**, 30–41 (2011).

12. D. Levy, S. Kenchaiah, M. G. Larson, E. J. Benjamin, M. J. Kupka, K. K. L. Ho, J. M. Murabito, R. S. Vasan, Long-Term Trends in the Incidence of and Survival with Heart Failure. *N. Engl. J. Med.* **347**, 1397–1402 (2002).

13. J. Chen, S.-L. T. Normand, Y. Wang, H. M. Krumholz, National and Regional Trends in Heart Failure Hospitalization and Mortality Rates for Medicare Beneficiaries, 1998-2008. *JAMA* **306**, 1669 (2011).

14. P. Ponikowski, S. D. Anker, K. F. AlHabib, M. R. Cowie, T. L. Force, S. Hu, T. Jaarsma, H. Krum, V. Rastogi, L. E. Rohde, U. C. Samal, H. Shimokawa, B. Budi Siswanto, K. Sliwa, G. Filippatos, Heart failure: preventing disease and death worldwide. *ESC Hear. Fail.* **1**, 4–25 (2014).

15. A. Mosterd, A. W. Hoes, Clinical epidemiology of heart failure. *Heart* **93**, 1137–46 (2007).

16. R. Vigen, T. M. Maddox, L. A. Allen, Aging of the United States population: impact on heart failure. *Curr. Heart Fail. Rep.* **9**, 369–74 (2012).

17. P. S. Jhund, K. Macintyre, C. R. Simpson, J. D. Lewsey, S. Stewart, A. Redpath, J. W. T. Chalmers, S. Capewell, J. J. V McMurray, Long-term trends in first hospitalization for heart failure and subsequent survival between 1986 and 2003: a population study of 5.1 million people. *Circulation* **119**, 515–23 (2009).

18. V. L. Roger, The heart failure epidemic. *Int. J. Environ. Res. Public Health* **7**, 1807–30 (2010).

19. S. Laribi, A. Aouba, M. Nikolaou, J. Lassus, A. Cohen-Solal, P. Plaisance, G. Pavillon, P. Jois, G. C. Fonarow, E. Jougla, A. Mebazaa, Trends in death attributed to heart failure over the past two decades in Europe. *Eur. J. Heart Fail.* **14**, 234–239 (2012).

20. C. A. Wasywich, G. D. Gamble, G. A. Whalley, R. N. Doughty, Understanding changing patterns of survival and hospitalization for heart failure over two decades in New Zealand:

utility of 'days alive and out of hospital' from epidemiological data. *Eur. J. Heart Fail.* **12**, 462–468 (2010).

21. H. Bueno, J. S. Ross, Y. Wang, J. Chen, M. T. Vidán, S.-L. T. Normand, J. P. Curtis, E. E. Drye, J. H. Lichtman, P. S. Keenan, M. Kosiborod, H. M. Krumholz, Trends in length of stay and short-term outcomes among Medicare patients hospitalized for heart failure, 1993-2006. *JAMA* **303**, 2141–7 (2010).

22. J. Chen, K. Dharmarajan, Y. Wang, H. M. Krumholz, National Trends in Heart Failure Hospital Stay Rates, 2001 to 2009. *J. Am. Coll. Cardiol.* **61**, 1078–1088 (2013).

23. M. Schaufelberger, K. Swedberg, M. Köster, M. Rosén, A. Rosengren, Decreasing one-year mortality and hospitalization rates for heart failure in Sweden Data from the Swedish Hospital Discharge Registry 1988 to 2000. *Eur. Heart J.* **25**, 300–307 (2004).

24. V. Askoxylakis, C. Thieke, S. T. Pleger, P. Most, J. Tanner, K. Lindel, H. A. Katus, J. Debus, M. Bischof, Long-term survival of cancer patients compared to heart failure and stroke: a systematic review. *BMC Cancer* **10**, 105 (2010).

25. M. P. Coleman, D. Forman, H. Bryant, J. Butler, B. Rachet, C. Maringe, U. Nur, E. Tracey, M. Coory, J. Hatcher, C. E. McGahan, D. Turner, L. Marrett, M. L. Gjerstorff, T. B. Johannesen, J. Adolfsson, M. Lambe, G. Lawrence, D. Meechan, E. J. Morris, R. Middleton, J. Steward, M. A. Richards, ICBP Module 1 Working Group, Cancer survival in Australia, Canada, Denmark, Norway, Sweden, and the UK, 1995-2007 (the International Cancer Benchmarking Partnership): an analysis of population-based cancer registry data. *Lancet (London, England)* **377**, 127–38 (2011).

26. E. Braunwald, The war against heart failure: The Lancet lecture. *Lancet* **385**, 812-24 (2015).

27. P. Ponikowski, A. A. Voors, S. D. Anker, H. Bueno, J. G. F. Cleland, A. J. S. Coats, V. Falk, J. R. González-Juanatey, V.-P. Harjola, E. A. Jankowska, M. Jessup, C. Linde, P. Nihoyannopoulos, J. T. Parissis, B. Pieske, J. P. Riley, G. M. C. Rosano, L. M. Ruilope, F. Ruschitzka, F. H. Rutten, P. van der Meer, G. Filippatos, J. J. V McMurray, V. Aboyans, S. Achenbach, S. Agewall, N. Al-Attar, J. J. Atherton, J. Bauersachs, A. John Camm, S. Carerj, C. Ceconi, A. Coca, P. Elliott, Ç. Erol, J. Ezekowitz, C. Fernández-Golfín, D. Fitzsimons, M. Guazzi, M. Guenoun, G. Hasenfuss, G. Hindricks, A. W. Hoes, B. Iung, T. Jaarsma, P. Kirchhof, J. Knuuti, P. Kolh, S. Konstantinides, M. Lainscak, P. Lancellotti, G. Y. H. Lip, F. Maisano, C. Mueller, M. C. Petrie, M. F. Piepoli, S. G. Priori, A. Torbicki, H. Tsutsui, D. J. van Veldhuisen, S. Windecker, C. Yancy, J. L. Zamorano, J. L. Zamorano, V. Aboyans, S. Achenbach, S. Agewall, L. Badimon, G. Barón-Esquivias, H. Baumgartner, J. J. Bax, H. Bueno, S. Carerj, V. Dean, Ç. Erol, D. Fitzsimons, O. Gaemperli, P. Kirchhof, P. Kolh, P. Lancellotti, G. Y. H. Lip, P. Nihoyannopoulos, M. F. Piepoli, P. Ponikowski, M. Roffi, A. Torbicki, A. Vaz Carneiro, S.

Windecker, H. S. Sisakian, E. Isayev, A. Kurlianskaya, W. Mullens, M. Tokmakova, P. Agathangelou, V. Melenovsky, H. Wiggers, M. Hassanein, T. Uuetoa, J. Lommi, E. S. Kostovska, Y. Juillière, A. Aladashvili, A. Luchner, C. Chrysohoou, N. Nyolczas, G. Thorgeirsson, J. Marc Weinstein, A. Di Lenarda, N. Aidargaliyeva, G. Bajraktari, M. Beishenkulov, G. Kamzola, T. Abdel-Massih, J. Celutkiene, S. Noppe, A. Cassar, E. Vataman, S. Abir-Khalil, P. van Pol, R. Mo, E. Straburzynska-Migaj, C. Fonseca, O. Chioncel, E. Shlyakhto, P. Otasevic, E. Goncalvesová, M. Lainscak, B. Díaz Molina, M. Schaufelberger, T. Suter, M. B. Yilmaz, L. Voronkov, C. Davies, 2016 ESC Guidelines for the diagnosis and treatment of acute and chronic heart failure. *Eur. Heart J.* **37**, 2129–2200 (2016).

28. J. J. V. McMurray, M. Packer, A. S. Desai, J. Gong, M. P. Lefkowitz, A. R. Rizkala, J. L. Rouleau, V. C. Shi, S. D. Solomon, K. Swedberg, M. R. Zile, Angiotensin–Neprilysin Inhibition versus Enalapril in Heart Failure. *N. Engl. J. Med.* **371**, 993–1004 (2014).

29. K. MacIntyre, S. Capewell, S. Stewart, J. W. Chalmers, J. Boyd, A. Finlayson, A. Redpath, J. P. Pell, J. J. McMurray, Evidence of improving prognosis in heart failure: trends in case fatality in 66 547 patients hospitalized between 1986 and 1995. *Circulation* **102**, 1126–31 (2000).

30. C. W. Yancy, M. Jessup, V. Chair, B. Bozkurt, J. Butler, D. E. Casey, M. H. Drazner, G. C. Fonarow, S. A. Geraci, T. Horwich, J. L. Januzzi, M. R. Johnson, E. K. Kasper, W. C. Levy, F. A. Masoudi, P. E. McBride, J. J. V McMurray, J. E. Mitchell, P. N. Peterson, B. Riegel, F. Sam, L. W. Stevenson, W. H. Wilson Tang, E. J. Tsai, B. L. Wilkoff, C. DE Jr, J. L. Anderson, A. K. Jacobs, N. M. Albert, R. G. Brindis, M. A. Creager, L. H. Curtis, D. DeMets, R. A. Guyton, J. S. Hochman, R. J. Kovacs, F. G. Kushner, E. Magnus Ohman, S. J. Pressler, F. W. Sellke, W.-K. Shen, W. G. Stevenson, 2013 ACCF/AHA Guideline for the Management of Heart Failure: Executive Summary: A Report of the American College of Cardiology Foundation/American Heart Association Task Force on Practice Guidelines. *J. Am. Coll. Cardiol.* **62**, 1495–1539 (2013).

31. C. W. Yancy, M. Jessup, B. Bozkurt, J. Butler, D. E. Casey, M. M. Colvin, M. H. Drazner, G. S. Filippatos, G. C. Fonarow, M. M. Givertz, S. M. Hollenberg, J. Lindenfeld, F. A. Masoudi, P. E. McBride, P. N. Peterson, L. W. Stevenson, C. Westlake, 2017 ACC/AHA/HFSA Focused Update of the 2013 ACCF/AHA Guideline for the Management of Heart Failure: A Report of the American College of Cardiology/American Heart Association Task Force on Clinical Practice Guidelines and the Heart Failure Society of America. *Circulation* **136**, e137–e161 (2017).

32. A. E. Moran, M. H. Forouzanfar, G. A. Roth, G. A. Mensah, M. Ezzati, A. Flaxman, C. J. L. Murray, M. Naghavi, The global burden of ischemic heart disease in 1990 and 2010: the Global Burden of Disease 2010 study. *Circulation* **129**, 1493–501 (2014).

33. L. R. Loehr, W. D. Rosamond, P. P. Chang, A. R. Folsom, L. E. Chambless, Heart Failure

Incidence and Survival (from the Atherosclerosis Risk in Communities Study). *Am. J. Cardiol.* **101**, 1016–1022 (2008).

34. J. S. Gottdiener, A. M. Arnold, G. P. Aurigemma, J. F. Polak, R. P. Tracy, D. W. Kitzman, J. M. Gardin, J. E. Rutledge, R. C. Boineau, Predictors of congestive heart failure in the elderly: the Cardiovascular Health Study. *J. Am. Coll. Cardiol.* **35**, 1628–37 (2000).

35. K. Hogg, K. Swedberg, J. McMurray, Heart failure with preserved left ventricular systolic function. *J. Am. Coll. Cardiol.* **43**, 317–327 (2004).

36. R. Lozano, M. Naghavi, K. Foreman, S. Lim, K. Shibuya, V. Aboyans, J. Abraham, T. Adair, R. Aggarwal, S. Y. Ahn, M. A. AlMazroa, M. Alvarado, H. R. Anderson, L. M. Anderson, K. G. Andrews, C. Atkinson, L. M. Baddour, S. Barker-Collo, D. H. Bartels, M. L. Bell, E. J. Benjamin, D. Bennett, K. Bhalla, B. Bikbov, A. Bin Abdulhak, G. Birbeck, F. Blyth, I. Bolliger, S. Boufous, C. Bucello, M. Burch, P. Burney, J. Carapetis, H. Chen, D. Chou, S. S. Chugh, L. E. Coffeng, S. D. Colan, S. Colquhoun, K. E. Colson, J. Condon, M. D. Connor, L. T. Cooper, M. Corriere, M. Cortinovis, K. C. de Vaccaro, W. Couser, B. C. Cowie, M. H. Criqui, M. Cross, K. C. Dabhadkar, N. Dahodwala, D. De Leo, L. Degenhardt, A. Delossantos, J. Denenberg, D. C. Des Jarlais, S. D. Dharmaratne, E. R. Dorsey, T. Driscoll, H. Duber, B. Ebel, P. J. Erwin, P. Espindola, M. Ezzati, V. Feigin, A. D. Flaxman, M. H. Forouzanfar, F. G. R. Fowkes, R. Franklin, M. Fransen, M. K. Freeman, S. E. Gabriel, E. Gakidou, F. Gaspari, R. F. Gillum, D. Gonzalez-Medina, Y. A. Halasa, D. Haring, J. E. Harrison, R. Havmoeller, R. J. Hay, B. Hoen, P. J. Hotez, D. Hoy, K. H. Jacobsen, S. L. James, R. Jasrasaria, S. Jayaraman, N. Johns, G. Karthikeyan, N. Kassebaum, A. Keren, J.-P. Khoo, L. M. Knowlton, O. Kobusingye, A. Koranteng, R. Krishnamurthi, M. Lipnick, S. E. Lipshultz, S. L. Ohno, J. Mabweijano, M. F. MacIntyre, L. Mallinger, L. March, G. B. Marks, R. Marks, A. Matsumori, R. Matzopoulos, B. M. Mayosi, J. H. McAnulty, M. M. McDermott, J. McGrath, Z. A. Memish, G. A. Mensah, T. R. Merriman, C. Michaud, M. Miller, T. R. Miller, C. Mock, A. O. Mocumbi, A. A. Mokdad, A. Moran, K. Mulholland, M. N. Nair, L. Naldi, K. M. V. Narayan, K. Nasseri, P. Norman, M. O'Donnell, S. B. Omer, K. Ortblad, R. Osborne, D. Ozgediz, B. Pahari, J. D. Pandian, A. P. Rivero, R. P. Padilla, F. Perez-Ruiz, N. Perico, D. Phillips, K. Pierce, C. A. Pope, E. Porrini, F. Pourmalek, M. Raju, D. Ranganathan, J. T. Rehm, D. B. Rein, G. Remuzzi, F. P. Rivara, T. Roberts, F. R. De León, L. C. Rosenfeld, L. Rushton, R. L. Sacco, J. A. Salomon, U. Sampson, E. Sanman, D. C. Schwebel, M. Segui-Gomez, D. S. Shepard, D. Singh, J. Singleton, K. Sliwa, E. Smith, A. Steer, J. A. Taylor, B. Thomas, I. M. Tleyjeh, J. A. Towbin, T. Truelsen, E. A. Undurraga, N. Venketasubramanian, L. Vijayakumar, T. Vos, G. R. Wagner, M. Wang, W. Wang, K. Watt, M. A. Weinstock, R. Weintraub, J. D. Wilkinson, A. D. Woolf, S. Wulf, P.-H. Yeh, P. Yip, A. Zabetian, Z.-J. Zheng, A. D. Lopez, C. J. Murray, Global and regional mortality from 235 causes of death for 20 age groups in 1990 and 2010: a systematic analysis for the Global Burden of Disease Study

2010. *Lancet* **380**, 2095–2128 (2012).

37. D. M. Yellon, D. J. Hausenloy, Myocardial Reperfusion Injury, *N. Engl. J. Med.* **357**, 1121–1135 (2007).

38. A. Torabi, J. G. Cleland, A. S. Rigby, N. Sherwi, Development and course of heart failure after a myocardial infarction in younger and older people. *J. Geriatr. Cardiol.* **11**, 1–12 (2014).

39. B. Ibáñez, G. Heusch, M. Ovize, F. Van de Werf, Evolving Therapies for Myocardial Ischemia/Reperfusion Injury. *J. Am. Coll. Cardiol.* **65**, 1454–1471 (2015).

40. R. B. Jennings, K. A. Reimer, Factors involved in salvaging ischemic myocardium: effect of reperfusion of arterial blood. *Circulation* **68**, I25-36 (1983).

41. P. R. Maroko, P. Libby, W. R. Ginks, C. M. Bloor, W. E. Shell, B. E. Sobel, J. Ross, Jr., Coronary artery reperfusion. I. Early effects on local myocardial function and the extent of myocardial necrosis. *J. Clin. Invest.* **51**, 2710–6 (1972).

42. W. R. Ginks, H. D. Sybers, P. R. Maroko, J. W. Covell, B. E. Sobel, J. Ross, Jr., Coronary artery reperfusion. II. Reduction of myocardial infarct size at 1 week after the coronary occlusion. *J. Clin. Invest.* **51**, 2717–23 (1972).

43. Effectiveness of intravenous thrombolytic treatment in acute myocardial infarction. Gruppo Italiano per lo Studio della Streptochinasi nell'Infarto Miocardico (GISSI). *Lancet (London, England)* **1**, 397–402 (1986).

44. G. W. Reed, J. E. Rossi, C. P. Cannon, Acute myocardial infarction. *Lancet* **389**, 197–210 (2017).

45. B. Ibanez, S. James, S. Agewall, M. J. Antunes, C. Bucciarelli-Ducci, H. Bueno, A. L. P. Caforio, F. Crea, J. A. Goudevenos, S. Halvorsen, G. Hindricks, A. Kastrati, M. J. Lenzen, E. Prescott, M. Roffi, M. Valgimigli, C. Varenhorst, P. Vranckx, P. Widimský, J.-P. Collet, S. D. Kristensen, V. Aboyans, A. Baumbach, R. Bugiardini, I. M. Coman, V. Delgado, D. Fitzsimons, O. Gaemperli, A. H. Gershlick, S. Gielen, V.-P. Harjola, H. A. Katus, J. Knuuti, P. Kolh, C. Leclercq, G. Y. H. Lip, J. Morais, A. N. Neskovic, F.-J. Neumann, A. Niessner, M. F. Piepoli, D. J. Richter, E. Shlyakhto, I. A. Simpson, P. G. Steg, C. J. Terkelsen, K. Thygesen, S. Windecker, J. L. Zamorano, U. Zeymer, S. Windecker, V. Aboyans, S. Agewall, E. Barbato, H. Bueno, A. Coca, J.-P. Collet, I. M. Coman, V. Dean, V. Delgado, D. Fitzsimons, O. Gaemperli, G. Hindricks, B. Iung, P. Jüni, H. A. Katus, J. Knuuti, P. Lancellotti, C. Leclercq, T. McDonagh, M. F. Piepoli, P. Ponikowski, D. J. Richter, M. Roffi, E. Shlyakhto, I. A. Simpson, J. L. Zamorano, M. Chettibi, H. G. Hayrapetyan, B. Metzler, F. Ibrahimov, V. Sujayeva, C. Beauloye, L. Dizdarevic-Hudic, K. Karamfiloff, B. Skoric, L. Antoniades, P. Tousek, P. J. Terkelsen, S. M. Shaheen, T. Marandi, M. Niemelä, S. Kedev, M. Gilard, A. Aladashvili, A. Elsaesser, I. G. Kanakakis, B. Merkely, T. Gudnason, Z. Iakobishvili, L. Bolognese, S. Berkinbayev, G.

Bajraktari, M. Beishenkulov, I. Zake, H. Ben Lamin, O. Gustiene, B. Pereira, R. G. Xuereb, S. Ztot, V. Juliebø, J. Legutko, A. T. Timóteo, G. Tatu-Chiţoiu, A. Yakovlev, L. Bertelli, M. Nedeljkovic, M. Studenčan, M. Bunc, A. M. García de Castro, P. Petursson, R. Jeger, M. S. Mourali, A. Yildirir, A. Parkhomenko, C. P. Gale, 2017 ESC Guidelines for the management of acute myocardial infarction in patients presenting with ST-segment elevation. *Eur. Heart J.* **39**, 119–177 (2018).

46. K. Smolina, F. L. Wright, M. Rayner, M. J. Goldacre, Determinants of the decline in mortality from acute myocardial infarction in England between 2002 and 2010: linked national database study. *BMJ* **344**, d8059 (2012).

47. H. K. Eltzschig, T. Eckle, Ischemia and reperfusion--from mechanism to translation. *Nat. Med.* **17**, 1391–401 (2011).

48. J. Inserte, M. Ruiz-Meana, A. Rodríguez-Sinovas, I. Barba, D. Garcia-Dorado, Contribution of Delayed Intracellular pH Recovery to Ischemic Postconditioning Protection. *Antioxid. Redox Signal.* **14**, 923–939 (2011).

49. C. Steenbergen, M. L. Hill, R. B. Jennings, Volume regulation and plasma membrane injury in aerobic, anaerobic, and ischemic myocardium in vitro. Effects of osmotic cell swelling on plasma membrane integrity. *Circ. Res.* **57**, 864–75 (1985).

50. C. E. Ganote, R. S. Vander Heide, Cytoskeletal lesions in anoxic myocardial injury. A conventional and high-voltage electron-microscopic and immunofluorescence study. *Am. J. Pathol.* **129**, 327–44 (1987).

51. R. S. Vander Heide, C. E. Ganote, Increased myocyte fragility following anoxic injury. *J. Mol. Cell. Cardiol.* **19**, 1085–103 (1987).

52. R. S. Vander Heide, J. P. Angelo, R. A. Altschuld, C. E. Ganote, Energy dependence of contraction band formation in perfused hearts and isolated adult myocytes. *Am. J. Pathol.* **125**, 55–68 (1986).

53. C. E. Ganote, M. A. Sims, R. S. VanderHeide, Mechanism of enzyme release in the calcium paradox. *Eur. Heart J.* **4 Suppl H**, 63–71 (1983).

54. D. Garcia-Dorado, P. Théroux, J. M. Duran, J. Solares, J. Alonso, E. Sanz, R. Munoz, J. Elizaga, J. Botas, F. Fernandez-Avilés, Selective inhibition of the contractile apparatus. A new approach to modification of infarct size, infarct composition, and infarct geometry during coronary artery occlusion and reperfusion. *Circulation* **85**, 1160–74 (1992).

55. M. V. Cohen, X.-M. Yang, J. M. Downey, The pH Hypothesis of Postconditioning: Staccato Reperfusion Reintroduces Oxygen and Perpetuates Myocardial Acidosis. *Circulation* **115**, 1895–1903 (2007).

56. F. Di Lisa, P. Bernardi, Mitochondria and ischemia–reperfusion injury of the heart: Fixing a hole. *Cardiovasc. Res.* **70**, 191–199 (2006).

57. C. Piot, P. Croisille, P. Staat, H. Thibault, G. Rioufol, N. Mewton, R. Elbelghiti, T. T. Cung, E. Bonnefoy, D. Angoulvant, C. Macia, F. Raczka, C. Sportouch, G. Gahide, G. Finet, X. André-Fouët, D. Revel, G. Kirkorian, J.-P. Monassier, G. Derumeaux, M. Ovize, Effect of Cyclosporine on Reperfusion Injury in Acute Myocardial Infarction. *N. Engl. J. Med.* **359**, 473–481 (2008).

58. K. P. Burton, J. M. McCord, G. Ghai, Myocardial alterations due to free-radical generation. *Am. J. Physiol. Circ. Physiol.* **246**, H776–H783 (1984).

59. D. J. Hearse, S. M. Humphrey, G. R. Bullock, The oxygen paradox and the calcium paradox: two facets of the same problem?. *J. Mol. Cell. Cardiol.* **10**, 641–68 (1978).

60. J. M. Zimmet, J. M. Hare, Nitroso-redox interactions in the cardiovascular system. *Circulation* **114**, 1531–44 (2006).

61. W. Grossman, W. J. Paulus, Myocardial stress and hypertrophy: A complex interface between biophysics and cardiac remodeling. *J. Clin. Invest.* **123**, 3701–3703 (2013).

62. A. J. LINZBACH, Heart failure from the point of view of quantitative anatomy. *Am. J. Cardiol.* **5**, 370–82 (1960).

63. W. Grossman, D. Jones, L. P. McLaurin, Wall stress and patterns of hypertrophy in the human left ventricle. *J. Clin. Invest.* **56**, 56–64 (1975).

64. J. J. Hunter, K. R. Chien, F. H. Epstein, Ed. Signaling Pathways for Cardiac Hypertrophy and Failure. *N. Engl. J. Med.* **341**, 1276–1283 (1999).

65. A. SCHAEFER, G. Klein, B. Brand, P. Lippolt, H. Drexler, G. P. Meyer, Evaluation of left ventricular diastolic function by pulsed Doppler tissue imaging in mice. *J. Am. Soc. Echocardiogr.* **16**, 1144–1149 (2003).

66. Q.-Q. Wu, Y. Xiao, Y. Yuan, Z.-G. Ma, H.-H. Liao, C. Liu, J.-X. Zhu, Z. Yang, W. Deng, Q. Tang, Mechanisms contributing to cardiac remodelling. *Clin. Sci.* **131**, 2319–2345 (2017).

67. H. H. Dale, On some physiological actions of ergot. *J. Physiol.* **34**, 163–206 (1906).

68. R. P. Ahlquist, A study of the adrenotropic receptors. *Am. J. Physiol. Content* **153**, 586–600 (1948).

69. A. M. Lands, A. Arnold, J. P. McAuliff, F. P. Luduena, T. G. Brown, Differentiation of receptor systems activated by sympathomimetic amines. *Nature* **214**, 597–8 (1967).

70. L. J. Emorine, S. Marullo, M. M. Briend-Sutren, G. Patey, K. Tate, C. Delavier-Klutchko, A. D. Strosberg, Molecular characterization of the human beta 3-adrenergic receptor. *Science (80-.).* **245**, 1118–21 (1989).

71. D. B. Bylund, D. C. Eikenberg, J. P. Hieble, S. Z. Langer, R. J. Lefkowitz, K. P. Minneman, P. B. Molinoff, R. R. Ruffolo, U. Trendelenburg, International Union of Pharmacology nomenclature of adrenoceptors. *Pharmacol. Rev.* **46**, 121–36 (1994).

72. M. P. Stapleton, Sir James Black and propranolol. The role of the basic sciences in the

history of cardiovascular pharmacology. *Texas Hear. Inst. J.* **24**, 336–42 (1997).

73. J. Bockaert, G-protein coupled receptors. Nobel Prize 2012 for chemistry to Robert J. Lefkowitz and Brian Kobilka. *Med. Sci.* **28**, 1133–1137 (2012).

74. R. A. Dixon, I. S. Sigal, M. R. Candelore, R. B. Register, W. Scattergood, E. Rands, C. D. Strader, Structural features required for ligand binding to the beta-adrenergic receptor. *EMBO J.* **6**, 3269–75 (1987).

75. H. G. Dohlman, M. G. Caron, A. DeBlasi, T. Frielle, R. J. Lefkowitz, Role of extracellular disulfide-bonded cysteines in the ligand binding function of the beta 2-adrenergic receptor. *Biochemistry* **29**, 2335–42 (1990).

76. G. Wallukat, A. Wollenberger, R. Morwinski, H. F. Pitschner, Anti-beta 1-adrenoceptor autoantibodies with chronotropic activity from the serum of patients with dilated cardiomyopathy: mapping of epitopes in the first and second extracellular loops. *J. Mol. Cell. Cardiol.* **27**, 397–406 (1995).

77. J. L. Benovic, L. J. Pike, R. A. Cerione, C. Staniszewski, T. Yoshimasa, J. Codina, M. G. Caron, R. J. Lefkowitz, Phosphorylation of the mammalian beta-adrenergic receptor by cyclic AMP-dependent protein kinase. Regulation of the rate of receptor phosphorylation and dephosphorylation by agonist occupancy and effects on coupling of the receptor to the stimulatory guanine nucleotide regulatory protein. *J. Biol. Chem.* **260**, 7094–101 (1985).

78. W. J. Koch, H. A. Rockman, P. Samama, R. A. Hamilton, R. A. Bond, C. A. Milano, R. J. Lefkowitz, Cardiac function in mice overexpressing the beta-adrenergic receptor kinase or a beta ARK inhibitor. *Science* . **268**, 1350–1353 (1995).

79. L. Kallal, A. W. Gagnon, R. B. Penn, J. L. Benovic, Visualization of agonist-induced sequestration and down-regulation of a green fluorescent protein-tagged beta2-adrenergic receptor. *J. Biol. Chem.* **273**, 322–8 (1998).

80. J. D. Port, L. Y. Huang, C. C. Malbon, Beta-adrenergic agonists that down-regulate receptor mRNA up-regulate a M(r) 35,000 protein(s) that selectively binds to beta-adrenergic receptor mRNAs. *J. Biol. Chem.* **267**, 24103–8 (1992).

81. J. R. Hadcock, M. Ros, C. C. Malbon, Agonist regulation of beta-adrenergic receptor mRNA. Analysis in S49 mouse lymphoma mutants. *J. Biol. Chem.* **264**, 13956–61 (1989).

82. M. R. Bristow, R. Ginsburg, V. Umans, M. Fowler, W. Minobe, R. Rasmussen, P. Zera, R. Menlove, P. Shah, S. Jamieson, Beta 1- and beta 2-adrenergic-receptor subpopulations in nonfailing and failing human ventricular myocardium: coupling of both receptor subtypes to muscle contraction and selective beta 1-receptor down- regulation in heart failure. *Circ. Res.* **59**, 297–309 (1986).

83. O. E. Brodde, Beta 1- and beta 2-adrenoceptors in the human heart: properties, function, and alterations in chronic heart failure. *Pharmacol. Rev.* **43** (1991).

84. B. Xu, J. Li, L. Gao, A. Ferro, Nitric oxide-dependent vasodilatation of rabbit femoral artery by β2-adrenergic stimulation or cyclic AMP elevation *in vivo*. *Br. J. Pharmacol.* **129**, 969–974 (2000).

85. E. N. Dedkova, Y. G. Wang, L. A. Blatter, S. L. Lipsius, Nitric oxide signalling by selective beta2-adrenoceptor stimulation prevents ACh-induced inhibition of beta2-stimulated Ca(2+) current in cat atrial myocytes. *J. Physiol.* **542**, 711–23 (2002).

86. S. Guimarães, D. Moura, Vascular adrenoceptors: an update. *Pharmacol. Rev.* **53**, 319–356 (2001).

87. A. Chruscinski, M. E. Brede, L. Meinel, M. J. Lohse, B. K. Kobilka, L. Hein, Differential distribution of beta-adrenergic receptor subtypes in blood vessels of knockout mice lacking beta(1)- or beta(2)-adrenergic receptors. *Mol. Pharmacol.* **60**, 955–62 (2001).

88. N. Flacco, V. Segura, M. Perez-Aso, S. Estrada, J. F. Seller, F. Jiménez-Altayõ, M. A. Noguera, P. D'Ocon, E. Vila, M. D. Ivorra, Different β-adrenoceptor subtypes coupling to cAMP or NO/cGMP pathways: Implications in the relaxant response of rat conductance and resistance vessels. *Br. J. Pharmacol.* **169**, 413–425 (2013).

89. D. Langin, G. Tavernier, M. Lafontan, Regulation of beta 3-adrenoceptor expression in white fat cells. *Fundam. Clin. Pharmacol.* **9**, 97–106 (1995).

90. M. Lafontan, M. Berlan, Fat cell adrenergic receptors and the control of white and brown fat cell function. *J. Lipid Res.* **34**, 1057–91 (1993).

91. A. M. Cypess, L. S. Weiner, C. Roberts-Toler, E. F. Elía, S. H. Kessler, P. A. Kahn, J. English, K. Chatman, S. A. Trauger, A. Doria, G. M. Kolodny, Activation of human brown adipose tissue by a beta3-adrenergic receptor agonist. *Cell Metab.* **21**, 33–38 (2015).

92. M. H. Fisher, a M. Amend, T. J. Bach, J. M. Barker, E. J. Brady, M. R. Candelore, D. Carroll, M. a Cascieri, S. H. Chiu, L. Deng, M. J. Forrest, B. Hegarty-Friscino, X. M. Guan, G. J. Hom, J. E. Hutchins, L. J. Kelly, R. J. Mathvink, J. M. Metzger, R. R. Miller, H. O. Ok, E. R. Parmee, R. Saperstein, C. D. Strader, R. a Stearns, D. E. MacIntyre, A selective human beta3 adrenergic receptor agonist increases metabolic rate in rhesus monkeys. *J. Clin. Invest.* **101**, 2387–2393 (1998).

93. G. Tavernier, P. Barbe, J. Galitzky, M. Berlan, D. Caput, M. Lafontan, D. Langin, Expression of beta3-adrenoceptors with low lipolytic action in human subcutaneous white adipocytes. *J. Lipid Res.* **37**, 87–97 (1996).

94. J. R. Arch, A. T. Ainsworth, M. A. Cawthorne, V. Piercy, M. V Sennitt, V. E. Thody, C. Wilson, S. Wilson, Atypical beta-adrenoceptor on brown adipocytes as target for anti-obesity drugs. *Nature* **309**, 163–5.

95. M. G. Ursino, V. Vasina, E. Raschi, F. Crema, F. De Ponti, The β3-adrenoceptor as a therapeutic target: Current perspectives. *Pharmacol. Res.* **59**, 221-34 (2009).

96. K. M. Tate, M. M. Briend-Sutren, L. J. Emorine, C. Delavier-Klutchko, S. Marullo, a D. Strosberg, Expression of three human beta-adrenergic-receptor subtypes in transfected Chinese hamster ovary cells. *Eur. J. Biochem.* **196**, 357–61 (1991).

97. C. Gauthier, G. Tavernier, F. Charpentier, D. Langin, H. Le Marec, C. Gauthier, G. Tavernier, F. Charpentier, D. Langin, H. Le Marec, Functional β3-Adrenoceptor in the Human Heart. *J. Clin. Invest* **98**, 556–562 (1996).

98. C. Dessy, S. Moniotte, P. Ghisdal, X. Havaux, P. Noirhomme, J. L. Balligand, Endothelial β3-adrenoceptors mediate vasorelaxation of human coronary microarteries through nitric oxide and endothelium-dependent hyperpolarization. *Circulation* **110**, 948–954 (2004).

99. P. D. Chamberlain, K. H. Jennings, F. Paul, J. Cordell, A. Berry, S. D. Holmes, J. Park, J. Chambers, M. V Sennitt, M. J. Stock, M. A. Cawthorne, P. W. Young, G. J. Murphy, The tissue distribution of the human beta3-adrenoceptor studied using a monoclonal antibody: direct evidence of the beta3-adrenoceptor in human adipose tissue, atrium and skeletal muscle. *Int. J. Obes. Relat. Metab. Disord.* **23**, 1057–65 (1999).

100. S. Moniotte, L. Kobzik, O. Feron, J. N. Trochu, C. Gauthier, J. L. Balligand, Upregulation of β3-Adrenoceptors and Altered Contractile Response to Inotropic Amines in Human Failing Myocardium. *Circulation* **103**, 1649–55 (2001).

101. A. Lymperopoulos, G. Rengo, W. J. Koch, Adrenergic nervous system in heart failure: pathophysiology and therapy. *Circ. Res.* **113**, 739–53 (2013).

102. A. van Spronsen, C. Nahmias, S. Krief, M. M. Briend-Sutren, A. D. Strosberg, L. J. Emorine, The promoter and intron/exon structure of the human and mouse beta 3-adrenergic-receptor genes. *Eur. J. Biochem.* **213**, 1117–24 (1993).

103. B. A. Evans, M. Papaioannou, S. Hamilton, R. J. Summers, Alternative splicing generates two isoforms of the beta3-adrenoceptor which are differentially expressed in mouse tissues. *Br. J. Pharmacol.* **127**, 1525–31 (1999).

104. F. Nantel, H. Bonin, L. J. Emorine, V. Zilberfarb, A. D. Strosberg, M. Bouvier, S. Marullo, The human beta 3-adrenergic receptor is resistant to short term agonist-promoted desensitization. *Mol. Pharmacol.* **43**, 548–55 (1993).

105. B. Rozec, C. Gauthier, β3-Adrenoceptors in the cardiovascular system: Putative roles in human pathologies. *Pharmacol. Ther.* **111**, 652–673 (2006).

106. E. Tagaya, J. Tamaoki, H. Takemura, K. Isono, A. Nagai, Atypical adrenoceptor-mediated relaxation of canine pulmonary artery through a cyclic adenosine monophosphate-dependent pathway. *Lung* **177**, 321–32 (1999).

107. C. Dessy, J. L. Balligand, Beta3-Adrenergic Receptors in Cardiac and Vascular Tissues. Emerging Concepts and Therapeutic Perspectives. *Adv. Pharmacol.* **59**, 135-163 (2010).

108. C. Gauthier, V. Leblais, L. Kobzik, J. N. Trochu, N. Khandoudi, A. Bril, J. L. Balligand, H.

Le Marec, The negative inotropic effect of beta3-adrenoceptor stimulation is mediated by activation of a nitric oxide synthase pathway in human ventricle. *J. Clin. Invest.* **102**, 1377–84 (1998).

109. V. L. Watts, F. M. Sepulveda, O. H. Cingolani, A. S. Ho, X. Niu, R. Kim, K. L. Miller, K. Vandegaer, D. Bedja, K. L. Gabrielson, G. Rameau, B. O'Rourke, D. A. Kass, L. A. Barouch, Anti-hypertrophic and anti-oxidant effect of beta3-adrenergic stimulation in myocytes requires differential neuronal NOS phosphorylation. *J. Mol. Cell. Cardiol.* **62**, 8–17 (2013).

110. X. Zhang, C. Szeto, E. Gao, M. Tang, J. Jin, Q. Fu, C. Makarewich, X. Ai, Y. Li, A. Tang, J. Wang, H. Gao, F. Wang, X. J. Ge, S. P. Kunapuli, L. Zhou, C. Zeng, K. Y. Xiang, X. Chen, Cardiotoxic and cardioprotective features of chronic β-Adrenergic signaling. *Circ. Res.* **112**, 498–509 (2013).

111. C. Pott, D. Steinritz, B. Bölck, U. Mehlhorn, K. Brixius, R. H. G. Schwinger, W. Bloch, eNOS translocation but not eNOS phosphorylation is dependent on intracellular Ca2+ in human atrial myocardium. *Am. J. Physiol. Cell Physiol.* **290**, C1437-45 (2006).

112. A. L. Moens, R. Yang, V. L. Watts, L. A. Barouch, Beta 3-adrenoreceptor regulation of nitric oxide in the cardiovascular system. *J. Mol. Cell. Cardiol.* **48**, 1088-95 (2010).

113. C. Belge, J. Hammond, E. Dubois-Deruy, B. Manoury, J. Hamelet, C. Beauloye, A. Markl, A. C. Pouleur, L. Bertrand, H. Esfahani, K. Jnaoui, K. R. Götz, V. O. Nikolaev, A. Vanderper, P. Herijgers, I. Lobysheva, G. Iaccarino, D. Hilfiker-Kleiner, G. Tavernier, D. Langin, C. Dessy, J. L. Balligand, Enhanced expression of β3-adrenoceptors in cardiac myocytes attenuates neurohormone-induced hypertrophic remodeling through nitric oxide synthase. *Circulation* **129**, 451–462 (2014).

114. T. a Kohout, H. Takaoka, P. H. McDonald, S. J. Perry, L. Mao, R. J. Lefkowitz, H. a Rockman, Augmentation of cardiac contractility mediated by the human beta(3)-adrenergic receptor overexpressed in the hearts of transgenic mice. *Circulation* **104**, 2485–2491 (2001).

115. N. C. Salazar, X. Vallejos, A. Siryk, G. Rengo, A. Cannavo, D. Liccardo, C. De Lucia, E. Gao, D. Leosco, W. J. Koch, A. Lymperopoulos, GRK2 blockade with βARKct is essential for cardiac β2-adrenergic receptor signaling towards increased contractility. *Cell Commun. Signal.* **11**, 64 (2013).

116. A. Cannavo, W. J. Koch, Targeting β3-adrenergic receptors in the heart: Selective agonism and β-blockade. *J. Cardiovasc. Pharmacol.* **69**, 1 (2016).

117. G. Tavernier, G. Toumaniantz, M. Erfanian, M. F. Heymann, K. Laurent, D. Langin, C. Gauthier, β3-adrenergic stimulation produces a decrease of cardiac contractility ex vivo in mice overexpressing the human β3-adrenergic receptor. *Cardiovasc. Res.* **59**, 288–96 (2003).

118. D. R. Sibley, R. J. Lefkowitz, Molecular mechanisms of receptor desensitization using the beta-adrenergic receptor-coupled adenylate cyclase system as a model. *Nature* **317**, 124–9 (1985).

119. S. Engelhardt, L. Hein, F. Wiesmann, M. J. Lohse, Progressive hypertrophy and heart failure in beta1-adrenergic receptor transgenic mice. *Proc. Natl. Acad. Sci. U. S. A.* **96**, 7059–64 (1999).

120. C. A. Milano, L. F. Allen, H. A. Rockman, P. C. Dolber, T. R. McMinn, K. R. Chien, T. D. Johnson, R. A. Bond, R. J. Lefkowitz, Enhanced . *Science.* **264**, 582–586 (1994).

121. S. B. Liggett, N. M. Tepe, J. N. Lorenz, A. M. Canning, T. D. Jantz, S. Mitarai, A. Yatani, G. W. Dorn, Early and delayed consequences of beta(2)-adrenergic receptor overexpression in mouse hearts: critical role for expression level. *Circulation* **101**, 1707–14 (2000).

122. H. A. Rockman, K. R. Chien, D. J. Choi, G. Iaccarino, J. J. Hunter, J. Ross, R. J. Lefkowitz, W. J. Koch, Expression of a beta-adrenergic receptor kinase 1 inhibitor prevents the development of myocardial failure in gene-targeted mice. *Proc. Natl. Acad. Sci. U. S. A.* **95**, 7000–5 (1998).

123. X. J. Du, D. J. Autelitano, R. J. Dilley, B. Wang, A. M. Dart, E. A. Woodcock, β2-adrenergic receptor overexpression exacerbates development of heart failure after aortic stenosis. *Circulation* **101**, 71–7 (2000).

124. S. A. Akhter, C. A. Skaer, A. P. Kypson, P. H. McDonald, K. C. Peppel, D. D. Glower, R. J. Lefkowitz, W. J. Koch, Restoration of beta-adrenergic signaling in failing cardiac ventricular myocytes via adenoviral-mediated gene transfer. *Proc. Natl. Acad. Sci. U. S. A.* **94**, 12100–5 (1997).

125. G. W. Dorn, N. M. Tepe, J. N. Lorenz, W. J. Koch, S. B. Liggett, Low- and high-level transgenic expression of beta2-adrenergic receptors differentially affect cardiac hypertrophy and function in Galphaq-overexpressing mice. *Proc. Natl. Acad. Sci. U. S. A.* **96**, 6400–5 (1999).

126. A. Morimoto, H. Hasegawa, H.-J. Cheng, W. C. Little, C.-P. Cheng, Endogenous β3-adrenoreceptor activation contributes to left ventricular and cardiomyocyte dysfunction in heart failure. *Am. J. Physiol. Circ. Physiol.* **286**, H2425–H2433 (2004).

127. R. Gan, W. Li, C. Xiu, J. Shen, X. Wang, S. Wu, Y. Kong, Chronic blocking of beta 3-adrenoceptor ameliorates cardiac function in rat model of heart failure. *Chin. Med. J. (Engl).* **120**, 2250–5 (2007).

128. S. Zhou, A. Y. Tan, O. Paz, M. Ogawa, C.-C. Chou, H. Hayashi, M. Nihei, M. C. Fishbein, L. S. Chen, S.-F. Lin, P.-S. Chen, Antiarrhythmic effects of beta3-adrenergic receptor stimulation in a canine model of ventricular tachycardia, *Hear. Rhythm* **5**, 289–297 (2008).

129. A. L. Moens, J. S. Leyton-Mange, X. Niu, R. Yang, O. Cingolani, E. K. Arkenbout, H. C.

Champion, D. Bedja, K. L. Gabrielson, J. Chen, Y. Xia, A. B. Hale, K. M. Channon, M. K. Halushka, N. Barker, F. L. Wuyts, P. M. Kaminski, M. S. Wolin, D. A. Kass, L. A. Barouch, Adverse ventricular remodeling and exacerbated NOS uncoupling from pressure-overload in mice lacking the beta3-adrenoreceptor. *J. Mol. Cell. Cardiol.* **47**, 576–85 (2009).

130. X. Niu, V. L. Watts, O. H. Cingolani, V. Sivakumaran, J. S. Leyton-Mange, C. L. Ellis, K. L. Miller, K. Vandegaer, D. Bedja, K. L. Gabrielson, N. Paolocci, D. A. Kass, L. A. Barouch, Cardioprotective effect of beta-3 adrenergic receptor agonism: Role of neuronal nitric oxide synthase. *J. Am. Coll. Cardiol.* **59**, 1979–1987 (2012).

131. B. Wang, M. Xu, W. Li, X. Li, Q. Zheng, X. Niu, Aerobic exercise protects against pressure overload-induced cardiac dysfunction and hypertrophy via β3-AR-nNOS-NO activation. *PLoS One* **12**, e0179648 (2017).

132. J. Wang, M. Li, X. Ma, K. Bai, L. Wang, Z. Yan, T. Lv, Z. Zhao, R. Zhao, H. Liu, W. R. Bauer, Ed. Autoantibodies against the β3-Adrenoceptor Protect from Cardiac Dysfunction in a Rat Model of Pressure Overload. *PLoS One* **8**, e78207 (2013).

133. N. Hermida, L. Michel, H. Esfahani, E. Dubois-Deruy, J. Hammond, C. Bouzin, A. Markl, H. Colin, A. Van Steenbergen, C. De Meester, C. Beauloye, S. Horman, X. Yin, M. Mayr, J.-L. Balligand, Cardiac myocyte β3-adrenergic receptors prevent myocardial fibrosis by modulating oxidant stress-dependent paracrine signaling. *Eur. Heart J.* **39**, 888–898 (2018).

134. J. P. Aragón, M. E. Condit, S. Bhushan, B. L. Predmore, S. S. Patel, D. B. Grinsfelder, S. Gundewar, S. Jha, J. W. Calvert, L. A. Barouch, M. Lavu, H. M. Wright, D. J. Lefer, Beta3-Adrenoreceptor Stimulation Ameliorates Myocardial Ischemia-Reperfusion Injury Via Endothelial Nitric Oxide Synthase and Neuronal Nitric Oxide Synthase Activation. *J. Am. Coll. Cardiol.* **58**, 2683–2691 (2011).

135. J. W. Calvert, M. E. Condit, J. P. Aragon, C. K. Nicholson, B. F. Moody, R. L. Hood, A. L. Sindler, S. Gundewar, D. R. Seals, L. A. Barouch, D. J. Lefer, Exercise Protects Against Myocardial Ischemia-Reperfusion Injury via Stimulation of {beta}3-Adrenergic Receptors and Increased Nitric Oxide Signaling: Role of Nitrite and Nitrosothiols. *Circ. Res.* **108**, 1448–1458 (2011).

136. J. García-Prieto, J. M. García-Ruiz, D. Sanz-Rosa, A. Pun, A. García-Alvarez, S. M. Davidson, L. Fernández-Friera, M. Nuno-Ayala, R. Fernández-Jiménez, J. A. Bernal, J. L. Izquierdo-Garcia, J. Jimenez-Borreguero, G. Pizarro, J. Ruiz-Cabello, C. Macaya, V. Fuster, D. M. Yellon, B. Ibanez, β3 adrenergic receptor selective stimulation during ischemia/reperfusion improves cardiac function in translational models through inhibition of mPTP opening in cardiomyocytes. *Basic Res. Cardiol.* **109**, 422 (2014).

137. Z. Zhang, L. Ding, Z. Jin, G. Gao, H. Li, L. Zhang, L. Zhang, X. Lu, L. Hu, B. Lu, X. Yu, T. Hu,

M. Bader, Ed. Nebivolol Protects against Myocardial Infarction Injury via Stimulation of Beta 3-Adrenergic Receptors and Nitric Oxide Signaling. *PLoS One* **9**, e98179 (2014).

138. X. Niu, L. Zhao, X. Li, Y. Xue, B. Wang, Z. Lv, J. Chen, D. Sun, Q. Zheng, β3-Adrenoreceptor stimulation protects against myocardial infarction injury via eNOS and nNOS activation. *PLoS One* **9**, e98713 (2014).

139. S. A. Sorrentino, C. Doerries, C. Manes, T. Speer, C. Dessy, I. Lobysheva, W. Mohmand, R. Akbar, F. Bahlmann, C. Besler, A. Schaefer, D. Hilfiker-Kleiner, T. F. Lüscher, J.-L. Balligand, H. Drexler, U. Landmesser, Nebivolol Exerts Beneficial Effects on Endothelial Function, Early Endothelial Progenitor Cells, Myocardial Neovascularization, and Left Ventricular Dysfunction Early After Myocardial Infarction Beyond Conventional β1-Blockade. *J. Am. Coll. Cardiol.* **57**, 601–611 (2011).

140. H. Bundgaard, C.-C. Liu, A. Garcia, E. J. Hamilton, Y. Huang, K. K. M. Chia, S. N. Hunyor, G. A. Figtree, H. H. Rasmussen, β3 Adrenergic stimulation of the cardiac Na+-K+ pump by reversal of an inhibitory oxidative modification. *Circulation* **122**, 2699–2708 (2010).

141. H. Bundgaard, A. Axelsson, J. Hartvig Thomsen, M. Sørgaard, K. F. Kofoed, R. Hasselbalch, N. A. S. Fry, N. Valeur, S. Boesgaard, F. Gustafsson, L. Køber, K. Iversen, H. H. Rasmussen, The first-in-man randomized trial of a beta3 adrenoceptor agonist in chronic heart failure: the BEAT-HF trial. *Eur. J. Heart Fail.* **19**, 566–575 (2017).

142. M. Vij, M. J. Drake, Clinical use of the β3 adrenoceptor agonist mirabegron in patients with overactive bladder syndrom. *Ther. Adv. Urol.* **7**, 241–248 (2015).

143. J.-L. Balligand, Cardiac beta3-adrenergic receptors in the clinical arena: the end of the beginning. *Eur. J. Heart Fail.* **19**, 576–578 (2017).

144. A. García-Álvarez, D. Pereda, I. García-Lunar, D. Sanz-Rosa, R. Fernández-Jiménez, J. García-Prieto, M. Nuño-Ayala, F. Sierra, E. Santiago, E. Sandoval, P. Campelos, J. Agüero, G. Pizarro, V. I. Peinado, L. Fernández-Friera, J. M. García-Ruiz, J. A. Barberá, M. Castellá, M. Sabaté, V. Fuster, B. Ibañez, Beta-3 adrenergic agonists reduce pulmonary vascular resistance and improve right ventricular performance in a porcine model of chronic pulmonary hypertension. *Basic Res. Cardiol.* **111**, 49 (2016).

145. K. Vintersten, C. Monetti, M. Gertsenstein, P. Zhang, L. Laszlo, S. Biechele, A. Nagy, Mouse in red: Red fluorescent protein expression in mouse ES cells, embryos, and adult animals. *Genesis* **40**, 241–246 (2004).

146. Y. Y. Kisanuki, R. E. Hammer, J. Miyazaki, S. C. Williams, J. A. Richardson, M. Yanagisawa, Tie2-Cre Transgenic Mice: A New Model for Endothelial Cell-Lineage Analysis in Vivo. *Dev. Biol.* **230**, 230–242 (2001).

147. K. Jiao, H. Kulessa, K. Tompkins, Y. Zhou, L. Batts, H. S. Baldwin, B. L. M. Hogan, An essential role of Bmp4 in the atrioventricular septation of the mouse heart.. *Genes Dev.* **17**,

2362–7 (2003).

148. V. S. Susulic, R. C. Frederich, J. Lawitts, E. Tozzo, B. B. Kahn, M. E. Harper, J. Himms-Hagen, J. S. Flier, B. B. Lowell, Targeted disruption of the beta 3-adrenergic receptor gene. *J. Biol. Chem.* **270**, 29483–92 (1995).

149. P. Pacher, T. Nagayama, P. Mukhopadhyay, S. Bátkai, D. A. Kass, Measurement of cardiac function using pressure-volume conductance catheter technique in mice and rats. *Nat. Protoc.* **3**, 1422–1434 (2008).

150. F. Halberg, H. Mult, G. Cornélissen, D. Hillman, L. A. Beaty, S. Hong, O. Schwartzkopff, Y. Watanabe, K. Otsuka, J. Siegelova, Chronobiologically Interpreted Ambulatory Blood Pressure Monitoring in Health and Disease. *Glob. Adv. Heal. Med.* **1**, 66–123 (2012).

151. R. Agarwal, Regulation of circadian blood pressure: from mice to astronauts. *Curr. Opin. Nephrol. Hypertens.* **19**, 51–58 (2010).

152. L. Campo, M. Ferrer, in *Methods in Mouse Atherosclerosis*. (2015), vol. 1339, pp. 255–276.

153. A. Cannavo, G. Rengo, D. Liccardo, A. Pun, E. Gao, A. J. George, G. Gambino, A. Rapacciuolo, D. Leosco, B. Ibanez, N. Ferrara, N. Paolocci, W. J. Koch, β1-Blockade Prevents Post-Ischemic Myocardial Decompensation Via β3AR-Dependent Protective Sphingosine-1 Phosphate Signaling. *J. Am. Coll. Cardiol.* **70**, 182–192 (2017).

154. T. Wai, J. García-Prieto, M. J. Baker, C. Merkwirth, P. Benit, P. Rustin, F. J. Rupérez, C. Barbas, B. Ibañez, T. Langer, Imbalanced OPA1 processing and mitochondrial fragmentation cause heart failure in mice. *Science* **350** 350(6265):aad0116 (2015).

155. F. M. Cruz, D. Sanz-Rosa, M. Roche-Molina, J. García-Prieto, J. M. García-Ruiz, G. Pizarro, L. J. Jiménez-Borreguero, M. Torres, A. Bernad, J. Ruíz-Cabello, V. Fuster, B. Ibáñez, J. A. Bernal, Exercise triggers ARVC phenotype in mice expressing a disease-causing mutated version of human plakophilin-2. *J. Am. Coll. Cardiol.* **65**, 1438–1450 (2015).

156. J. G. Baker, The selectivity of beta-adrenoceptor agonists at human beta1-, beta2- and beta3-adrenoceptors. *Br. J. Pharmacol.* **160**, 1048–61 (2010).

157. C. Hoffmann, M. R. Leitz, S. Oberdorf-Maass, M. J. Lohse, K. N. Klotz, Comparative pharmacology of human β-adrenergic receptor subtypes - Characterization of stably transfected receptors in CHO cells. *Naunyn. Schmiedebergs. Arch. Pharmacol.* **369**, 151–159 (2004).

158. C. Dessy, J. Saliez, P. Ghisdal, G. Daneau, I. I. Lobysheva, F. Frérart, C. Belge, K. Jnaoui, P. Noirhomme, O. Feron, J. L. Balligand, Endothelial β3-adrenoreceptors mediate nitric oxide-dependent vasorelaxation of coronary microvessels in response to the third-generation β-blocker nebivolol. *Circulation* **112**, 1198–1205 (2005).

159. C. A. Pacak, C. S. Mah, B. D. Thattaliyath, T. J. Conlon, M. A. Lewis, D. E. Cloutier, I.

Zolotukhin, A. F. Tarantal, B. J. Byrne, Recombinant adeno-associated virus serotype 9 leads to preferential cardiac transduction in vivo. *Circ. Res.* **99**, e3-9 (2006).

160. P. R. Konkalmatt, R. J. Beyers, D. M. O'Connor, Y. Xu, M. E. Seaman, B. A. French, Cardiac-selective expression of extracellular superoxide dismutase after systemic injection of adeno-associated virus 9 protects the heart against post-myocardial infarction left ventricular remodeling. *Circ. Cardiovasc. Imaging* **6**, 478-86 (2013).

161. S. C. Kolwicz, R. Tian, R. Tian, Glucose metabolism and cardiac hypertrophy. *Cardiovasc. Res.* **90**, 194–201 (2011).

162. L. Chen, J. Song, S. Hu, Metabolic remodeling of substrate utilization during heart failure progression. *Heart Fail. Rev.* , 1–12 (2018).

163. Y. Guo, Z. Wang, X. Qin, J. Xu, Z. Hou, H. Yang, X. Mao, W. Xing, X. Li, X. Zhang, F. Gao, Enhancing fatty acid utilization ameliorates mitochondrial fragmentation and cardiac dysfunction via rebalancing optic atrophy 1 processing in the failing heart. *Cardiovasc. Res.* **114**, 1–13 (2018).

164. K. Y. Goh, J. Qu, H. Hong, T. Liu, L. J. Dell'Italia, Y. Wu, B. O'Rourke, L. Zhou, Impaired mitochondrial network excitability in failing guinea-pig cardiomyocytes. *Cardiovasc. Res.* **109**, 79–89 (2016).

165. G. Rengo, C. Zincarelli, G. Femminella, D. Liccardo, G. Pagano, C. de Lucia, G. Altobelli, V. Cimini, D. Ruggiero, P. Perrone-Filardi, E. Gao, N. Ferrara, A. Lymperopoulos, W. Koch, D. Leosco, Myocardial β2-adrenoceptor gene delivery promotes coordinated cardiac adaptive remodelling and angiogenesis in heart failure. *Br. J. Pharmacol.* **166**, 2348–2361 (2012).

166. S. T. Pleger, A. Remppis, B. Heidt, M. Völkers, J. K. Chuprun, M. Kuhn, R. H. Zhou, E. Gao, G. Szabo, D. Weichenhan, O. J. Müller, A. D. Eckhart, H. A. Katus, W. J. Koch, P. Most, S100A1 gene therapy preserves in vivo cardiac function after myocardial infarction. *Mol. Ther.* **12**, 1120-1129 (2005).

167. S. T. Pleger, P. Most, M. Boucher, S. Soltys, J. K. Chuprun, W. Pleger, E. Gao, A. Dasgupta, G. Rengo, A. Remppis, H. A. Katus, A. D. Eckhart, J. E. Rabinowitz, W. J. Koch, Stable Myocardial-Specific AAV6-S100A1 Gene Therapy Results in Chronic Functional Heart Failure Rescue. *Circulation* **115**, 2506–2515 (2007).

168. S. T. Pleger, C. Shan, J. Ksienzyk, R. Bekeredjian, P. Boekstegers, R. Hinkel, S. Schinkel, B. Leuchs, J. Ludwig, G. Qiu, C. Weber, P. Raake, W. J. Koch, H. A. Katus, O. J. Müller, P. Most, Cardiac AAV9-S100A1 gene therapy rescues post-ischemic heart failure in a preclinical large animal model. *Sci. Transl. Med.* **3**, 92ra64 (2011).

169. B. E. Jaski, M. L. Jessup, D. M. Mancini, T. P. Cappola, D. F. Pauly, B. Greenberg, K. Borow, H. Dittrich, K. M. Zsebo, R. J. Hajjar, Calcium Up-Regulation by Percutaneous Administration of Gene Therapy In Cardiac Disease (CUPID) Trial Investigators, Calcium

upregulation by percutaneous administration of gene therapy in cardiac disease (CUPID Trial), a first-in-human phase 1/2 clinical trial. *J. Card. Fail.* **15**, 171–81 (2009).

170. S. Masutani, H.-J. Cheng, A. Morimoto, H. Hasegawa, Q.-H. Han, W. C. Little, C. P. Cheng, β3-Adrenergic receptor antagonist improves exercise performance in pacing-induced heart failure. *Am. J. Physiol. Heart Circ. Physiol.* **305**, H923-30 (2013).

171. J. L. Montastruc, P. Verwaerde, M. Pelat, J. Galitzky, D. Langin, M. Lafontan, M. Berlan, Peripheral cardiovascular actions of SR 58611 A, a beta 3-adrenoceptor agonist, in the dog: Lack of central effect. *Fundam. Clin. Pharmacol.* **13**, 180–186 (1999).

172. H. Cernecka, C. Sand, M. C. Michel, The odd sibling: features of β3-adrenoceptor pharmacology. *Mol. Pharmacol.* **86**, 479–84 (2014).

173. Y.-T. Shen, P. Cervoni, T. Claus, S. F. Vatner, Differences in beta 3-adrenergic receptor cardiovascular regulation in conscious primates, rats and dogs. *J. Pharmacol. Exp. Ther.* **278**, 1435–1443 (1996).

174. D. K. Rohrer, A. Chruscinski, E. H. Schauble, D. Bernstein, B. K. Kobilka, Cardiovascular and Metabolic Alterations in Mice Lacking Both β1- and β2-Adrenergic Receptors. *J. Biol. Chem.* **274**, 16701–16708 (1999).

175. T. T. Shen, H. Zhang, S. F. Vatner, Peripheral vascular effects of beta-3 adrenergic receptor stimulation in conscious dogs. *J. Pharmacol. Exp. Ther.* **268**, 466–473 (1994).

176. G. Tavernier, J. Galitzky, A. Bousquet-Melou, J. L. Montastruc, M. Berlan, The positive chronotropic effect induced by BRL 37344 and CGP 12177, two beta-3 adrenergic agonists, does not involve cardiac beta adrenoceptors but baroreflex mechanisms. *J. Pharmacol. Exp. Ther.* **263**, 1083–90 (1992).

177. J. N. Trochu, V. Leblais, Y. Rautureau, F. Bévérelli, H. Le Marec, A. Berdeaux, C. Gauthier, Beta 3-adrenoceptor stimulation induces vasorelaxation mediated essentially by endothelium-derived nitric oxide in rat thoracic aorta. *Br. J. Pharmacol.* **128**, 69–76 (1999).

178. J. A. Smith, A. M. Shah, M. J. Lewis, Factors released from endocardium of the ferret and pig modulate myocardial contraction. *J. Physiol.* **439**, 1–14 (1991).

179. R. Schulz, M. Kelm, G. Heusch, Nitric oxide in myocardial ischemia/reperfusion injury. *Cardiovasc. Res.* **61**, 402–413 (2004).

180. G. Heusch, K. Boengler, R. Schulz, Cardioprotection: nitric oxide, protein kinases, and mitochondria. *Circulation* **118**, 1915–9 (2008).

181. M. Seddon, A. M. Shah, B. Casadei, Cardiomyocytes as effectors of nitric oxide signalling. *Cardiovasc. Res.* **75**, 315–326 (2007).

182. E. Murphy, C. Steenbergen, Mechanisms underlying acute protection from cardiac ischemia-reperfusion injury. *Physiol. Rev.* **88**, 581–609 (2008).

183. D. M. Trappanese, Y. Liu, R. C. McCormick, A. Cannavo, G. Nanayakkara, M. M. Baskharoun, H. Jarrett, F. J. Woitek, D. M. Tillson, A. R. Dillon, F. A. Recchia, J.-L. Balligand, S. R. Houser, W. J. Koch, L. J. Dell'Italia, E. J. Tsai, Chronic β1-adrenergic blockade enhances myocardial β3-adrenergic coupling with nitric oxide-cGMP signaling in a canine model of chronic volume overload: new insight into mechanisms of cardiac benefit with selective β1-blocker therapy. *Basic Res. Cardiol.* **110**, 456 (2015).

184. V. Sharma, H. Parsons, M. F. Allard, J. H. McNeill, Metoprolol increases the expression of β3-adrenoceptors in the diabetic heart: Effects on nitric oxide signaling and forkhead transcription factor-3. *Eur. J. Pharmacol.* **595**, 44–51 (2008).

185. X. Rossello, A. Piñero, R. Fernández-Jiménez, J. Sánchez-González, G. Pizarro, C. Galán-Arriola, M. Lobo-Gonzalez, J. P. Vilchez, J. García-Prieto, J. M. García-Ruiz, A. García-Álvarez, D. Sanz-Rosa, B. Ibanez, Mirabegron, a Clinically Approved β3 Adrenergic Receptor Agonist, Does Not Reduce Infarct Size in a Swine Model of Reperfused Myocardial Infarction. *J. Cardiovasc. Transl. Res.* **11**, 310–318 (2018).

186. C. A. Milano, L. F. Allen, H. A. Rockman, P. C. Dolber, T. R. McMinn, K. R. Chien, T. D. Johnson, R. A. Bond, R. J. Lefkowitz, Enhanced myocardial function in transgenic mice overexpressing the beta 2-adrenergic receptor. *Science .* **264**, 582–6 (1994).

187. A. R. Wende, M. K. Brahma, G. R. McGinnis, M. E. Young, Metabolic Origins of Heart Failure. *JACC. Basic to Transl. Sci.* **2**, 297–310 (2017).

188. J. C. Osorio, W. C. Stanley, A. Linke, M. Castellari, Q. N. Diep, A. R. Panchal, T. H. Hintze, G. D. Lopaschuk, F. A. Recchia, Impaired myocardial fatty acid oxidation and reduced protein expression of retinoid X receptor-alpha in pacing-induced heart failure. *Circulation* **106**, 606–12 (2002).

189. T. Kato, S. Niizuma, Y. Inuzuka, T. Kawashima, J. Okuda, Y. Tamaki, Y. Iwanaga, M. Narazaki, T. Matsuda, T. Soga, T. Kita, T. Kimura, T. Shioi, Analysis of Metabolic Remodeling in Compensated Left Ventricular Hypertrophy and Heart Failure. *Circ. Hear. Fail.* **3**, 420–430 (2010).

190. S. C. Kolwicz, D. P. Olson, L. C. Marney, L. Garcia-Menendez, R. E. Synovec, R. Tian, R. Tian, Cardiac-specific deletion of acetyl CoA carboxylase 2 prevents metabolic remodeling during pressure-overload hypertrophy. *Circ. Res.* **111**, 728–38 (2012).

191. L. Cheng, G. Ding, Q. Qin, Y. Huang, W. Lewis, N. He, R. M. Evans, M. D. Schneider, F. A. Brako, Y. Xiao, Y. E. Chen, Q. Yang, Cardiomyocyte-restricted peroxisome proliferator-activated receptor-δ deletion perturbs myocardial fatty acid oxidation and leads to cardiomyopathy. *Nat. Med.* **10**, 1245–1250 (2004).

192. H. Tuunanen, E. Engblom, A. Naum, K. Någren, B. Hesse, K. E. J. Airaksinen, P. Nuutila, P. Iozzo, H. Ukkonen, L. H. Opie, J. Knuuti, Free fatty acid depletion acutely decreases

cardiac work and efficiency in cardiomyopathic heart failure. *Circulation* **114**, 2130–7 (2006).

193. K. M. R. Prasad, Y. Xu, Z. Yang, S. T. Acton, B. A. French, Robust cardiomyocyte-specific gene expression following systemic injection of AAV: In vivo gene delivery follows a Poisson distribution. *Gene Ther.* **18**, 43-52. (2011).

194. S. Kaimoto, A. Hoshino, M. Ariyoshi, Y. Okawa, S. Tateishi, K. Ono, M. Uchihashi, K. Fukai, E. Iwai-Kanai, S. Matoba, Activation of PPAR-α in the early stage of heart failure maintained myocardial function and energetics in pressure-overload heart failure. *Am. J. Physiol. Circ. Physiol.* **312**, H305–H313 (2017).

195. F. Brigadeau, P. Gelé, M. Wibaux, C. Marquié, F. Martin-Nizard, G. Torpier, J.-C. Fruchart, B. Staels, P. Duriez, D. Lacroix, The PPARalpha Activator Fenofibrate Slows Down the Progression of the Left Ventricular Dysfunction in Porcine Tachycardia-Induced Cardiomyopathy. *J. Cardiovasc. Pharmacol.* **49**, 408–415 (2007).

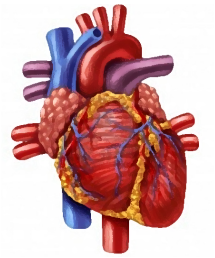

Annex I: Publications

During this thesis, the following publications have been generated:

1. **A. Pun-Garcia,** , M. Gómez, D. Sanz-Rosa, B. Prados, L. del Campo, V. Andrés, V. Fuster, J.L. De la Pompa, E. Oliver, B Ibañez. Cardiomyocyte- and not endothelial-specific β3-adrenergic receptor stimulation protects the heart against ischemia/reperfusion injury. (In preparation).

2. **A. Pun-Garcia,** R Villena-Gutierrez, M Gómez, D Sanz-Rosa, B Prados, E Oliver, A Cannavo, J. A. Bernal, W. J. Koch, V. Fuster, J. L. De la Pompa and B Ibanez. Beta-3-adrenergic receptor overexpression reverses aortic stenosis-induced heart failure and restores balanced mitochondrial dynamics, Journal of Experimental Medicine (in revision).

In addition, the doctoral student has participated in the following collaborative publications:

3. J. García-Prieto, J. M. García-Ruiz, D. Sanz-Rosa, **A. Pun**, A. García-Alvarez, S. M. Davidson, L. Fernández-Friera, M. Nuno-Ayala, R. Fernández-Jiménez, J. A. Bernal, J. L. Izquierdo-Garcia, J. Jimenez-Borreguero, G. Pizarro, J. Ruiz-Cabello, C. Macaya, V. Fuster, D. M. Yellon, B. Ibanez, β3 adrenergic receptor selective stimulation during ischemia/reperfusion improves cardiac function in translational models through inhibition of mPTP opening in cardiomyocytes. *Basic Res. Cardiol.* **109**, 422 (2014).

4. L. A. Grisanti, A. M. Gumpert, C. J. Traynham, J. E. Gorsky, A. A. Repas, E. Gao, R. L. Carter, D. Yu, J. W. Calvert, **A. Pun García**, B. Ibáñez, J. E. Rabinowitz, W. J. Koch, D. G. Tilley, Leukocyte-Expressed β2-Adrenergic Receptors Are Essential for Survival After Acute Myocardial Injury. *Circulation* **134**, 153–67 (2016).

5. A. Cannavo, G. Rengo, D. Liccardo, **A. Pun**, E. Gao, A. J. George,

G. Gambino, A. Rapacciuolo, D. Leosco, B. Ibanez, N. Ferrara, N. Paolocci, W. J. Koch, β1-Blockade Prevents Post-Ischemic Myocardial Decompensation Via β3AR-Dependent Protective Sphingosine-1 Phosphate Signaling. *J. Am. Coll. Cardiol.* **70**, 182–192 (2017).

6. J. García-Prieto, R. Villena-Gutiérrez, M. Gómez, E. Bernardo, **A. Pun-García**, I. García-Lunar, G. Crainiciuc, R. Fernández-Jiménez, V. Sreeramkumar, R. Bourio-Martínez, J. M. García-Ruiz, A. S. Del Valle, D. Sanz-Rosa, G. Pizarro, A. Fernández-Ortiz, A. Hidalgo, V. Fuster, B. Ibanez, Neutrophil stunning by metoprolol reduces infarct size. *Nat. Commun.* **8**, 14780 (2017).

7. A. Binek, R. Fernández-Jiménez, I. Jorge, E. Camafeita, J. A. López, N. Bagwan, C. Galán-Arriola, **A. Pun**, J. Agüero, V. Fuster, B. Ibanez, J. Vázquez, Proteomic footprint of myocardial ischemia/reperfusion injury: Longitudinal study of the at-risk and remote regions in the pig model. *Sci. Rep.* **7**, 12343 (2017).